Table 7-8

MARAD Series Model H - Nondimensional Stability and Control Derivatives, Hull Constants, and Stability Indices for Various H/T Values

(Values are based on a 200,000 ton full load displacement at a reference speed of 8 knots.)

	Nondimensional Value				Ratio to Deep Water Value			
	H/T = ∞	H/T = 2.5	H/T = 1.5	H/T = 1.2	H/T = ∞	H/T = 2.5	H/T = 1.5	H/T = 1.2
Y_v'	-0.01165	-0.01218	-0.02811	-0.06510	1.000	1.045	2.413	5.588
N_v'	-0.00665	-0.00814	-0.01584	-0.02643		1.224	2.382	3.974
Y_r'	0.00346	0.00355	0.00750	0.01106		1.026	2.167	3.197
N_r'	-0.00240	-0.00265	-0.00396	-0.006475		1.104	1.650	2.698
$Y_{\dot{v}}'$	-0.01218	-0.01315	-0.02169	-0.05859		1.080	1.780	4.811
$N_{\dot{v}}'$	-0.00004	-0.00003	0.000016	0.000155		0.750	-0.400	-3.875
$Y_{\dot{r}}'$	-0.00035	-0.00035	-0.00038	-0.00105		1.000	1.086	3.000
$N_{\dot{r}}'$	-0.000761	-0.000781	-0.00108	-0.00141		1.025	1.419	1.853
$Y_{\delta r}'$	0.00335	0.00333	0.00340	0.00413		0.994	1.015	1.233
$N_{\delta r}'$	-0.00174	-0.00174	-0.00178	-0.00186		1.000	1.023	1.069
m'	0.01341	0.01341	0.01341	0.01341		1.000	1.000	1.000
I_z'	0.000838	0.000838	0.000838	0.000838		1.000	1.000	1.000
$-Y_{\dot{v}}'/m'$	0.9080	0.9806	1.617	4.369		1.080	1.780	4.811
σ_{1h}'	0.4063	0.4515	-0.1591	-0.7528		1.111	-0.392	-1.852
σ_{2h}'	-2.2970	-2.4705	-2.6128	-2.8662		1.076	1.137	1.248
σ_{1h}''	0.07661	0.08513	-0.02995	-0.1419		1.111	-0.392	-1.853
ι_v'	0.5708	0.6683	0.5635	0.4060		1.171	0.987	0.711
ι_r'	0.2414	0.2690	0.7525	2.3354		1.114	3.117	9.674
ι_d'	-0.3294	-0.3993	0.1889	1.9294	1.000	1.213	-0.573	-5.857

Table 7-9

Comparison of Stability and Control Derivatives and Stability Indices for MARAD Series at H/T = ∞ and H/T = 1.2

(Values are based on a 200,000 ton full load displacement at a reference speed of 8 knots.)

	H/T = ∞				H/T = 1.2			
	E	K	L	H	E	K	L	H
Y_v'	-0.01914	-0.01294	-0.00935	-0.01165	-0.13107	-0.10675	-0.09770	-0.06510
N_v'	-0.01072	-0.00687	-0.00448	-0.00665	-0.05238	-0.03903	-0.03705	-0.02643
Y_r'	0.00554	0.00342	0.00251	0.00346	0.01278	0.01105	0.01223	0.01106
N_r'	-0.00460	-0.00314	-0.00250	-0.00240	-0.00898	-0.00717	-0.00632	-0.006475
$Y_{\dot{v}}'$	-0.02017	-0.01349	-0.00981	-0.01218	-0.09543	-0.06487	-0.05009	-0.05859
$N_{\dot{r}}'$	-0.00136	-0.000857	-0.000586	-0.000761	-0.00255	-0.00166	-0.001433	-0.00141
$Y_{\delta r}'$	0.00545	0.000456	0.00359	0.00335	0.00650	0.00657	0.00581	0.00413
$N_{\delta r}'$	-0.00286	-0.00238	-0.001865	-0.00174	-0.00293	-0.00265	-0.00212	-0.00186
m'	0.02267	0.01813	0.01511	0.01341	0.02267	0.01813	0.01511	0.01341
I_z'	0.001417	0.001133	0.000944	0.000838	0.001417	0.001133	0.000944	0.00838
σ_{lh}'	0.3331	0.4139	0.3740	0.4063	-0.5608	-0.7574	-0.8506	-0.7528
σ_{lh}''	0.07482	0.08630	0.07338	0.07661	-0.1259	-0.1579	-0.1669	-0.1419
ℓ_d'	-0.2912	-0.3184	0.2806	-0.3294	0.5102	0.6481	1.820	1.9294

Notes: MARAD Series Ships E, K, and L represent B/T variations of 3.00, 3.75, and 4.50, respectively, with constant C_B = 0.85 and L/B = 5.00.

MARAD Series Ships E and H represent L/B variations of 5.00 and 6.50, respectively, with constant C_B = 0.85 and B/T = 3.00.

Table 7-10

Incremental Contribution to Stability and Control Derivatives of MARAD Series 200,000 Ton Ships Due to Change in Propeller Loading Coefficient at Various H/T

Ship	H/T	$Y_{v\eta}'$	$N_{v\eta}'$	$Y_{r\eta}'$	$N_{r\eta}'$	$Y_{\delta r\eta}'$	$N_{\delta r\eta}'$
E	∞	-0.00316	0.00164	0.00159	-0.00085	0.00545	-0.00286
	2.5	-0.00310	0.00163	0.00162	-0.00087	0.00547	-0.00287
	1.5	-0.00466	0.00243	0.00246	-0.00128	0.00773	-0.00405
	1.2	-0.00871	0.00392	0.00391	-0.00177	0.01538	-0.00693
K	∞	-0.00228	0.00119	0.00119	-0.00062	0.00456	-0.00238
	2.5	-0.00236	0.00123	0.00121	-0.00079	0.00475	-0.00251
	1.5	-0.00527	0.00278	0.00276	-0.00145	0.00748	-0.00392
	1.2	-0.01076	0.00434	0.00431	-0.00204	0.01339	-0.00540
L	∞	-0.00154	0.00080	0.00080	-0.00042	0.00359	-0.00187
	2.5	-0.00234	0.00088	0.00095	-0.00068	0.00372	-0.00186
	1.5	-0.00564	0.00280	0.00283	-0.00144	0.00766	-0.00383
	1.2	-0.01398	0.00510	0.00611	-0.00174	0.02002	-0.00730
H	∞	-0.00178	0.00092	0.00093	-0.00048	0.00335	-0.00174
	2.5	-0.00191	0.00094	0.00101	-0.00052	0.00339	-0.00179
	1.5	-0.00372	0.00194	0.00186	-0.00097	0.00516	-0.00270
	1.2	-0.00645	0.00295	0.00231	-0.00161	0.01026	-0.00462

Table 7-11

Comparison of Dimensional Angular Acceleration Parameters for 200,000 Ton Displacement in Deep and Shallow Water of Various Depths

(Values are for an approach speed of 8 knots.)

Ship	H/T	cp, sec^{-2}	t_2, sec	
			Col. 1	Col. 2
E	∞	0.9053×10^{-4}	52	52
	2.5	0.9052	52	52
	1.5	0.7735	55	55
	1.2	0.6492	62	67
K	∞	0.9058	52	52
	2.5	0.9022	53	53
	1.5	0.8081	56	56
	1.2	0.7185	61	64
L	∞	0.8174	56	56
	2.5	0.7804	57	57
	1.5	0.6778	59	59
	1.2	0.5981	64	70
H	∞	0.6740	61	61
	2.5	0.6657	62	62
	1.5	0.5748	67	68
	1.2	0.5125	69	79

Notes: Col. 1 values are read from Figure 7-26.
Col. 2 values are from computer simulations.

Table 7-12

MARAD Series Ship E - Nondimensional Hydrodynamic Coefficients and Constants for Various H/T Values

(Values are based on a 200,000 ton full load displacement at a reference speed of 8 knots.)

(a) X-Equation

Nondimensional Coefficient	Value			
	H/T = ∞	H/T = 2.5	H/T = 1.5	H/T = 1.2
$X_{\dot{u}}'$	-0.00133	-0.00168	-0.00350	-0.00629
X_{vr}'	0.01608	0.01888	0.03939	0.07051
X_{vv}'	0.00248	0.00395	0.00536	0.04236
$X_{\delta r\delta r}'(\eta=0)$	-0.00170	-0.00150	-0.00123	-0.00030
X_{rr}'	0.0	0.0	0.0	0.0
$X_{vv\eta}'$	0.00100	0.00336	0.00864	0.01330
$X_{\delta r\delta r\eta\eta}'$	-0.00139	-0.00130	-0.00142	-0.00159
a_1	-0.000021	0.0	0.0	0.0
b_1	-0.002054	-0.001888	-0.001842	-0.002516
c_1	0.002086	-.002061	0.002212	0.002774
a_2	-0.000838	-0.000892	-0.001040	-0.001251
b_2	-0.000849	-0.000896	-0.001023	-0.001149
c_2	0.001687	0.001788	0.002063	0.002401
a_3	-0.000838	-0.000892	-0.001040	-0.001251
b_3	0.001201	0.001127	0.000723	0.000385
c_3	-0.000054	-0.000283	-0.000795	-0.001434
a_4	-0.001291	-0.001270	-0.001191	-0.001149
b_4	-0.000114	+0.000108	0.000386	0.000704
c_4	-0.000916	-0.000924	-0.000981	-0.001220

Note: Segments 1, 2, 3 and 4 for X' as a function of η correspond to $2 \leq \eta \leq \infty$, $0 \leq \eta \leq 2.0$, $-1.0 \leq \eta \leq 0$, and $-\infty \leq \eta \leq -1.0$, respectively.

Table 7-12 (Continued)

(b) Y-Equation

Nondimensional Coefficient	Value			
	H/T = ∞	H/T = 2.5	H/T = 1.5	H/T = 1.2
$Y_{\dot{v}}'$	-0.02017	-0.02547	-0.05304	-0.09543
Y_{*}'	0.000084	0.000091	0.000112	0.000143
Y_{v}'	-0.01506	-0.027014	-0.05231	-0.132715
$Y_{v\|v\|}'$	-0.0534	-0.07510	-0.159091	-0.36113
Y_{r}'	0.00538	0.00547	0.00659	0.01278
$Y_{r\|r\|}'$	0.0020	0.00331	0.00560	0.01600
$Y_{r\|\delta r\|}'$	0.0	0.0	0.0	0.0
$Y_{v\|r\|}'$	-0.01630	-0.01762	-0.06325	-0.15028
$Y_{\dot{r}}'$	-0.00035	-0.00043	-0.00125	-0.00300
$Y_{\delta r}'$	0.00545	0.00547	0.00554	0.00650
$Y_{\delta r\eta}'$	0.00545	0.00547	0.00773	0.01538
$Y_{r\eta}'$	0.00159	0.00162	0.00246	0.00391
$Y_{v\eta}'$	-0.00316	-0.00310	-0.00466	-0.00871
$Y_{*\eta}'$	0.000084	0.000091	0.000112	0.000143
m'	0.02267	0.002267	0.002267	0.002267

Table 7-12 (Concluded)

(c) N-Equation

Nondimensional Coefficient	Value			
	H/T = ∞	H/T = 2.5	H/T = 1.5	H/T = 1.2
$N_{\dot{r}}'$	-0.00136	-0.00137	-0.00189	-0.00255
N_{*}'	-0.000044	-0.000049	-0.000059	-0.000075
N_{v}'	-0.01098	-0.012803	-0.02773	-0.05238
$N_{v\|v\|}'$	0.01327	0.009091	0.01062	0.0
N_{r}'	-0.00430	-0.00435	-0.00535	-0.00898
$N_{r\|r\|}'$	-0.00018	-0.00039	-0.00054	-0.00153
$N_{r\delta r}'$	0.0	0.0	0.0	0.0
$N_{\|v\|r}'$	-0.00515	-0.00624	-0.01683	-0.03675
$N_{\dot{v}}'$	0.00002	0.00004	0.00055	0.00201
$N_{\delta r}'$	-0.00286	-0.00287	-0.00291	-0.00293
$N_{\delta r\eta}'$	-0.00286	-0.00287	-0.00405	-0.00693
$N_{v\eta}'$	0.00164	0.00163	0.00243	0.00392
$N_{r\eta}'$	-0.000854	-0.000865	-0.00128	-0.001766
$N_{*\eta}'$	-0.000044	-0.000049	-0.000059	-0.000075
I_{z}'	0.001417	0.001417	0.001417	0.001417

Note: Value of I_z' is based on $k_z' = 0.25$.

Table 7-13

MARAD Series Ship K - Nondimensional Hydrodynamic Coefficients and Constants for Various H/T Values

(Values are based on a 200,000 ton full load displacement at a reference speed of 8 knots.)

(a) X-Equation

Nondimensional Coefficient	Value			
	H/T = ∞	H/T = 2.5	H/T = 1.5	H/T = 1.2
$X_{\dot{u}}'$	-0.00107	-0.001435	-0.003139	-0.005145
X_{vr}'	0.01012	0.01241	0.02963	0.04865
X_{vv}'	0.00188	0.00204	0.004458	0.02167
$X_{\delta r\delta r}'(\eta=0)$	-0.000513	-0.000507	-0.0004268	-0.000361
X_{rr}'	0.0	0.0	0.0	0.0
$X_{vv\eta}'$	0.000994	0.001095	0.003582	0.01411
$X_{\delta r\delta r\eta\eta}'$	-0.001167	-0.00119	-0.00139	-0.00215
a_1	0.0	0.0	0.0	0.0
b_1	-0.001448	-0.001447	-0.001424	-0.001761
c_1	0.001658	0.001660	0.001758	0.002052
a_2	-0.000906	-0.000958	-0.001273	-0.001555
b_2	-0.000513	-0.000461	-0.000183	-0.000011
c_2	0.001419	0.001419	0.001456	0.001566
a_3	-0.000906	-0.000958	-0.001273	-0.001555
b_3	0.000474	0.000455	0.000332	0.000228
c_3	-0.000445	-0.000474	-0.000915	-0.001439
a_4	-0.000741	-0.000772	-0.000902	-0.001283
b_4	-0.000112	-0.000089	0.000350	0.000459
c_4	-0.001196	-0.001204	-0.001268	-0.001480

Note: Segments 1, 2, 3 and 4 for X' as a function of η correspond to $2 \leq \eta \leq \infty$, $0 \leq \eta \leq 2.0$, $-1.0 \leq \eta \leq 0$, and $-\infty \leq \eta \leq -1.0$, respectively.

Table 7-13 (Continued)

(b) Y-Equation

Nondimensional Coefficient	Value			
	H/T = ∞	H/T = 2.5	H/T = 1.5	H/T = 1.2
$Y_{\dot{v}}'$	-0.01349	-0.01876	-0.03958	-0.06487
Y_{*}'	0.000086	0.000084	0.000090	0.000098
Y_{v}'	-0.01031	-0.01399	-0.03885	-0.11135
$Y_{v\|v\|}'$	-0.03718	-0.04853	-0.08909	-0.18113
Y_{r}'	0.00335	0.03685	0.00659	0.01105
$Y_{r\|r\|}'$	0.00107	0.00161	0.00791	0.00994
$Y_{r\|\delta r\|}'$	0.0	0.0	0.0	0.0
$Y_{v\|r\|}'$	-0.0163	-0.0160	-0.02043	-0.05241
$Y_{\dot{r}}'$	-0.00024	-0.00041	-0.00105	-0.00218
$Y_{\delta r}'$	0.00456	0.00451	0.00477	0.00657
$Y_{\delta r\eta}'$	0.00456	0.00475	0.00748	0.01339
$Y_{r\eta}'$	0.00119	0.00121	0.00276	0.00431
$Y_{v\eta}'$	-0.00228	-0.00236	-0.00527	-0.01076
$Y_{*\eta}'$	0.000086	0.000086	0.000090	0.000098
m'	0.01813	0.01813	0.01813	0.01813

Table 7-13 (Concluded)

(c) N-Equation

Nondimensional Coefficient	Value			
	H/T = ∞	H/T = 2.5	H/T = 1.5	H/T = 1.2
$N_{\dot{r}}'$	-0.000857	-0.000865	-0.00121	-0.00166
N_{*}'	-0.000045	-0.000045	-0.000047	-0.000052
N_{v}'	-0.00728	-0.00766	-0.01907	-0.03903
$N_{v\|v\|}'$	0.00895	0.00658	0.001136	0.0
N_{r}'	-0.00314	-0.00325	-0.00411	-0.00717
$N_{r\|r\|}'$	-0.00074	-0.00078	-0.00145	-0.00191
$N_{r\delta r}'$	0.0	0.0	0.0	0.0
$N_{\|v\|r}'$	-0.00515	-0.00839	-0.02609	-0.03491
$N_{\dot{v}}'$	-0.00016	-0.00007	0.000596	0.00250
$N_{\delta r}'$	-0.00238	-0.00238	-0.00250	-0.00265
$N_{\delta r\eta}'$	-0.00238	-0.00251	-0.00392	-0.00540
$N_{v\eta}'$	0.00119	0.00123	0.00278	0.00434
$N_{r\eta}'$	-0.00062	-0.00079	-0.00145	-0.00204
$N_{*\eta}'$	-0.000045	-0.000045	-0.000047	-0.000052
I_{z}'	0.001133	0.001133	0.001133	0.001133

Note: Value of I_{z}' is based on $k_{z}' = 0.25$.

Table 7-14

MARAD Series Ship L - Nondimensional Hydrodynamic Coefficients and Constants for Various H/T Values

(Values are based on a 200,000 ton full load displacement at a reference speed of 8 knots.)

(a) X-Equation

Nondimensional Coefficient	Value			
	H/T = ∞	H/T = 2.5	H/T = 1.5	H/T = 1.2
$X_{\dot{u}}'$	-0.000888	-0.001025	-0.0024983	-0.004534
X_{vr}'	0.00736	0.00741	0.02071	0.03757
X_{vv}'	0.000657	0.00128	0.00669	0.02694
$X_{\delta r\delta r}'(\eta=0)$	-0.000492	-0.000443	-0.0003345	-0.0003283
X_{rr}'	0.0	0.0	0.0	0.0
$X_{vv\eta}'$	0.00092	0.00162	0.00477	0.00940
$X_{\delta r\delta r\eta\eta}'$	-0.00154	-0.00162	-0.00177	-0.00251
a_1	0.0	0.0	0.0	0.0
b_1	-0.001381	-0.001415	-0.001787	-0.002003
c_1	0.001515	0.001531	0.001946	0.002304
a_2	-0.000649	-0.000686	-0.001136	-0.001554
b_2	-0.000674	-0.000651	-0.000400	-0.000274
c_2	0.001324	0.001352	0.001536	0.001822
a_3	-0.000649	-0.000686	-0.001136	-0.001554
b_3	0.000578	0.000563	0.000362	0.000135
c_3	-0.000189	-0.000198	-0.000248	-0.000302
a_4	-0.000537	-0.000535	-0.000409	-0.000347
b_4	-0.000164	-0.000151	0.000149	0.000319
c_4	-0.001042	-0.001053	-0.001188	-0.001325

Note: Segments 1, 2, 3 and 4 for X' as a function of η correspond to $2 \leq \eta \leq \infty$, $0 \leq \eta \leq 2.0$, $-1.0 \leq \eta \leq 0$, and $-\infty \leq \eta \leq -1.0$, respectively.

Table 7-14 (Continued)

(b) Y-Equation

Nondimensional Coefficient	Value			
	H/T = ∞	H/T = 2.5	H/T = 1.5	H/T = 1.2
$Y_{\dot{v}}'$	-0.00981	-0.01379	-0.02760	-0.05009
Y_{*}'	0.000086	0.000075	0.000077	0.000096
Y_{v}'	-0.00751	-0.01269	-0.03724	-0.09881
$Y_{v\|v\|}'$	-0.02622	-0.04935	-0.1093	-0.34113
Y_{r}'	0.00251	0.00271	0.00555	0.01223
$Y_{r\|r\|}'$	0.00115	0.00193	0.00474	0.00698
$Y_{r\|\delta r\|}'$	0.0	0.0	0.0	0.0
$Y_{v\|r\|}'$	-0.0163	-0.01942	-0.0609	-0.1551
$Y_{\dot{r}}'$	-0.00011	-0.00021	0.001033	0.002217
$Y_{\delta r}'$	0.00359	0.00361	0.00414	0.00581
$Y_{\delta r\eta}'$	0.00359	0.00372	0.00766	0.02002
$Y_{r\eta}'$	0.00080	0.00095	0.00283	0.00611
$Y_{v\eta}'$	-0.00154	-0.00234	-0.00564	-0.01398
$Y_{*\eta}'$	0.000086	0.000075	0.000077	0.000096
m'	0.01511	0.01511	0.01511	0.01511

Table 7-14 (Concluded)

(c) N-Equation

Nondimensional Coefficient	Value			
	H/T = ∞	H/T = 2.5	H/T = 1.5	H/T = 1.2
N_r'	-0.000586	-0.000663	-0.001104	-0.001433
N_*'	-0.000045	-0.000041	-0.000040	-0.000051
N_v'	-0.00475	-0.00635	-0.01984	-0.03721
$N_{v\|v\|}'$	0.00423	0.00342	0.000910	-0.002213
N_r'	-0.0025	-0.00259	-0.00350	-0.00632
$N_{r\|r\|}'$	-0.00028	-0.00042	-0.000561	-0.000961
$N_{r\delta r}'$	0.0	0.0	0.0	0.0
$N_{\|v\|r}'$	-0.00515	-0.00811	-0.022326	-0.06672
$N_{\dot{v}}'$	-0.00016	-0.00015	0.000374	0.001117
$N_{\delta r}'$	-0.001865	-0.00187	-0.00207	0.00212
$N_{\delta r\eta}'$	-0.001865	-0.00186	-0.00383	-0.00730
$N_{v\eta}'$	0.000803	0.000875	0.00280	0.00510
$N_{r\eta}'$	-0.00042	-0.00068	-0.00144	-0.00174
$N_{*\eta}'$	-0.000045	-0.000041	-0.000040	-0.000051
I_z'	0.000944	0.000944	0.000944	0.000944

Note: Value of I_z' is based on $k_z' = 0.25$.

Table 7-15

MARAD Series Ship H - Nondimensional Hydrodynamic Coefficients and Constants for Various H/T Values

(Values are based on a 200,000 ton full load displacement at a reference speed of 8 knots.)

(a) X-Equation

Nondimensional Coefficient	Value			
	H/T = ∞	H/T = 2.5	H/T = 1.5	H/T = 1.2
$X_{\dot{u}}'$	-0.000671	-0.000689	-0.001195	-0.003228
X_{vr}'	0.00914	0.00938	0.01627	0.04394
X_{vv}'	0.00197	0.00199	0.00340	0.0109
$X_{\delta r\delta r}'(\eta = 0)$	-0.00087	-0.00084	-0.000659	-0.000442
X_{rr}'	0.0	0.0	0.0	0.0
$X_{vv\eta}'$	0.00103	0.00121	0.00761	0.0157
$X_{\delta r\delta r\eta\eta}'$	-0.00109	-0.00110	-0.00117	-0.00129
a_1	0.0	0.0	0.0	0.0
b_1	-0.001169	-0.001182	-0.001317	-0.001417
c_1	0.001304	0.001319	0.001483	0.001627
a_2	-0.000641	-0.000660	-0.000876	-0.001419
b_2	-0.000438	-0.000409	-0.000285	0.000291
c_2	0.001080	0.001081	0.001101	0.001128
a_3	-0.000641	-0.000660	-0.000876	-0.001419
b_3	0.000883	0.000855	0.000509	0.000190
c_3	-0.000285	-0.000297	-0.000421	-0.000609
a_4	-0.001189	-0.001182	-0.000952	-0.000885
b_4	-0.000272	-0.000268	0.000091	0.000332
c_4	-0.000892	-0.000898	-0.000945	-0.001001

Note: Segments 1, 2, 3 and 4 for X' as a function of η correspond to $2 \leq \eta \leq \infty$, $0 \leq \eta \leq 2.0$, $-1.0 \leq \eta \leq 0$, and $-\infty \leq \eta \leq -1.0$, respectively.

Table 7-15 (Continued)

(b) Y-Equation

Nondimensional Coefficient	Value			
	H/T = ∞	H/T = 2.5	H/T = 1.5	H/T = 1.2
$Y_{\dot{v}}'$	-0.01218	-0.01315	-0.02169	-0.05859
Y_{*}'	0.00006	0.000058	0.000058	0.000075
Y_{v}'	-0.00924	-0.01055	-0.02834	-0.06636
$Y_{v\|v\|}'$	-0.03702	-0.05092	-0.10319	-0.19233
Y_{r}'	0.00335	0.00368	0.00750	0.01046
$Y_{r\|r\|}'$	0.00230	0.00295	0.00633	0.00907
$Y_{r\|\delta r\|}'$	0.0	0.0	0.0	0.0
$Y_{v\|r\|}'$	-0.0144	-0.0199	-0.02898	-0.05769
$Y_{\dot{r}}'$	-0.00035	-0.00035	-0.00038	-0.00105
$Y_{\delta r}'$	0.00335	0.00333	0.00340	0.00413
$Y_{\delta r\eta}'$	0.00335	0.00339	0.00516	0.01026
$Y_{r\eta}'$	0.00093	0.00101	0.00186	0.00231
$Y_{v\eta}'$	-0.00178	-0.00191	-0.00372	-0.00645
$Y_{*\eta}'$	0.00006	0.000058	0.000058	0.000075
m'	0.01341	0.01341	0.01341	0.01341

Table 7-15 (Concluded)

(c) N-Equation

Nondimensional Coefficient	Value			
	H/T = ∞	H/T = 2.5	H/T = 1.5	H/T = 1.2
$N_{\dot{r}}'$	-0.000761	-0.000781	-0.00108	-0.00141
N_{*}'	-0.000031	-0.000031	-0.000031	-0.000040
N_{v}'	-0.00515	-0.00738	-0.01691	-0.02893
$N_{v\|v\|}'$	0.0020	0.00179	0.0007515	0.0
N_{r}'	-0.00240	-0.00265	-0.00396	-0.00611
$N_{r\|r\|}'$	-0.00044	-0.00089	-0.00133	-0.00181
$N_{r\delta r}'$	0.0	0.0	0.0	0.0
$N_{\|v\|r}'$	-0.00483	-0.00995	-0.021563	-0.038427
$N_{\dot{v}}'$	-0.00004	-0.00003	0.000016	0.000155
$N_{\delta r}'$	-0.00174	-0.00174	-0.00178	-0.00186
$N_{\delta r\eta}'$	-0.00174	-0.00179	-0.00270	-0.00462
$N_{v\eta}'$	0.000923	0.000936	0.001938	0.00295
$N_{r\eta}'$	-0.00048	-0.00052	-0.000969	-0.00161
$N_{*\eta}'$	-0.000031	-0.000031	-0.000031	-0.000040
I_{z}'	0.000838	0.000838	0.000838	0.000838

Note: Value of I_{z}' is based on $k_{z}' = 0.25$.

Table 7-16

Comparison of Numerical Measures from Spiral Maneuvers
in Deep and Shallow Water of Various Depths
200,000 Ton Displacement

(Values are for an approach speed of 8 knots.)

Ship	H/T	Height of Loop deg/sec	Width of Loop deg	Neutral Rudder Angle deg	Rate at Rudder Angle 20° R deg/sec	Rate at Rudder Angle 10° R deg/sec	Rate at Rudder Angle 0 deg/sec	Rate at Rudder Angle 10° L deg/sec	Rate at Rudder Angle 20° L deg/sec
E	∞	0.285	4.8	1.0R	0.206	0.187	-	-0.194	-0.215
	2.5	0.284	3.3	1.0R	0.233	0.206	-	-0.204	-0.241
	1.5	0.187	1.7	1.5R	0.269	0.220	-0.118	-0.225	-0.273
	1.2	0.0	0.0	1.2R	0.199	0.122	0.019	-0.133	-0.215
K	∞	0.251	6.8	1.0R	0.186	0.169	-	-0.176	-0.487
	2.5	0.218	4.6	1.0R	0.187	0.166	-	-0.174	-0.188
	1.5	0.071	0.9	1.0R	0.194	0.154	-0.060	-0.166	-0.197
	1.2	0.0	0.0	1.0R	0.180	0.103	-0.015	-0.118	-0.188
L	∞	0.211	5.2	1.2R	0.164	0.148	-	-0.159	-0.175
	2.5	0.210	4.7	1.2R	0.185	0.165	-	-0.172	-0.192
	1.5	0.094	0.7	0.9R	0.196	0.158	-0.078	-0.172	-0.210
	1.2	0.0	0.0	1.0R	0.151	0.082	0.010	-0.101	-0.164
H	∞	0.191	4.0	1.0R	0.186	0.156	-	-0.164	-0.189
	2.5	0.195	4.1	1.0R	0.182	0.156	-	-0.164	-0.184
	1.5	0.0	0.0	0.8R	0.178	0.125	-0.026	-0.137	-0.183
	1.2	0.0	0.0	1.0R	0.135	0.072	-0.019	-0.086	-0.140

Table 7-17

Comparison of Numerical Measures from Zigzag Maneuvers
200,000 Ton Displacement in Deep and Shallow Water

(Values are for an approach speed of 8 knots.)

(a) 5-5 Zigzag

Ship	H/T	First Overshoot						Reach (sec)	Second Overshoot Heading Angle (deg)	Third Overshoot Heading Angle (deg)	Period (sec)
		Time to Reach Execute Heading Change (sec)	Overshoot Angle (deg)	Total Heading Change (deg)	Width of Path at Execute (ft)	Overshoot Width of Path (ft)	Total Width of Path (ft)				
E	∞	111	5.16	10.16	19	534	553	402	-	-	-
	2.5	112	3.55	8.55	23	364	387	345	29.85	28.35	1688
	1.5	124	3.27	8.27	26	344	370	342	22.17	16.29	920
	1.2	165	0.80	5.80	58	175	233	332	2.61	1.91	635
K	∞	111	4.94	8.94	16	427	443	383	-	-	-
	2.5	119	2.71	7.71	22	315	337	343	26.23	19.02	1105
	1.5	125	2.28	7.28	33	276	309	332	11.23	2.36	773
	1.2	134	0.64	5.64	61	128	209	303	1.68	1.73	578
L	∞	122	2.74	7.74	14	340	354	370	-	-	-
	2.5	124	2.85	7.85	19	349	368	370	28.61	18.23	1240
	1.5	129	2.41	7.41	29	290	319	335	9.40	5.62	730
	1.2	171	0.50	5.50	71	145	216	273	1.31	0.49	519
H	∞	135	2.79	7.79	22	368	390	395	21.42	17.63	1175
	2.5	136	3.57	8.57	22	450	472	420	27.79	19.72	1294
	1.5	155	1.56	6.56	47	254	301	362	4.87	2.61	695
	1.2	213	0.47	5.47	87	187	274	315	1.28	1.48	767

Table 7-17 (Continued)

(b) 10-10 Zigzag

Ship	H/T	First Overshoot						Reach (sec)	Second Overshoot Heading Angle (deg)	Third Overshoot Heading Angle (deg)	Period (sec)
		Time to Reach Execute Heading Change (sec)	Overshoot Angle (deg)	Total Heading Change (deg)	Width of Path at Execute (ft)	Overshoot Width of Path (ft)	Total Width of Path (ft)				
E	∞	105	9.33	19.33	28	996	1024	405	29.90	22.23	955
	2.5	105	7.61	17.61	39	784	823	362	23.76	19.40	805
	1.5	116	7.30	17.30	61	744	805	360	18.77	13.83	734
	1.2	156	1.94	11.94	116	380	496	342	3.54	2.39	504
K	∞	104	7.35	17.35	25	834	859	388	22.30	15.29	910
	2.5	112	5.47	15.47	42	657	699	361	25.31	11.08	788
	1.5	124	4.96	14.96	70	597	667	351	10.53	7.81	682
	1.2	145	1.58	11.58	109	337	446	311	2.58	1.83	573
L	∞	121	5.49	15.49	36	701	737	383	17.26	11.04	899
	2.5	124	5.55	15.55	51	696	747	375	15.73	11.08	816
	1.5	129	4.70	14.70	65	583	648	343	8.44	6.19	641
	1.2	167	1.24	11.24	135	323	458	342	1.90	1.15	613
H	∞	131	5.91	15.91	51	773	824	416	15.78	11.88	889
	2.5	129	6.12	16.12	48	823	871	415	15.83	11.71	890
	1.5	144	3.08	13.08	85	531	616	312	5.57	3.98	676
	1.2	212	1.25	11.24	167	415	582	362	1.86	1.32	758

Table 7-17 (Concluded)

(c) 20-20 Zigzag

Ship	H/T	First Overshoot						Reach (sec)	Second Overshoot Heading Angle (deg)	Third Overshoot Heading Angle (deg)	Period (sec)
		Time to Reach Execute Heading Change (sec)	Overshoot Angle (deg)	Total Heading Change (deg)	Width of Path at Execute (ft)	Overshoot Width of Path (ft)	Total Width of Path (ft)				
E	∞	111	17.23	37.23	83	1685	1768	415	26.95	17.84	860
	2.5	112	14.48	34.48	101	1401	1502	372	26.75	19.19	780
	1.5	119	12.35	32.35	131	1250	1381	309	17.27	13.65	680
	1.2	151	4.30	24.30	216	804	1020	300	5.72	4.75	630
K	∞	111	13.58	33.58	64	1473	1537	403	19.21	13.28	330
	2.5	112	10.08	30.08	76	1212	1288	372	13.92	10.58	750
	1.5	123	8.22	28.22	130	1075	1205	361	10.03	8.07	661
	1.2	154	3.57	23.57	235	696	931	340	4.23	3.68	615
L	∞	120	10.43	30.43	73	1295	1368	402	17.40	11.12	850
	2.5	121	9.75	29.75	91	1252	1343	391	13.88	9.85	729
	1.5	138	7.38	27.38	175	975	1150	355	8.43	6.84	642
	1.2	176	2.94	22.94	291	662	953	300	3.18	2.70	660
H	∞	131	10.97	30.97	96	1400	1496	420	16.62	12.22	860
	2.5	133	9.43	29.43	131	1316	1447	422	12.38	9.63	820
	1.5	151	5.25	25.25	188	981	1169	397	6.26	5.36	730
	1.2	204	2.67	22.67	325	855	1180	360	3.18	2.79	816

Table 7-18

Comparison of Numerical Measures from Steady Turning Maneuvers of 200,000 ton Ships in Deep and Shallow Water

(Values are for an approach speed of 8 knots.)

(a) 10 Degree Right Rudder Angle Turn

Ship	H/T	Time to Change Heading 90 Deg seconds	Time to Change Heading 180 Deg seconds	Speed Remaining in Steady Turn knots	Advance feet	Transfer feet	Tactical Diameter feet	Steady Turning Diameter feet
E	∞	403	812	4.58	4048	1813	4541	4499
	2.5	399	748	4.93	4005	2054	4435	4423
	1.5	433	804	5.99	4227	2567	5265	5259
	1.2	898	1721	7.51	7995	6852	13652	13308
K	∞	458	938	5.01	4545	2289	5638	5718
	2.5	498	983	5.31	4813	2688	6185	6168
	1.5	542	1021	6.26	5051	3415	7072	6779
	1.2	921	1796	7.51	8097	7108	14327	14073
L	∞	532	1084	5.18	5254	2707	6624	6661
	2.5	528	1017	5.78	5131	2971	6706	6712
	1.5	593	1122	6.83	5472	4037	8231	8076
	1.2	1143	1373	7.58	9875	8983	18133	17996
H	∞	534	1044	5.24	5265	2799	6412	6427
	2.5	738	1087	5.71	5393	3195	7105	7042
	1.5	767	1474	7.11	6986	5441	11135	10906
	1.2	1190	2581	7.63	11439	8617	20820	20518

(b) 20 Degree Right Rudder Angle Turn

E	∞	305	675	3.58	2998	1234	3358	3254
	2.5	357	589	3.79	2301	1425	3113	3016
	1.5	314	600	4.86	2991	1757	3609	3472
	1.2	515	973	6.42	4575	3559	7032	6343
K	∞	291	774	3.96	3396	1625	4196	4121
	2.5	368	788	4.14	3508	1823	4469	4294
	1.5	391	763	4.91	3561	2325	4842	4303
	1.2	712	1022	6.36	4636	3752	7461	6855
L	∞	400	879	3.99	3829	1821	4756	4608
	2.5	390	805	4.54	3718	2027	4801	4681
	1.5	422	820	5.59	3810	2639	5487	5167
	1.2	634	1207	6.80	5372	4502	9040	8603
H	∞	395	840	4.05	3761	1875	4443	4319
	2.5	423	870	4.49	3955	2237	5134	4942
	1.5	514	1007	5.88	4601	3349	6923	6514
	1.2	726	1403	6.59	6392	5232	10345	9530

Table 7-18 (Concluded)

(c) 35 Degree Right Rudder Angle Turn

Ship	H/T	Time to Change Heading 90 Deg seconds	Time to Change Heading 180 Deg seconds	Speed Remaining in Steady Turn knots	Advance feet	Transfer feet	Tactical Diameter feet	Steady Turning Diameter feet
E	∞	248	615	2.50	2325	901	2448	2314
	2.5	239	493	2.61	2212	945	2181	2003
	1.5	246	478	3.53	2258	1212	2481	2204
	1.2	348	643	4.42	3051	2086	4090	3120
K	∞	283	691	2.76	2655	1099	3104	2850
	2.5	293	685	2.81	2712	1284	3235	2887
	1.5	307	631	3.16	2701	1607	3408	2876
	1.2	363	703	4.23	3091	2241	4354	3445
L	∞	316	735	2.74	2915	1201	3379	3047
	2.5	311	706	2.78	2839	1386	3405	3076
	1.5	326	657	3.54	2834	1797	3719	3161
	1.2	403	763	4.86	3344	2498	4743	3855
H	∞	309	695	2.64	2830	1233	3031	2761
	2.5	342	751	3.00	3031	1565	3655	3278
	1.5	388	778	3.72	3312	2201	4515	3919
	1.2	497	930	4.49	4101	3004	5719	4420

(d) 45 Degree Right Rudder Angle Turn

E	∞	225	620	1.88	2110	712	2071	1858
	2.5	217	474	1.98	2024	794	1804	1586
	1.5	228	434	2.79	2065	1005	2040	1672
	1.2	308	574	3.24	2741	1701	3203	2214
K	∞	261	692	2.05	2419	890	2656	2283
	2.5	269	672	2.06	2458	1021	2741	2286
	1.5	285	605	2.15	2457	1363	2848	2195
	1.2	317	623	2.56	2725	1750	3387	2417
L	∞	293	830	1.57	2627	951	2779	2197
	2.5	289	709	1.67	2561	1124	2815	2232
	1.5	300	655	2.30	2551	1458	3024	2291
	1.2	347	627	3.43	2886	1895	3428	2404
H	∞	287	737	1.82	2551	984	2512	2088
	2.5	318	742	2.06	2741	1268	3020	2503
	1.5	357	718	2.55	2968	1828	3626	2785
	1.2	433	824	3.16	3696	2412	4445	2865

Table 7-19

Comparison of Nondimensional Tactical and Steady Turning Diameters for 200,000 Ton Displacement in Deep and Shallow Water at H/T = 1.2

Ship	Rudder Angle deg R	TD/L		D/L		Ratio to Deep Water Value	
		H/T = ∞	H/T = 1.2	H/T = ∞	H/T = 1.2	TD/L	D/L
E	10	5.33	16.03	5.28	15.63	3.01	2.96
	20	3.94	8.26	3.82	7.45	2.09	1.95
	35	2.87	4.80	2.72	3.66	1.67	1.35
	45	2.43	3.76	2.18	2.60	1.55	1.19
K	10	6.15	15.62	6.23	15.34	2.54	2.46
	20	4.57	8.13	4.49	7.46	1.78	1.66
	35	3.38	4.75	3.11	3.76	1.40	1.21
	45	2.90	3.69	2.49	2.63	1.28	1.06
L	10	6.79	18.60	6.84	18.46	2.74	2.70
	20	4.88	9.27	4.73	8.83	1.90	1.87
	35	3.47	4.87	3.13	3.95	1.40	1.27
	45	2.85	3.52	2.25	2.47	1.23	1.09
H	10	6.32	20.52	6.34	20.23	3.25	3.19
	20	4.38	10.20	4.26	9.39	2.33	2.21
	35	2.99	5.64	2.72	4.36	1.88	1.60
	45	2.48	4.38	2.06	2.82	1.77	1.37

Table 7-20

Comparison of Numerical Measures from Stopping Maneuvers for 200,000 Ton Displacement in Deep and Shallow Water at H/T = 1.2

Ship	Depth Draft Ratio H/t	Rudder Fixed at Zero				Rudder Held at Angle of 35 Degrees Right			
		Head Reach feet	Side Reach feet	Time to Reach Zero Speed seconds	Heading Change degrees	Head Reach feet	Side Reach feet	Time to Reach Zero Speed seconds	Heading Change degrees
E	∞	5555	-360	670	-47	2860	1279	490	109
	1.2	6234	-138	955	-5	4272	2887	880	71
K	∞	4714	-129	619	-28	3135	1050	519	84
	1.2	6020	-114	883	-4	4001	2898	824	76
L	∞	5227	-145	679	-28	3507	1184	530	81
	1.2	5913	-111	841	-3	4295	2606	790	70
H	∞	5408	-126	759	-18	3405	1345	569	95
	1.2	6237	-69	958	-1	5030	2552	899	49

CHAPTER 8
NUMERICAL EXAMPLE

Introduction

The numerical example presented in this chapter is intended to provide guidance to the user of the data given in the previous chapters. In addition, the performance of a MARAD series hull form is compared with the performance of an equivalent conventional hull form representative of existing full-form vessels in current service.

The selected design example is the 390,000 deadweight ton U.S. flag tanker U.S.T. ATLANTIC, with proportions and form characteristics that lie within the MARAD Series matrix of hull form parameters. The resistance, propulsion, and PMM maneuvering tests of the 24 foot model were carried out in the Hydronautics Ship Model Basin (HSMB) in 1975, and results were reported in Reference 40. Full scale Raydist trials conducted in 1979, were reported in Reference 41. The availability of these reports provided the opportunity to compare performance predictions by use of the MARAD Series data charts with model test predictions and full scale trial results.

Model-Ship Characteristics

Principal characteristics of the U.S.T. ATLANTIC, MARAD design designation T11-S-116a, are summarized in Table 8-1. Characteristics of the equivalent HSMB model 7530-1 are also included in the table. The hull form of the "T11" design consists of a cylindrical bow, similar to that of the NSMB Series, Reference 10, and the MARAD Series, and a conventional transom stern with semi-balanced rudder and supporting shoe piece. The primary difference between the "T11" and MARAD Series hull forms is in the afterbody geometry, with the Series forms having the characteristic buttock-flow run with open stern configuration and spade or horn rudder.

Speed-Power Predictions

The speed-power predictions were prepared using the computer program developed in 1977 and reported in detail in Reference 42. The complete listing for this program is included in Appendix D. Program descriptions included in this chapter are limited to brief discussions of applying the resistance and propulsion data to design studies, including interpolation methods incorporated in the program. The charts included in Chapters 4 and 5 for prediction of resistance and powering characteristics can be used manually in the traditional manner, employing linear interpolations as appropriate. However, more sophisticated interpolation methods were incorporated into the program.

Resistance - For a given combination of values of B/T, L/B, F_N, and C_B, the program provides for the following interpolation and computation sequence to obtain C_R:

- Interpolate on B/T, using a three-point parabolic fit.
- Interpolate on L/B using a three-point parabolic fit.
- Interpolate or extrapolate on F_N.

If the F_N value falls in the range of 0.13 to 0.19, a fourth order polynomial fit is used. If F_N is less than 0.13, then the C_R is set equal to the C_R value at F_N = 0.13. If F_N is greater than 0.17, a linear extrapolation is used, based on the slope of C_R between F_N = 0.185 and F_N = 0.190, as determined by a 4th order polynomial.

- Interpolate on C_B.

Due to the shape of the C_R versus C_B curve, three different interpolation methods are used, depending on the value of C_B. When C_B falls between 0.80 and 0.85, a weighted average of linear and 2nd order polynomial estimates is used. If C_B lies between 0.850 and 0.875, the interpolation is made using a second order polynomial.

Effective Horsepower, EHP - Estimated values of EHP are given in Table 8-2, the computer program output.

Assumptions and modifications to the principal characteristics summarized in Table 8-1, as required for the resistance estimates for this example, are summarized in the following notes:

(1) Wetted surface - The wetted surface coefficient, $C_S = S/(\nabla L)^{1/2}$, corresponding to the actual wetted surface, Table 8-1, is 2.754. However, the existing form of the computer program only provides for a wetted surface coefficient based on the equivalent MARAD Series model. For this case the value computed was 2.805.

(2) Appendage drag - Results of the Series resistance tests indicated that the increased resistance due to presence of the rudder was essentially in direct proportion to the increased wetted surface. Since wetted surface of the series model exceeds the actual wetted surface by about 1.9%, this correction was ignored in the example.

(3) Correlation allowance - Based on experience with earlier expansions of model test results for large full-form hulls, a value of $C_A = 0$ was assumed.

(4) Frictional resistance - Frictional resistance coefficient, C_F, was obtained from the 1957 ITTC line, Reference 13, corresponding to the appropriate values of Reynolds number, R_N.

EHP was computed for a range of speeds, by means of the following relationships:

$$CT = C_R + C_F + C_A$$

$$EHP = \frac{C_T \times \frac{\rho}{2} Sv^3}{550 \text{ ft-lb/sec}}$$

Powering Estimate - Values of (1-t), (1-w), and e_{rr} were taken from the data given in Chapter 5 and interpolated in the same manner as the C_R values. These factors are functions of

B/T, L/B, and C_B, and are constant with Froude number. In the computer program, (1-t), (1-w), and e_{rr} are each arranged in a separate array made up of a matrix of values of B/T, L/B, and C_B. For given values of B/T, L/B, and C_B, the interpolation sequence in the program is as follows:

- Interpolate on B/T, using a three-point parabolic fit.
- Interpolate on L/B, using a three-point parabolic fit.
- Interpolate on C_B as follows:
  For $0.80 \leq C_B \geq 0.850$, a weighted average of linear and second order polynomial interpolation;
  For $0.85 < C_B \leq 0.875$, a second order polynomial interpolation;

Then hull efficiency, $e_h = (1-t)/(1-w)$, and propulsive coefficient, $PC = (e_h)(e_p)(e_{rr})$.

The propeller efficiency in open water is calculated using the results of the open water tests conducted with four and five-bladed propellers of the Wageningen B-screw series results as reported in Reference 43. The propeller is optimized for the design speed with respect to operating rpm, blade-area ratio, pitch-diameter ratio (P/D), and diameter (D). Required shaft horsepower, SHP, is computed from the expression:

$$SHP = \frac{EHP_{Total}}{PC}$$

Results of the powering calculations are summarized in the computer printout of Table 8-2.

Comparison of Results - EHP, SHP, PC, and RPM values for speeds of 12 to 18 knots are summarized in Table 8-3 and compared graphically in Figure 8-1 for the computer model prediction, model test, and full scale trials. The following should be noted when making comparisons:

(1) Optimum propeller selected in the computer model, based on the Wageningen "B" Series data bank, resulted in the selection of the propeller characteristics summarized in the following

tabulation. Characteristics of the propeller used in the model test and installed on the ship are also listed.

Item	MARAD Series Optimum	Model and Full Scale
Diameter	30.5 ft	31.5 ft
Number of blades	5	6
P/D	0.776	0.614
BAR	0.672	0.599

(2) EHP data are not available from the trial analysis.

(3) Trial speeds did not exceed 16 knots.

A comparison of the predicted EHP values from the MARAD Series computer program and from the model tests indicates that resistance of the MARAD Series is lower for the range of speeds investigated. However, PC is significantly greater for the model than for the MARAD Series. The low value of PC for the series results from the low values of e_h which are inherent characteristics of the MARAD Series hull form. The significant difference in RPM prediction, comparing the trial and model test results with the Series prediction, results from the unusually low values of wake fraction characteristic of the MARAD Series hull form.

The trial and model test SHP curves are essentially parallel. However, at the maximum continuous power level of 45,000 SHP, speed predicted by model test is approximately 0.3 knots higher than measured on trials. The MARAD Series SHP curve is significantly steeper than either the model or trial curves, though the curves intersect at the nominal 16 knot design speed.

As in the case of this example, the Series data and computer model are expected to be used frequently for speed-power predictions of conventional hull forms having the Series parameters. Development of EHP ratio "worm curves" with experience will increase the utility of the Series for this purpose. For the

current example, EHP_{model}/EHP_{MARAD} varies from 1.13 at low speeds to about 1.10 at design speed. Development of such empirical data with experience has been common practice for application of the earlier Taylor and Series 60 data for prediction purposes.

Predictions of Maneuvering Characteristics

Predictions of ship maneuvering performance of the U.S.T. ATLANTIC using the MARAD Series data were carried out in three steps:

(1) Estimation of the nondimensional coefficients and constants used as an input to the maneuvering simulation model.

(2) Limited simulations of the standard definitive maneuvers such as turns, zigzags, and stops.

(3) Analysis and comparison of the simulated results with the available results from the sea trials and from computer predictions based on the model test data analysis.

Estimation of the Hydrodynamic Coefficients - Results of the captive model tests presented in Chapter 6, were used to predict the nondimensional hydrodynamic coefficients for the U.S.T. ATLANTIC ship in surge, sway, and yaw. Three models from the MARAD Series, designated E, G, and K, respectively, have similar values of B/T, L/B, and C_B, as shown in the following tabulation:

Ship/Model	B/T	L/B	C_B
U.S.T. ATLANTIC	3.081	5.073	0.816
Series Ship E	3.000	5.000	0.850
Series Ship G	3.000	5.000	0.800
Series Ship K	3.750	5.000	0.800

Values of L/B ratio are nearly identical and B/T ratio for Ships E, G, and the U.S.T. ATLANTIC are close. For further interpolation, Ship E was selected as the best candidate vessel for the following reasons:

(1) Values of B/T and L/B are close to those of the U.S.T. ATLANTIC. Difference in block coefficients will have relatively minor effects on ship maneuvering coefficients for the full scale vessels.

(2) Testing and analysis for the Ship E hull model was the most comprehensive and is considered very reliable.

Analysis of the test data and maneuvering performance of the MARAD Series carried out in Chapter 6 indicates that in the range of variation of block coefficients from 0.80 to 0.85 the nondimensional hydrodynamic forces depend primarily on the ratio B/T and, to a lesser degree, on the ratio L/T. Variation of C_B for the Series models had only a secondary effect on the hydrodynamic forces.

Corrections to the hull forces due to differences in B/T, L/B, and C_B values were determined using the appropriate charts, figures, and tables in Chapter 6. The values of these corrections were quite small, rarely exceeding five to seven percent of the total value of the coefficient.

Due to the significant differences in the size of the rudder and propeller for both vessels, the corresponding corrections to the terms related to the performance of the rudder and propeller were significant. The values of the U.S.T. ATLANTIC rudder and propeller coefficients are less than the corresponding values for Ship E by an average 20 to 30 percent. A summary of the hydrodynamic maneuvering coefficients for the U.S.T. ATLANTIC is compared with the Ship E coefficients in Table 8-4.

(1) As expected, the values of the hull hydrodynamic linear and nonlinear coefficients, for all three sets are very close. Some of the differences between predictions and model basin measurements can be attributed to differences in curve fitting

procedures which determine the linear and quadratic terms as a function of ship motion parameters. For example, nondimensional values of the total yaw damping moment estimated by predictions from the MARAD Series and measured in the model basin are very close in the practical range of ship rates, $r' = rL/U$, between 0.5 and 0.9. The linear and quadratic yaw damping coefficients, N_r' and $N_{r|r|}'$, respectively, are given in the following tabulation, for the interpolated and model test values:

Data Source	Coefficient, N_r'	Coefficient, $N_{r\|r\|}'$
Prediction from MARAD Series Interpolation	-0.004150	-0.000262
Experiment from PMM Model Tests and Analysis	-0.003682	-0.000690

The values differ significantly due to the different emphasis on the relative contribution of the linear and nonlinear terms defining the total yaw damping force coefficient.

(2) The hydrodynamic forces due to the rudder and propeller were estimated from the MARAD Series data by taking into account the relative dimensions of the rudder and propeller on the U.S.T. ATLANTIC, which are about 25 percent smaller than in MARAD Series models. The resulting predicted and measured values of the rudder forces are very close, hence the proposed procedure seems reasonable.

(3) Resistance and propulsion hydrodynamic forces are determined by the coefficients a_i, b_i, and c_i. Again some of the differences between predicted and measured values of the coefficients could be attributed to the curve fitting technique. In addition, the limiting values of the ship propulsion ratio

value, η, defining four segments of resistance and propulsion terms, differed in the following manner:

- Segments 1 and 2 in the MARAD Series interpolation were defined as:

  Segment 1: $1 \leq \eta \leq \infty$

  Segment 2: $0 \leq \eta \leq 1.0$

- Segments 1, 2, and 3 in the PMM model test data were defined as:

  Segment 1: $2.0 \leq \eta \leq \infty$

  Segment 2: $0.2 \leq \eta \leq 2.0$

  Segment 3: $-1.0 \leq \eta \leq 0.2$

Limits for Segment 4 were similar.

(4) In the PMM model test data, hydrodynamic forces due to variation in the propeller loading are described by the original simplified mathematical model which assumes only the linear dependence of these forces from the propeller revolutions, n, on the ship propulsion ratio, η. Then any force component is expressed by the sum:

$$F = [F]_{\eta=1} + (\eta-1)\,[F_{\eta}]$$

where F corresponds to X, Y, and N components of the rudder and asymmetric forces. The first term corresponds to the coefficient at self propulsion point (η=1) and the second term gives the linear contributions proportional to the η-derivative coefficients. The following values were derived from the PMM model test data:

$Y_{\delta r\eta}' = 0.00442$ $\qquad$ $Y_{\star}'_{\eta} = Y_{\star}' = 0.000045$

$N_{\delta r\eta}' = -0.00230$ $\qquad$ $N_{\star}'_{\eta} = N_{\star}' = -0.000023$

Simulations of the Definitive Maneuvers - Simulations of the standard definitive maneuvers were performed for full-ahead and half-ahead forward speeds. Comparison of the simulated results

obtained from the MARAD Series interpolation with the numerical results based on the model tests shows that both predictions are quite close, with differences no greater than six to ten percent for all simulations. Selected results are given in Tables 8-5 and 8-6.

The ship maneuvering trial data of the U.S.T. ATLANTIC reported in Reference 41 includes the trajectory plots for turns with 35 degree rudder, time history of the rudder and heading angle for 20-20 zigzag and trajectory of the crash stop maneuver from full-ahead speed. These results without correction for wind and speed are shown on Figures 8-2 through 8-5. It should be emphasized that the weather conditions during trials were such that the recorded ship trajectories were strongly influenced by environmental conditions, particularly the wave drift forces. For comparison of the simulated and trial maneuvers, the ship trial trajectories were corrected for the influence of wind and waves using a two step "reverse" simulation procedure. The initial step involved the attempt to simulate the trial record as closely as possible. The actual values of environmental disturbances were determined by an iteration process. In the second step these values were used again in reverse for the specific trial turns. The principal numerical measures of the corrected trial turning maneuver are tabulated in Table 8-5 together with the results of the simulations. The corresponding ship trajectories are shown in Figures 8-6 and 8-7, indicating good agreement between predictions and measurements.

The results of 20-20 zigzag maneuvers are given in Table 8-6 and the time history of the ship heading angle is shown on Figures 8-8 and 8-9. The simulated and measured results are also in close agreement. The results of the simulated crash stop maneuver are shown on Figure 8-9 together with the uncorrected trial measurements. The main characteristics of this maneuver, head reach and time to stop, are in satisfactory agreement with the trial records. The measured value of the side reach, however, is significantly larger than the simulated value, probably due to the influence of wave drift on the vessel,

particularly at the last stages of the maneuver.

Results of the analysis of the simulated and measured maneuvering performance at the U.S.T. ATLANTIC, can be briefly summarized as follows:

(1) The comprehensive ship maneuvering information obtained from the MARAD Series results provides a good basis for predicting ship maneuvering characteristics for hull forms similar to those of the Series. The surge, sway, and yaw hydrodynamic forces acting on a ship hull in a maneuver can be reliably estimated from the results of Chapter 6 by considering the effects of variation of C_B, L/B, and B/T. Predicted values can be used for further simulation studies based on the mathematical model described in Chapter 6.

(2) In the prediction of the rudder and propulsion forces, consideration should be given to the dimensions of the rudder and propeller of the studied ship and the MARAD Series equivalent. It can be reasonably assumed that the basic hydrodynamic interaction between ship hull, rudder, and propeller will be the same for the Series form and the hull form under study.

Although the environmental effects during the U.S.T. ATLANTIC sea trials were significant, results of measured and predicted maneuvers are in reasonably good agreement.

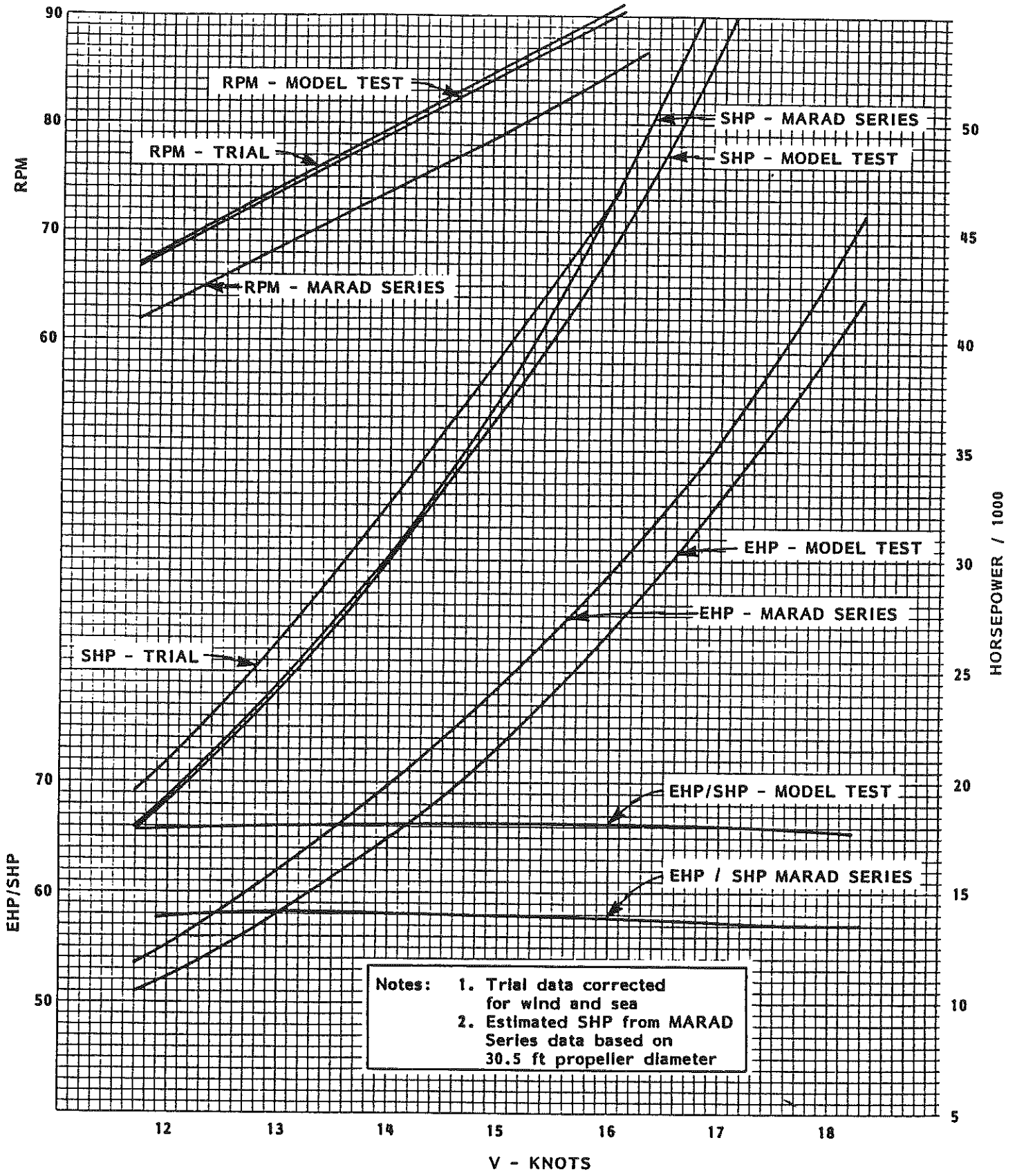

FIGURE 8-1 - COMPARISON OF ESTIMATES AND TRIAL PERFORMANCE
390,000 DWT U.S.T. ATLANTIC

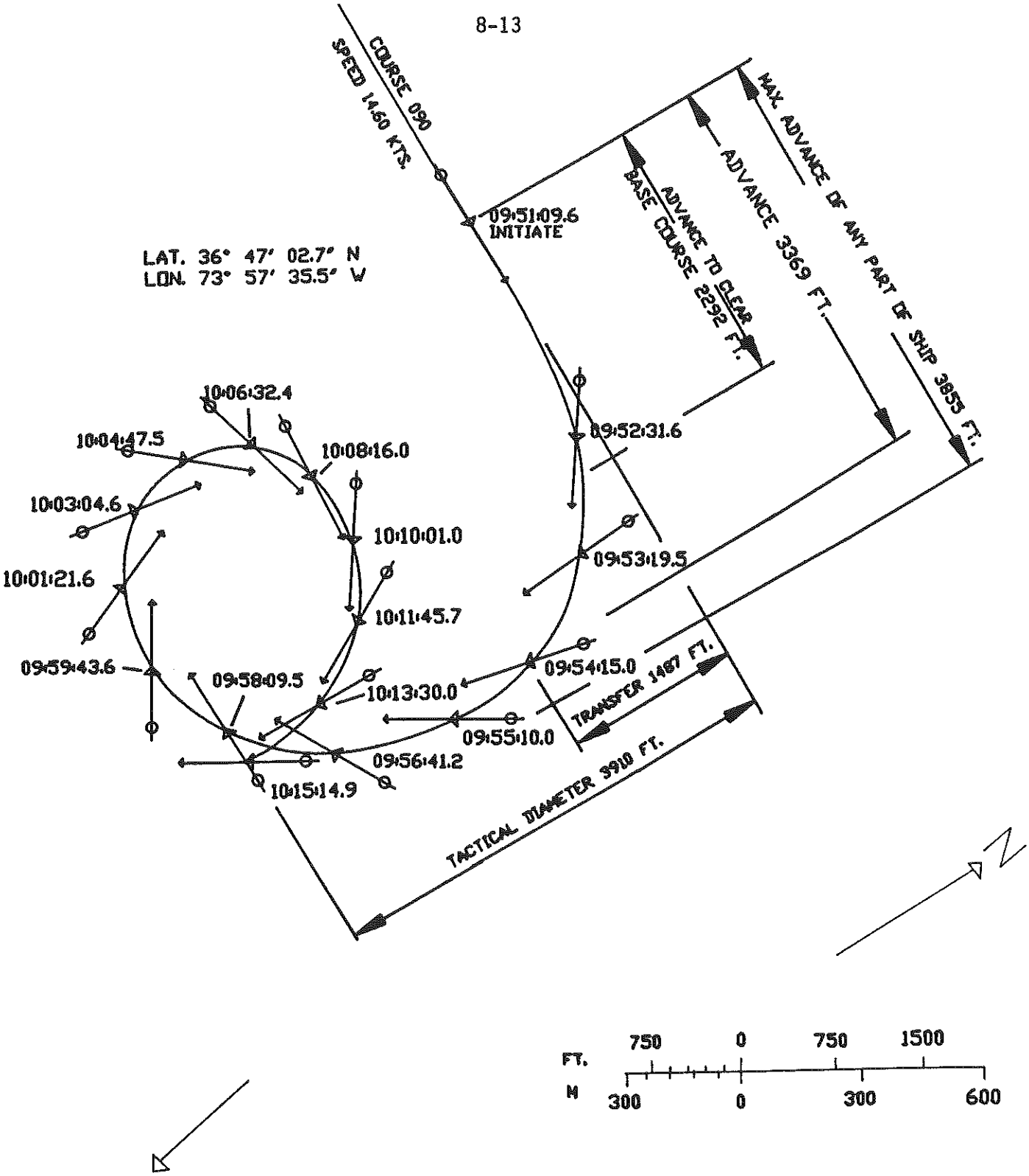

WIND : 12 KTS. FROM 350 (T)

TITLE: RIGHT TURNING CIRCLE
ENGINE: 89 RPM AHEAD
BALLAST: 74 FT. - FULL LOAD
RUDDER: HARD RIGHT (35° RIGHT)
ID: NNSDDCO HULL 613 UST ATLANTIC
DATE: 12 FEB. 79
○-RAYDIST ANTENNA
△-CENTER OF GRAVITY
TELEDYNE HASTINGS - RAYDIST FEB 79
HB-10857 SHEET 1 OF 5

FIGURE 8-2 - VESSEL TRAJECTORY FOR 35° RIGHT RUDDER ANGLE, FULL AHEAD SPEED

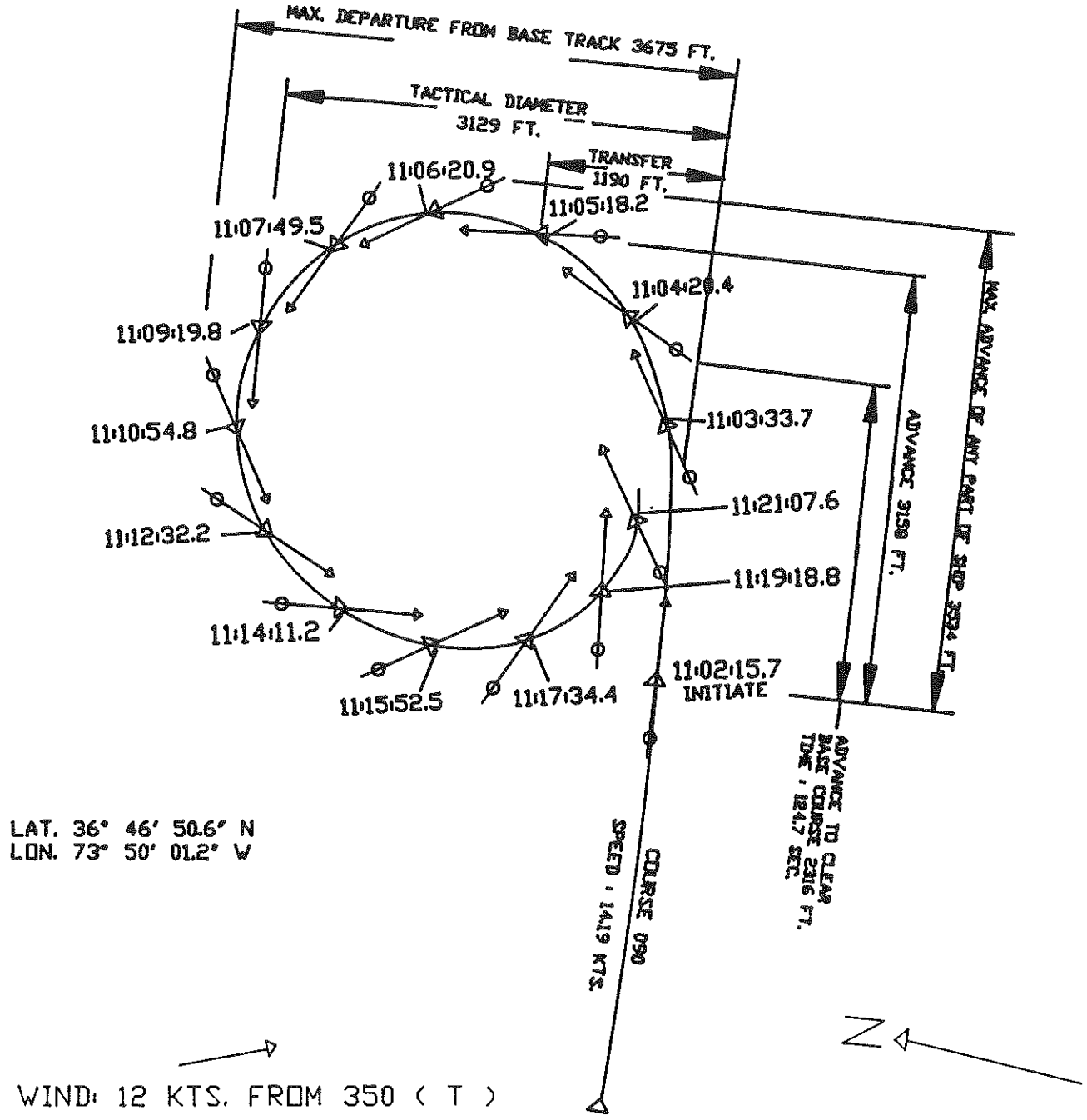

FT. 750 0 750 1500
M 300 0 300 600

TITLE: LEFT TURNING CIRCLE
ENGINE: 89 RPM AHEAD
BALLAST: 74 FT. - FULL LOAD
RUDDER: HARD LEFT (35° LEFT)
ID: NNSDDCD HULL 613 UST ATLANTIC
DATE: 12 FEB. 79
O-RAYDIST ANTENNA
△-CENTER OF GRAVITY
TELEDYNE HASTINGS - RAYDIST FEB 79
HB-10857 SHEET 2 OF 5

FIGURE 8-3 - VESSEL TRAJECTORY FOR 35° LEFT RUDDER ANGLE, FULL AHEAD SPEED

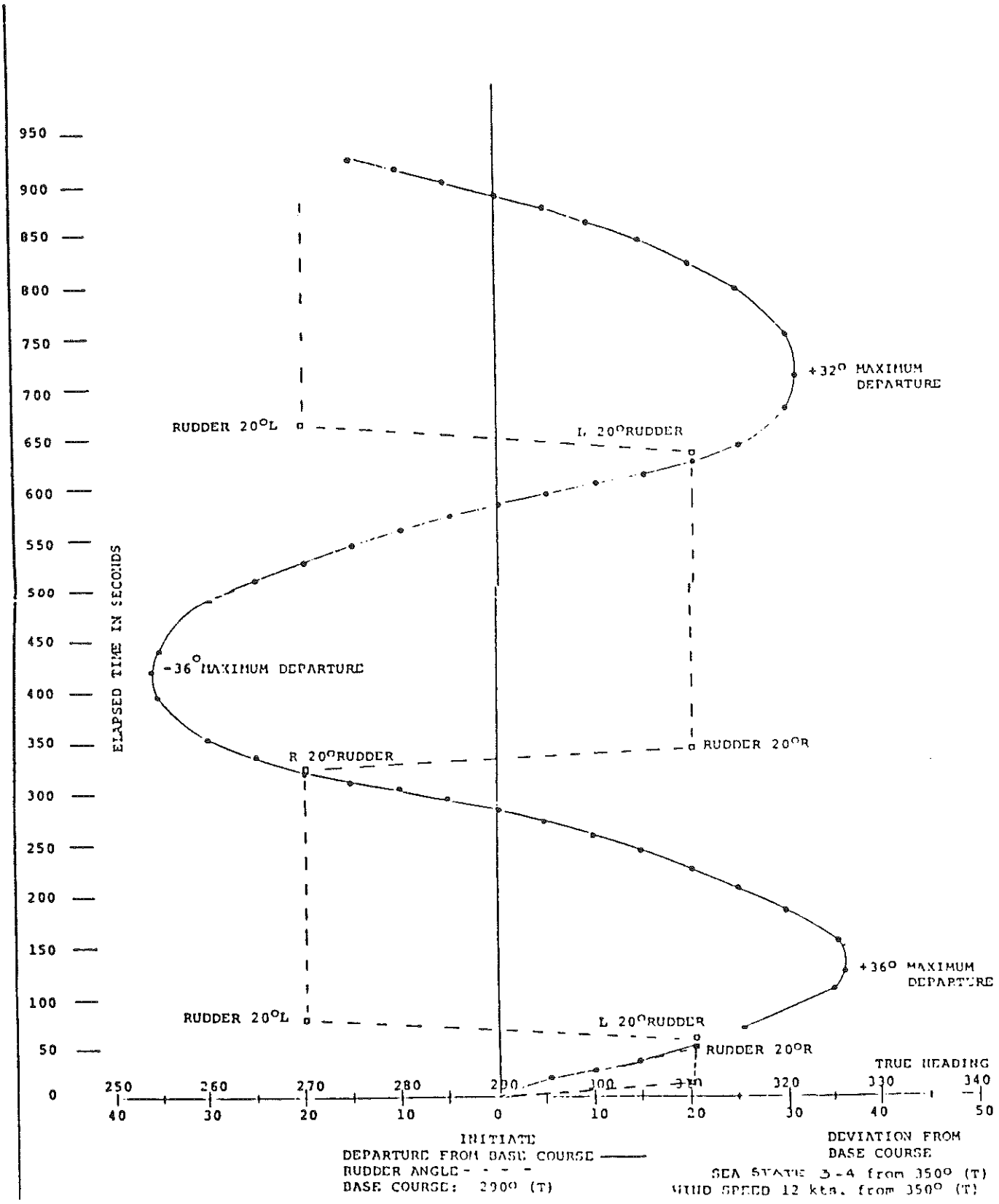

FIGURE 8-4 - 20-20 ZIGZAG MANEUVER, FULL AHEAD SPEED

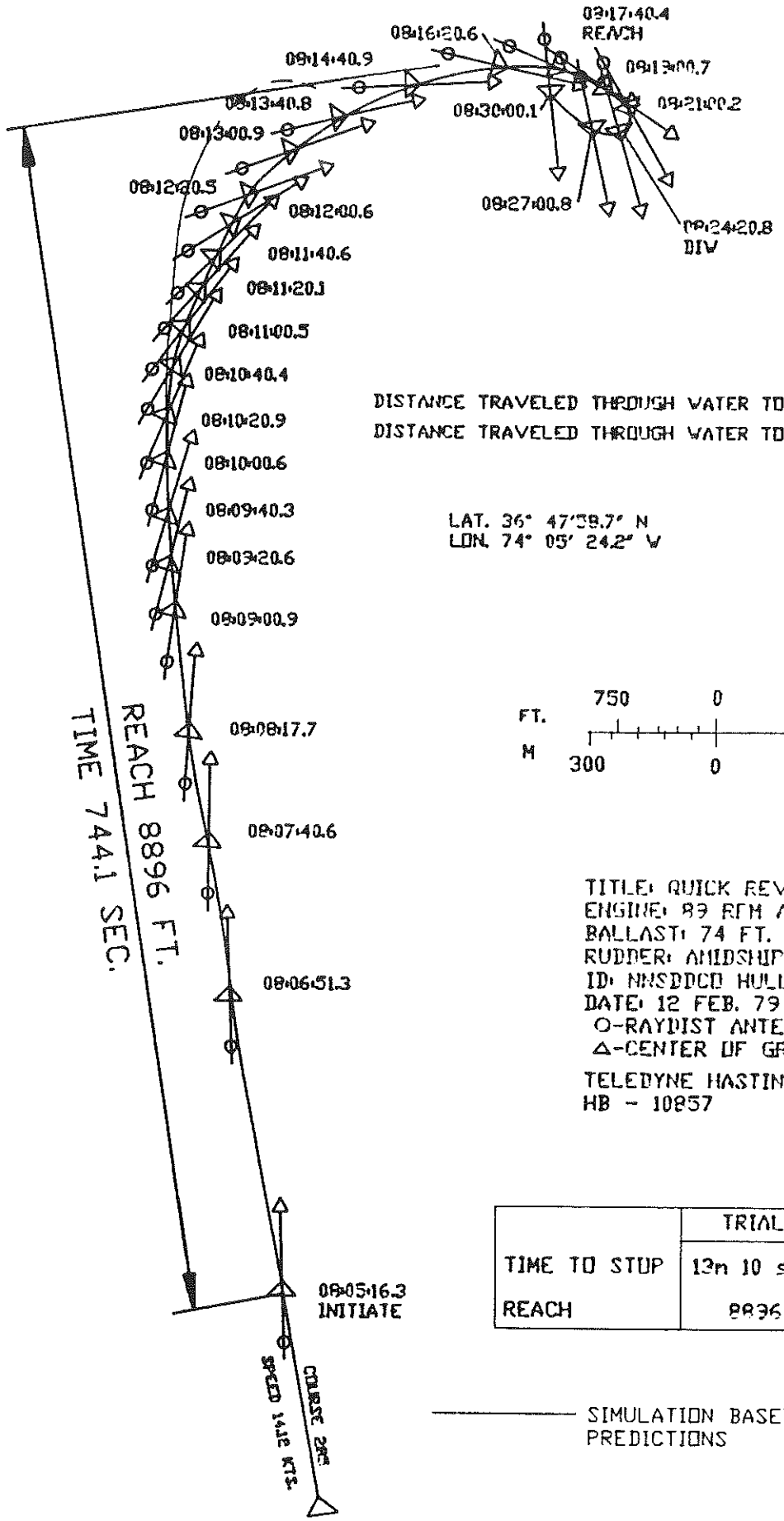

	TRIAL	SIMULATOR
TIME TO STOP	13m 10 sec	14m 15 sec
REACH	8836	8929

——— SIMULATION BASED ON MARAD SERIES PREDICTIONS

FIGURE 8 -5 - VESSEL TRAJECTORY OF CRASH STOP MANEUVER, FROM FULL AHEAD TO FULL ASTERN

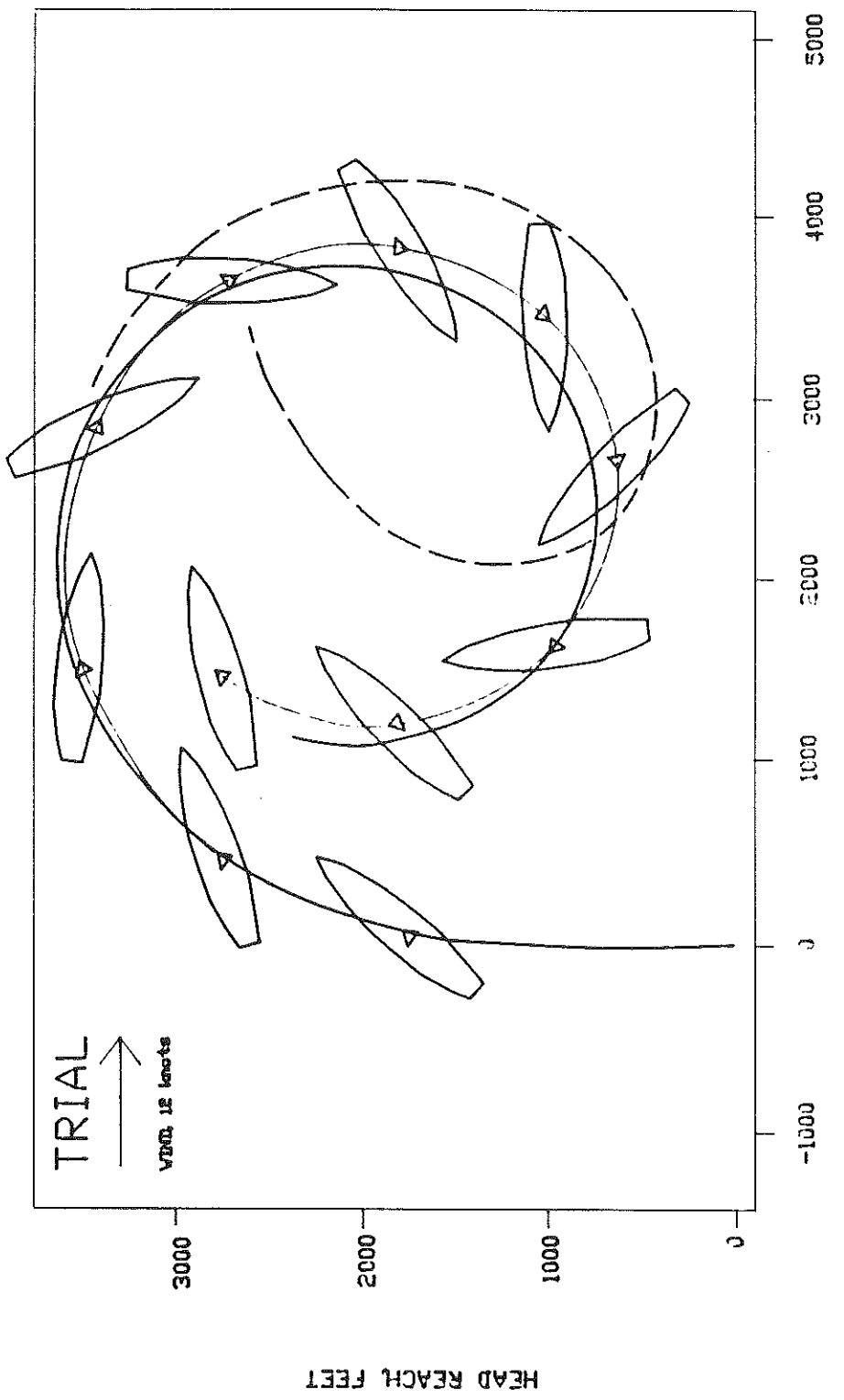

FIGURE 8-6 - PREDICTED AND MEASURED SHIP TRAJECTORIES
FOR 35° RIGHT RUDDER ANGLE, FULL AHEAD SPEED

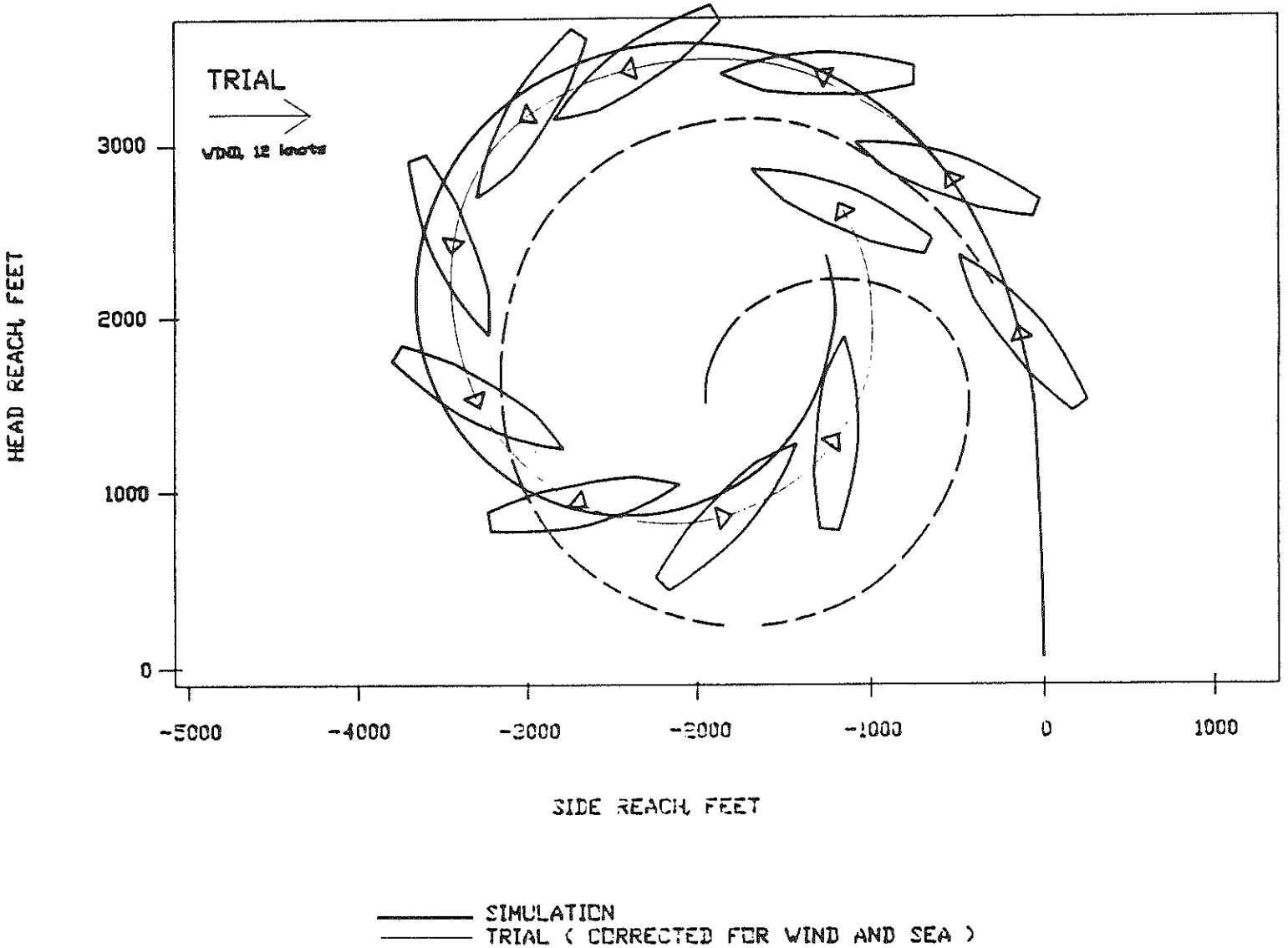

FIGURE 8-7 - PREDICTED AND MEASURED SHIP TRAJECTORIES FOR 35° LEFT RUDDER ANGLE, FULL AHEAD SPEED

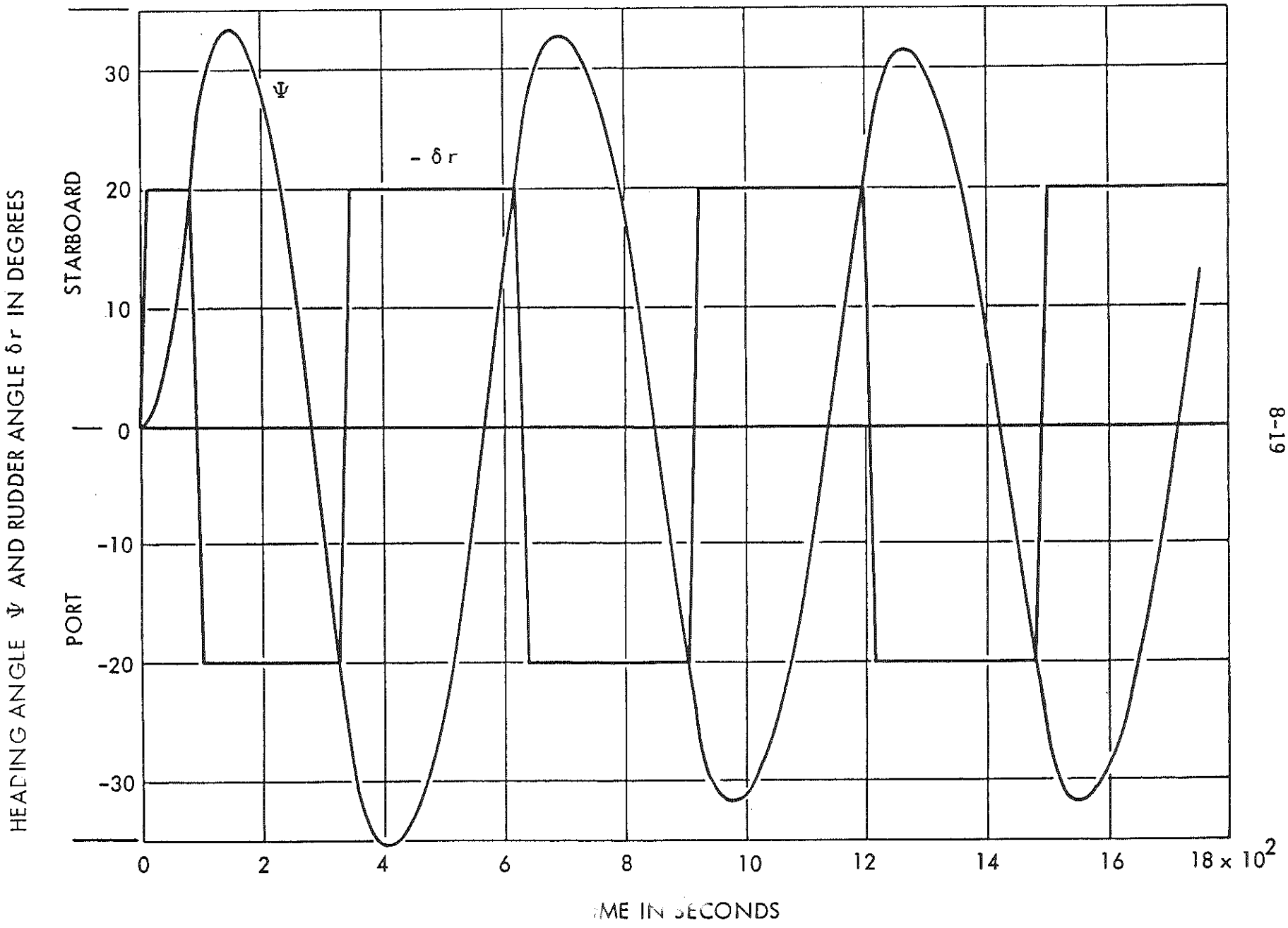

FIGURE 8-8 - SIMULATED PREDICTIONS BASED ON PMM MODEL TESTS

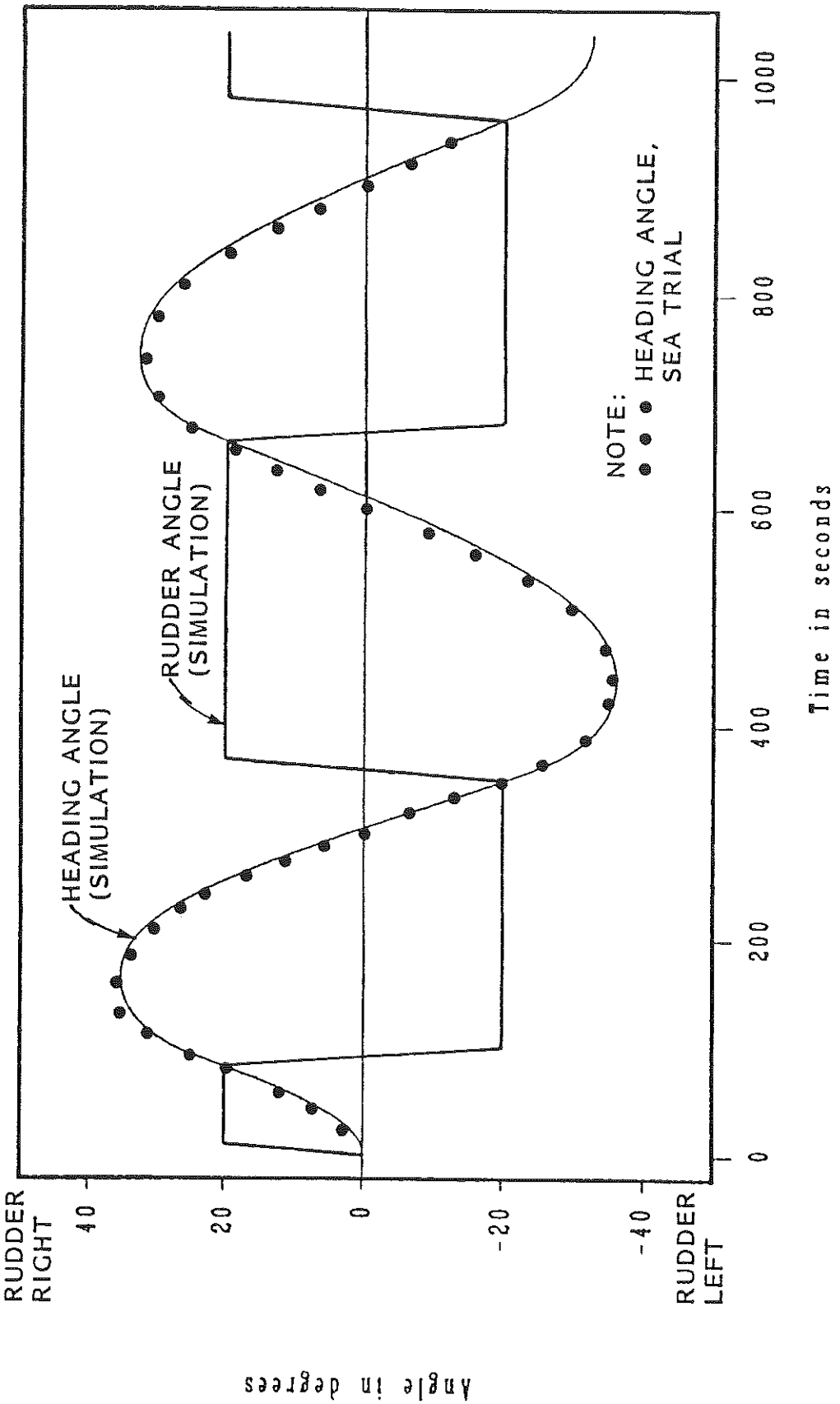

FIGURE 8-9 - 20-20 ZIGZAG MANEUVER - COMPARISON OF PREDICTION AND SEA TRIALS

Table 8-1

Principal Geometric Characteristics of
390,000 DWT U.S.T. ATLANTIC
Full Load Condition

Item	Ship	Model
L, ft	1,143	24.191
B, ft	228	4.825
T, mean, ft	74	1.566
FP	74	1.566
AP	74	1.566
Δ, mld	449,840 tons	4,264 lbs
S, appended, sq. ft.	369,440	165.478
L/B	5.013	5.013
B/T	3.081	3.081
C_B	0.816	0.816
C_p	0.818	
C_{wp}	0.899	
LCB aft of FP, ft	547.5	
% fwd amidships	2.123	2.123

TABLE 8-2

MARAD SERIES

***** PROPULSION SUMMARY - FULL LOAD CONDITION *****

** SHIP CHARACTERISTICS *****

LBP = 1143.00 FT.	DISPL. = 449840. TONS			L/B = 5.013		PROP. DIAM. = 30.50	
BEAM = 228.00 FT.	LCB = 2 PERCENT FWD MIDSHIPS			B/T = 3.081		PITCH/DIAM = 0.776	
DRAFT = 74.00 FT.	CB = 0.8164			CS = 2.805		BAR = 0.672	
W.S. = 376276. SQ. FT.				CIRC-S = 5.990		NO. OF BLADES = 5	
DESIGN SPEED = 16.0 KNOTS							

** SPEED - POWER INFORMATION *****

KNOTS	FN	SLR	CIRC-K	EHP BARE HULL	EHP APP	EHP TOTAL	SHP	P.C.	1-T	1-W	EH	ERR	EP	RPM
11.0	0.0969	0.3254	1.8772	8684.	0.	8684.	15041.	0.577	0.793	0.711	1.115	0.986	0.525	58.3
12.0	0.1057	0.3549	2.0479	11189.	0.	11189.	19349.	0.578	0.793	0.711	1.115	0.986	0.526	63.4
13.0	0.1145	0.3845	2.2186	14128.	0.	14128.	24393.	0.579	0.793	0.711	1.115	0.986	0.527	68.6
14.0	0.1233	0.4141	2.3892	17535.	0.	17535.	30225.	0.580	0.793	0.711	1.115	0.986	0.528	73.7
15.0	0.1322	0.4437	2.5599	21597.	0.	21597.	37288.	0.579	0.793	0.711	1.115	0.986	0.527	79.1
16.0	0.1410	0.4733	2.7305	26798.	0.	26798.	46490.	0.576	0.793	0.711	1.115	0.986	0.524	85.0
17.0	0.1498	0.5028	2.9012	32820.	0.	32820.	57217.	0.574	0.793	0.711	1.115	0.986	0.522	90.9
18.0	0.1586	0.5324	3.0719	39797.	0.	39797.	69725.	0.571	0.793	0.711	1.115	0.986	0.519	96.9

KNOTS	FN	SLR	CIRC-K	REY. NO.	CF X 1000	CA X 1000	CR X 1000	CT X 1000	CIRC-C
11.0	0.0969	0.3254	1.8772	0.1657E+10	1.439	0.000	0.549	1.988	0.474
12.0	0.1057	0.3549	2.0479	0.1807E+10	1.424	0.000	0.549	1.973	0.470
13.0	0.1145	0.3845	2.2186	0.1958E+10	1.411	0.000	0.549	1.960	0.467
14.0	0.1233	0.4141	2.3892	0.2109E+10	1.398	0.000	0.549	1.947	0.464
15.0	0.1322	0.4437	2.5599	0.2259E+10	1.387	0.000	0.563	1.950	0.465
16.0	0.1410	0.4733	2.7305	0.2410E+10	1.376	0.000	0.617	1.994	0.475
17.0	0.1498	0.5028	2.9012	0.2561E+10	1.367	0.000	0.669	2.036	0.485
18.0	0.1586	0.5324	3.0719	0.2711E+10	1.357	0.000	0.722	2.079	0.496

NOTES -
1. SEA WATER AT 59 DEG. F.
2. 1957 ITTC FRICTION LINE
3. PROPELLER CHARACTERISTICS BASED ON 5 BLADED WAGENINGEN B-SCREW SERIES PROPELLER
4. APPENDAGE ALLOWANCE = 0.000 X BARE HULL EHP
5. CORRELATION ALLOWANCE = 0.000000

Table 8-3

Speed-Power Prediction and Trial Comparison

V_K, knots	EHP		SHP			PC		RPM		
	MARAD Series Prediction	Model Test	MARAD Series Prediction	Model Test	Trial	MARAD Series Prediction	Model Test	MARAD Series	Model Test	Trial
12	11,189	12,650	19,349	19,200	21,530	0.578	0.659	63.4	68.3	68.6
13	14,128	15,990	24,393	24,230	26,500	0.583	0.660	68.6	73.7	74.1
14	17,535	19,870	30,225	30,060	32,500	0.580	0.661	73.7	79.3	79.6
15	21,597	24,310	37,288	36,720	39,300	0.579	0.662	79.1	84.7	85.1
16	26,798	29,370	46,490	44,300	46,550	0.576	0.663	85.0	90.0	90.6
17	32,820	35,540	57,217	53,850	--	0.574	0.660	90.9	95.8	--
18	39,797	43,150	69,725	65,780	--	0.571	0.656	96.9	101.7	--

Table 8-4

Nondimensional Hydrodynamic Coefficients
for Ship Maneuvering Simulations
390,000 DWT U.S.T. ATLANTIC

Nondimensional Coefficient	Data Source		
	MARAD Series Ship E	390,000 DWT Model PMM Tests	MARAD Series Data Interpolation
X_u'	-0.00133	-0.001233	-0.00129
X_{vr}'	0.01608	0.01436	0.01559
X_{vv}'	0.00248	0.0	0.00243
$X_{\delta r \delta r}'$	-0.00290	-0.00225	-0.00196
X_{rr}'	0.0	0.0	0.0
$X_{vv\eta}'$	0.00100	0.0	0.00088
a_1	-0.000021	-0.0003199	-0.000250
b_1	-0.002054	-0.0009317	-0.001000
c_1	0.002097	0.0012458	-0.001300
a_2	-0.000838	-0.0006399	-0.000750
b_2	-0.000849	-0.0004412	-0.000350
c_2	0.001687	0.0010811	0.001100
a_3	-0.000838	-0.0007296	-0.000750
b_3	0.001201	0.0003765	0.001200
c_3	-0.000054	-0.0007660	-0.000850
a_4	-0.001291	-0.0007487	-0.000750
b_4	-0.000114	0.0002911	0.001100
c_4	-0.000916	-0.0008314	-0.000850

Table 8-4 - Continued

Nondimensional Coefficient	Data Source		
	MARAD Series Ship E	390,000 DWT Model PMM Tests	MARAD Series Data Interpolation
Y_v'	-0.02017	-0.01915	-0.01956
Y_*'	0.000084	0.000045	0.000080
Y_v'	-0.01506	-0.01554	-0.01487
$Y_{v\|v\|}'$	-0.05340	-0.051745	-0.0535
Y_r'	0.00538	0.005936	0.00530
$Y_{r\|r\|}'$	0.00200	0.00310	0.00191
$Y_{v\|r\|}'$	-0.01630	-0.01630	-0.01610
Y_r'	-0.00035	-0.00040	-0.00034
$Y_{\delta r}'$	0.00545	0.00384	0.00395
$Y_{r\eta}'$	0.00159	0.00126	0.00125
$Y_{v\eta}'$	-0.00316	-0.00192	-0.00229
m'	0.022679	0.021086	0.021086
d, $n \geq 0$	0.280	-	0.280
d, $n < 0$	0.280	-	0.280
e, $n \geq 0$	0.345	-	0.345
e, $n \leq 0$	0.200	-	0.200
f, $n \geq 0$	0.065	-	0.0715
f, $n \leq 0$	-0.001	-	-0.001

Table 8-4 - Concluded

Nondimensional Coefficient	Data Source		
	MARAD Series Ship E	390,000 DWT Model PMM Tests	MARAD Series Data Interpolation
N_r'	-0.00136	-0.001090	-0.001296
N_*'	-0.000044	-0.000023	-0.000042
N_v'	-0.01098	-0.008875	-0.00998
$N_{v\|v\|}'$	0.01327	0.009072	0.01287
N_r'	-0.00430	-0.003682	-0.00415
$N_{r\|r\|}'$	-0.00018	-0.000690	-0.000262
$N_{v\|r\|}'$	-0.00515	-0.00515	-0.00511
N_v'	0.00002	-0.000193	-0.0000185
$N_{\delta r}'$	-0.00286	-0.001992	-0.00200
$N_{v\eta}'$	0.00164	0.000976	0.001190
$N_{r\eta}'$	-0.000854	-0.000659	-0.000650
I_z'	0.001417	0.001017	0.001017
d_* $n \geq 0$	0.0	-	0.0
$n < 0$	0.0	-	0.0
e_* $n \geq 0$	0.450	-	0.275
$n \leq 0$	-0.149	-	-0.110
f_* $n \geq 0$	0.117	-	0.110
$n < 0$	-0.282	-	-0.235

Table 8-5

Comparison of Numerical Measures from Steady Turning Maneuvers for 390,000 DWT U.S.T. ATLANTIC

Data Source	Approach Speed Knots	Rudder Angle, Degrees	Time to Change Heading 90 Degrees, Seconds	Time to Change Heading 180 Degrees, Seconds	Speed at 90 Degrees Heading Change, Knots	Speed at 180 Degrees Heading Change, Knots	Percent Loss of Speed in Steady Turns	Advance, Feet	Transfer, Feet	Tactical Diameter, Feet	Steady Turning Diameter, Feet
Model PMM Tests	16.0	-35	184	426	9.01	4.54	77.3	3447	1517	3628	2774
	16.0	+35	182	420	8.98	4.50	77.5	3395	1474	3521	2678
Full Scale Trial	16.0	-35	-	-	-	-	-	3369	1405	3694	2485
	16.0	+35	-	-	-	-	-	3242	1310	3340	2154
MARAD Series Data	16.0	-35	188	428	8.72	4.99	74.35	3531	1464	3629	2595
	16.0	+35	184	417	8.74	4.86	75.24	3468	1428	3520	2367

Table 8-6

Comparison of Numerical Measures from Zigzag Maneuvers for 390,000 DWT U.S.T. ATLANTIC

Data Source	Approach Speed Knots	Execute Heading Change, Degrees	Rudder Angle, Degrees	First Overshoot						Second Overshoot		
				Time to Reach Execute Heading Change, Seconds	Overshoot Angle, Degrees	Total Heading Change, Degrees	Width of Path Execute, Feet	Overshoot Width of Path, Feet	Total Width of Path, Feet	Time to Reach Execute Heading Change, Seconds	Overshoot Angle, Degrees	Total Heading Change, Degrees
Model PMM Tests	16	20	20	79	13.4	33.4	137	2056	2193	326	15.3	35.3
Full Scale Trial	16	20	20	71	16.0	36.0	-	-	-	291	16.0	36.0
MARAD Series Data	16	20	20	81	15.3	35.3	122	2356	2477	306	16.1	36.1

APPENDIX A
TEST APPARATUS, TESTING TECHNIQUES, AND PROCEDURES

APPENDIX A
TEST APPARATUS, TESTING TECHNIQUES, AND PROCEDURES

The model test program was conducted in the Hydronautics Ship Model Basin (HSMB) located in Laurel, Maryland. Principal characteristics of the HSMB are summarized in the following tabulation:

Length .....418 feet
Width ..... 25 feet
Operating Water
Depth .....0-13 feet
Towing Carriage Speeds
- Main carriage .....0-20 ft/sec
- High speed carriage .....0-30 ft/sec

Wave Maker
- Hydraulically driven, wedge plunger type

Wave Characteristics
- Regular or irregular (Pierson Moskowitz, JONSWAP, or other spectra, as required)
- Heights up to 20 inches
- Lengths up to 50 feet

A beach consisting of a grating fabricated from rectangular steel tubing is installed at one end of the basin to minimize wave reflection from deep water towing tests and waves generated by the wavemaker in seakeeping tests.

Resistance and Propulsion Test Apparatus

The towing system used in the HSMB for resistance and propulsion tests is shown in the schematic diagram of Figure A-1. The resistance or X-gages are 4-inch variable reluctance block gages. Each gage is sensitive to only a single component of force exerted in a direction normal to the flexural face of the cube; interaction effects from other force components are negligible. For ship model resistance and propulsion tests,

X-gages rated for a range of ±50 pounds with a sensitivity of 100 millivolts per pound are typically used.

The measurement system for propulsion tests shown in Figure A-1 consists of a 3/4 horsepower DC motor with gear box which drives the propeller through a transmission dynamometer in direct line with the propeller shaft. Propeller shaft revolutions are measured by a magnetic pulse pickup unit located between the motor and gear box.

The variable reluctance transmission dynamometer used for propulsion tests is designed to measure torque and thrust on a rotating armature shaft without the use of slip rings. This is accomplished by the use of "magnitorque" and "magnithrust" elements that rotate with the dynamometer shaft concentrically within each of two variable reluctance coils fixed to the stationary housing. The transmission dynamometer has a measurement range of ±50 pounds thrust and ±50 inch-pounds torque and is usually operated at sensitivities of 100 millivolts per pound and 50 millivolts per inch-pound, respectively. The same transmission dynamometer installed in a strut-pod system is used for theopen water propeller tests associated with propulsion experiments.

Planar-Motion Mechanism System

The Planar Motion Mechanism (PMM) system used at the time of the deep water test program had the following characteristics:

Sway amplitude	± 2.9 inches
Frequency range	0.085 - 3.0 Hz
Yaw table rotation	± 15 degrees

Prior to conduct of the shallow water PMM tests a new Large Amplitude Planar Motion Mechanism (LAHPMM) system with the following characteristics was installed:

Sway amplitude	± 3.0 feet
Frequency range	0-0.25 Hz
Yaw amplitude	± 30.0 degrees

Captive model tests to determine the dynamic stability and control characteristics in deep water were carried out by means

of the PMM system shown schematically in Figure A-2. The PMM system incorporated in one device a means for experimentally determining all of the hydrodynamic stability coefficients required for the equations of motion of a body moving on the surface in three degrees of freedom, including the three categories of static, rotary, and acceleration coefficients. The basic PMM system, described in detail in References 1 and 2, is a complete system that embraces all mechanical, electrical, and electronic components necessary to perform all functions from model handling to final processing of data preparatory to analysis.

The PMM system adaptor, yaw table, and the rest of the system necessary to produce the motions and to make the force measurements in the horizontal plane is shown in the schematic sketch in Figure A-2b. The resulting forced-motion mechanism had the capability for oscillating large surface ship models in swaying and yawing motions over a continuous range of frequencies.

The same 4-inch variable reluctance block gages used in the resistance test apparatus were also used for the PMM. The gages were installed in the model so that force components were measured with respect to a body axis system with the origin at the model center of gravity (CG). Thus, the Y and X gages sensed the lateral and longitudinal force components, respectively. With the arrangement shown in Figure A-2, the total Y-force exerted on the model was experienced as pure reaction at each of the gimbal centers, i.e., the moment about each of these centers was zero. The reaction Y-forces were measured by block gages Y_1 and Y_2 and the total Y-force equaled the sum. These forces were then resolved with respect to the CG to obtain yawing moment. Because of symmetry, the yawing moment was the difference between Y_1 and Y_2 times the distance from one gimbal center to the CG. The total X-force exerted on the model was also experienced as pure reaction forces at each of the two gimbal centers. The sum of the forces measured by the X_1 and X_2 gages was equal to the

total X-force. Since the reaction X-forces were aligned with the longitudinal axis, there was no contribution to the yawing moment. For standard PMM tests on ship models, the Y-gages were rated for a range of ±500 pounds with a sensitivity of 50 millivolts per pound and the X-gages were rated for a range of ±50 pounds with a sensitivity of 100 millivolts per pound.

The specific apparatus used for the shallow water tests was the Large Amplitude Horizontal Planar Motion Mechanism system, (LAHPMM) described in detail in Reference 38. The LAHPMM system, like its predecessor PMM system, is a complete system which includes all mechanical, electrical, and electronic components necessary to perform all functions associated with PMM testing. A diagram showing the towing arrangement and principal electromechanical components of the overall system is given in Figure A-3.

For the static yaw mode, drift angle settings are made in two degree increments and cover a range of ±30 degrees. For the dynamic modes, the sinusoidal motions are produced by two separate servo-motor drive systems controlled through a signal generator using a single cup sine-cosine potentiometer. Sinusoidal motions can be produced to cover a range of frequencies from about 0.01 to 0.20 Hertz with swaying (single) amplitudes up to 3.0 feet and yawing (single) amplitudes up to 30 degrees. LAHPMM system dynamometry is the same as described for the earlier PMM system.

Resistance Tests

Standard procedures for conducting resistance tests in the HSMB and for reducing the data are in general accordance with the recommendations of the International Towing Tank Conference (ITTC). All tests were conducted with the model equipped with appropriately located turbulence stimulation studs. Selected tests were also made with studs removed to determine if a correction was necessary to account for parasitic drag of the studs exclusive of the turbulence stimulation effect.

The procedures for reducing the resistance test data to nondimensional coefficient form and extrapolating the results to obtain values of effective horsepower, EHP, for the full scale ship are essentially as given in Reference 38. However, an additional step was taken to account for the tank blockage correction and the ITTC 1957 Line was used for the frictional resistance coefficients both in the model and full scale ship ranges. The Hughes tank blockage correction, Reference 12, used at HSMB was the most widely used among the modern formulations and is relatively simple to apply. In the event that a new frictional resistance coefficient formulation and/or tank blockage correction is adopted in the future, the resistance data may be readily converted accordingly.

The Hughes method provides for an effective velocity increase based on the following relationship:

$$\frac{\delta V}{V} = k \frac{m}{1-m-F_{Nh}} \qquad [A1]$$

where: V is the towing carriage speed,
δV is the effective speed increase,
m is the mean area blockage ratio, equal to ∇/LA_T,
∇ is the model displacement volume,
L is the model length,
A_T is the cross-sectional area of the towing tank,
F_{Nh} is the Froude number based on towing tank depth, h, equal to $V/\sqrt{gh}$, and
k is an empirical constant equal to a mean value of 1.7, based on test data reported in Reference 12.

The MARAD Series models have approximately equal maximum section areas at the full load and ballast conditions. Accordingly, the speed corrections to account for tank blockage effects are approximately the same for all models and amount to about 2.7 and 1.5 percent effective increase in speed for the full load and ballast conditions, respectively.

The procedural steps for the reduction of the resistance test data in the model range are as follows:

1) Multiply towing carriage speed for each run by the calculated value of $1 + \delta v/v$ to obtain tabulated values of model resistance in pounds versus effective speed based on tank blockage corrections for each model test condition.

2) Using the corrected data, calculate values of the total resistance coefficient

$$C_{Tm} = \frac{R_T}{\frac{\rho}{2} Sv^2} \qquad [A2]$$

where v is the corrected speed.

3) Calculate model Reynolds number vL/ν using corrected speed and towing tank water temperature to obtain the values of model frictional resistance coefficient, C_{Fm}, for each of the data points from the tables of Reference 12.

4) Calculate values of residuary resistance coefficient, C_R, as follows:

$$C_R = \frac{R_R}{\frac{\rho}{2} Sv^2} = C_T - C_F \qquad [A3]$$

5) Plot values of C_R versus Froude number, $v/\sqrt{gL}$, based on corrected speed and fair the plots to obtain curves such as those presented in Appendix B.

6) Cross-fair values of C_R at equal values of F_N, as functions of pertinent geometric parameters for the series, to obtain the design charts of the type given in Figures 4-4 through 4-16.

7) Calculate values of F_N corresponding to even speeds in knots for the full scale ship and enter the appropriate curve of C_R versus F_N to obtain values of C_R.

8) Calculate Reynolds number for the full scale ship at each selected speed and at standard conditions of salt water of

3.5 percent salinity and 59 degrees F, and obtain values of ship frictional resistance coefficient, C_{Fs}, from the tables of Reference 13.

9) Calculate values of total resistance coefficient for the full scale ship at each speed as follows:

$$C_{Ts} = C_R + C_{Fs} + C_A = \frac{R_{Ts}}{\frac{\rho}{2} Sv^2} \qquad [A4]$$

where C_A is the correlation allowance coefficient, assumed equal to 0.00015 for the 350,000 ton full scale designs.

10) Convert values of C_{Ts} to EHP at each speed using full scale dimensions and sea conditions as follows:

$$EHP = \frac{R_T v}{550} = C_{Ts} \left[\frac{\frac{\rho}{2} SV_k^3}{550} \right] (1.689)^3 \qquad [A5]$$

where V_k is the ship speed in knots.

Propulsion Tests

Standard procedures at the HSMB for conducting propulsion tests are in general accordance with procedures recommended by the ITTC. Two basic methods of conducting propulsion tests were used for each model. The first is the standard method used in the United States for evaluating the propulsion characteristics of specific surface ship designs. The method consists in propelling the model at full scale "ship propulsion point" at each of several speeds covering the design range scaled in accordance with the Froude Law of Similitude. Thus two conditions must be satisfied:

1) The model speed in each case must correspond to the speed of the particular full scale ship of specified dimensions, i.e., at equal F_N.

2) The model propeller rpm at each F_N value must be adjusted so that the delivered thrust overcomes a model

resistance derived from the predicted full scale resistance, i.e., C_T versus F_N for ship and model are equal.

In the current state of the art it is assumed that the wake fractions and thrust deductions for model and full scale are equal when these two conditions are met. Various procedures have been advocated in an attempt to correct for scale effects on the propeller-hull interactions. In the absence of general acceptance, however, none of the proposed corrections were incorporated in the HSMB model test and data reduction procedures.

The second method used is similar to that recommended by the British Towing Tank Panel. Here the model speed is held constant and the model propeller RPM is varied in discrete increments through a range of overloads and underloads with respect to either the model or ship resistance or loading coefficients. This method is particularly advantageous in connection with systematic series studies since it produces generalized data which can be used to predict the propulsion characteristics of any size geometrically similar ship at any service condition that falls within the range of overloads and underloads.

Step by step procedures used in conducting the propulsion tests are given in detail in Appendix D of Reference 1.

The procedures for reducing and analyzing the data derived from the propulsion tests were divided into three stages. First, the measured test values were processed, including application of tares to T and Q, to obtain final model values of v, T, Q, and n. These data were then reduced to nondimensional coefficients and cross-faired against related parameters. Finally, discrete values of the faired coefficients were converted to obtain values of SHP and RPM for various evenly-spaced speeds in knots for the full scale ship of specified dimensions. For systematic series work or where an arbitrary stock propeller is used, the second stage is of most interest and was performed as follows:

1) Values of F_N, J_a, C_{Ti}', PC, 1-t, K_T, and K_Q were calculated directly using the final model values from the propulsion tests, where

$$K_T = \frac{T}{\rho n^2 D^4} \qquad [A6]$$

$$K_Q = \frac{Q}{\rho n^2 D^5} \qquad [A7]$$

2) The values of K_T and K_Q were used with the open water characteristic curves for the same propeller as used in the propulsion tests to obtain the true advance coefficients J_{tT} and J_{tQ}. These, in turn, were used to obtain the Taylor wake fractions for thrust and torque identity, respectively, by the following relationships:

$$1 - w_T = \frac{J_{tT}}{J_a} \qquad [A8]$$

$$1 - w_Q = \frac{J_{tQ}}{J_a} \qquad [A9]$$

3) The values of the propeller open water efficiency, e_p, were also obtained from the propeller characteristic curve at the corresponding values of J_{tT}. Then the hull efficiency, e_h, and relative rotative efficiency, e_{rr}, were obtained from the following relationships:

$$e_h = \frac{1-t}{1-w_T} \qquad [A10]$$

$$e_{rr} = \frac{PC}{e_p\, e_h} \qquad [A11]$$

4) The coefficient data from the overload and underload test (1-t, $1-w_T$, $1-w_Q$, PC, e_h, e_p, and e_{rr}) were plotted as functions of C_{Ti}'. The individual coefficient curves were faired and these curves were then cross-faired until

the relationship given in Equation [A11] was satisfied over the entire range of C_{Ti}' values. The curves of e_p and PC were not presented in the final plots since, for a stock propeller, these curves are arbitrary.

5) For the ship propulsion point type of test, the data were treated similarly but were plotted as a function of F_N. For the case of specific propeller designs, curves of J_a, PC, and e_p were given in the final plots. For the case of a stock propeller, the curves presented for J_a, PC, and e_p were obtained from the propeller series data, for an optimal propeller of the same diameter as the stock propeller.

The faired data of Step 5 can be converted to the dimensional values for the corresponding full scale design as follows:

6) At each value of F_N corresponding to a number of even ship speeds in knots, read the values of PC and J_a. At the same speeds read the predicted values of EHP previously obtained and tabulated, with an allowance included for the EHP added by the rudder. Then,

$$SHP = \frac{EHP}{PC} \qquad [A12]$$

and,

$$RPM = 101.33 \frac{V_k}{J_a D} \qquad [A13]$$

where V_K is the ship speed in knots and

D is the diameter of the ship propeller in feet.

Planar Motion Mechanism Tests

Standard procedures developed at HSMB for conducting PMM tests with large surface ship models generally follow the ITTC recommendations given in References 18, 19, and 22. In all such tests, the model has freedom in pitch and heave but is restrained in all other degrees of freedom. The model propeller is operated at the ship point of propulsion for all reference tests and the force and moment data are taken with respect to a body-axis

system with the origin at the ship longitudinal center of gravity. The principles of operation, the general test procedures to be followed, and the data reduction methods are reviewed briefly in the following paragraphs. Detailed discussion is included in References 1 and 2.

Three basic types of tests were conducted with the PMM to obtain all of the hydrodynamic coefficients or derivatives necessary to make an analysis of the directional stability characteristics of a specific ship. These are called static (steady-state), pure swaying, and pure yawing tests. The modes of motion associated with each of these types of tests are shown schematically in Figure A-4 and are accomplished as follows:

Static tests - The model was towed at constant velocity so that its center of gravity moved in a straight path with discrete settings of yaw angle held constant for each run. The yaw angles were set remotely by means of the yaw bridge installed on the towing carriage, Figure A-2. For a completely appended model, the static stability tests were conducted with rudder fixed on center and with the model propeller RPM set at the ship propulsion point for zero drift angle and zero rudder angle. For large full-form surface ship models, the Y_1, Y_2, X_1, and X_2 force components sensed by the block gages during each run were recorded after a 30 second integration period. A waiting period of 10 minutes was usually allowed between each run.

Pure sway tests - While being towed at constant velocity, the model was oscillated in the lateral direction so that the centerline remained parallel to the direction of motion of the towing carriage while the center of gravity moved in a sinusoidal path. The desired forced motion was produced by oscillating the two model support points in phase. The tests were conducted with propeller RPM at the ship propulsion point and with the rudder fixed at zero degrees. The range of oscillation frequencies was kept below 0.3 cycles per second to avoid tank resonant standing wave effects. Each run was made with both carriage speed and oscillation frequency held constant while measurements were

taken. The force component separator system of the PMM instrumentation was used to directly resolve the periodic Y_1 and Y_2 forces sensed by the block gages into in-phase and quadrature force components. Integrations were made over a discrete number of cycles. Usually, for large surface ship models, integrations are made for one complete cycle at a time because of the low oscillation frequencies involved. A typical run includes a one-cycle integration in normal mode to simultaneously obtain both the in-phase and quadrature readings on the Y_1 and Y_2 gages followed by another one-cycle simultaneous integration in "reverse" mode (gage-signal polarity reversed) and subsequent recording of readings. The normal and reversed readings are combined to obtain the desired in-phase and quadrature force components.

Pure yawing tests - While being towed at constant velocity the model was oscillated so that its longitudinal centerline always remained tangent to the path described by its center of gravity. The desired forced motion was produced by oscillating the two model support points with a predetermined phase angle between them obtained by setting the phase-changer of the PMM according to the following relationship:

$$\cos \phi_s = \frac{1 - \left(\frac{\omega x}{U}\right)^2}{1 + \left(\frac{\omega x}{U}\right)^2}$$

where

ϕ_s is the phase angle between support points,

ω is the frequency of oscillation,

x is the distance of each gimbal point from the model center of gravity, and

U is the forward speed of the model.

The remaining procedures for conducting the pure yawing tests and processing the data are essentially the same as described for the pure swaying tests.

In addition to conducting the basic PMM tests for inherent (controls fixed) directional stabilility analyses, PMM tests were performed to provide a complete set of hydrodynamic coefficents for the equations of motion in three degrees of freedom, to establish the mathematical models needed to perform computer simulation studies of full scale ships. These tests are usually performed concurrently with the basic PMM tests and cover a wide range of kinematic variables to provide all of the hydrodynamic stability and control coefficients, including the nonlinear and coupling coefficients, to simulate the various calm water maneuvers within the capability of the given ship. The tests are predominantly of the steady state variety and usually include discrete variations over the entire range of rudder angles (δr = -5.0 to +40 degrees) for each of several drift angles ranging up to 15 degrees with propeller at ship-propulsion point (η = 1.0) and overload and underload tests (η between -1.0 and 2.0) for selected values of δr and β.

Standard methods are applied to reduce the data obtained from PMM tests to nondimensional coefficients and derivatives for subsequent use in stability and control analyses and computer simulation studies. The stability and control derivatives used for analyses based on linearized equations of motion are obtained as follows:

The values for the nondimensional static derivatives Y_v', N_v', $Y_{\delta r}'$, and $N_{\delta r}'$ are taken from the slopes through zero of the appropriate faired curves of Y', N' versus β and δr, respectively, such as those presented in Appendix C. In general, the derivative is based on the average slope over at least ± 4 degrees of either β or δr. All angular measurements are in radians.

The values of the rotary and acceleration derivatives are derived by substituting into the values from the graphs of the in-phase and quadrature force components, obtained as the result of the pure swaying and pure yawing test reduction equations given in Table A-1.

The foregoing stability derivatives can be used to obtain the nondimensional directional stability indices σ_{1h}' and σ_{2h}' by solving for the roots of the quadratic characteristic equation

$$A\sigma^2 + B\sigma + C = 0 \qquad [A14]$$

where

$$A = (Y_{\dot{v}}' - m')(N_{\dot{r}}' - I_z') - Y_{\dot{r}}' Y_{\dot{r}}' N_{\dot{v}}'$$

$$B = Y_v'(N_{\dot{r}}' - I_z') + N_r'(Y_{\dot{v}}' - m) - N_{\dot{v}}'(Y_{\dot{r}}' - m') - Y_{\dot{r}}' N_v'$$

$$C = Y_v' N_r' - N_v'(Y_r' - m')$$

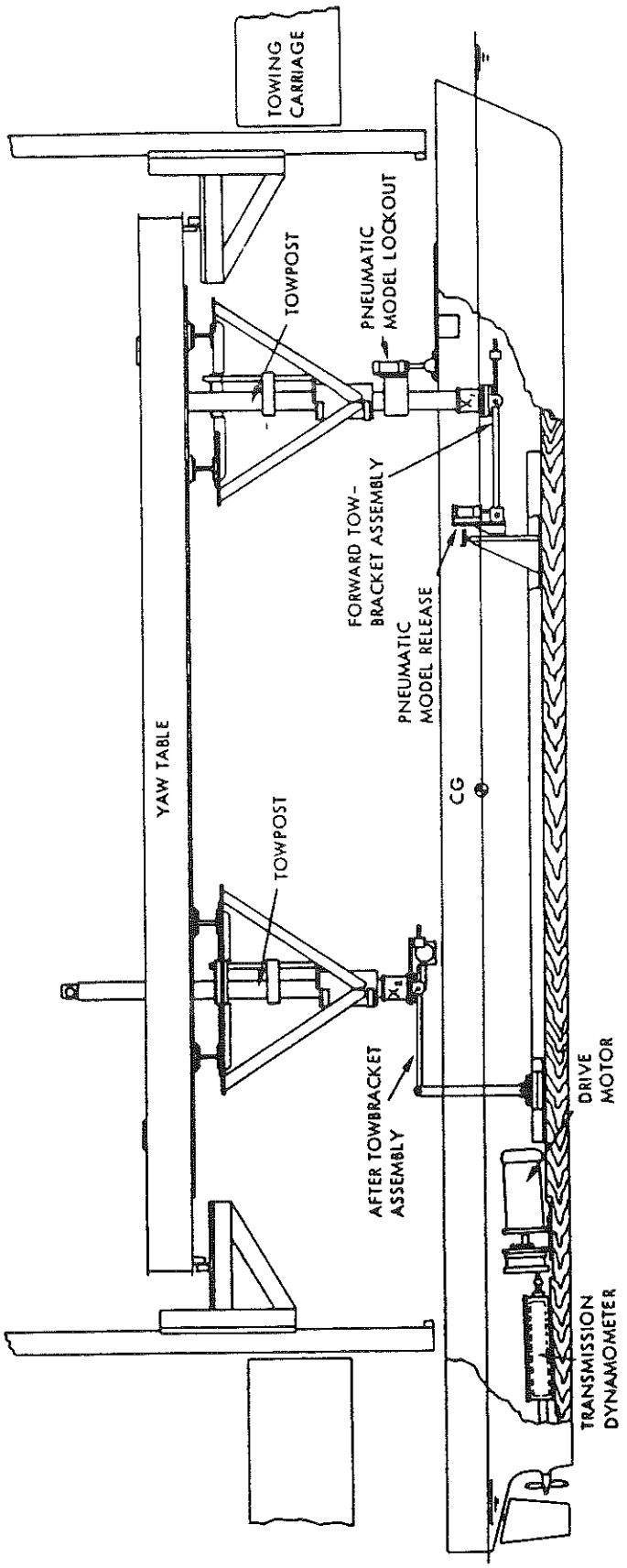

FIGURE A-1 - SCHEMATIC OF TOWING SYSTEM AND DYNAMOMETRY USED FOR RESISTANCE AND PROPULSION TESTS

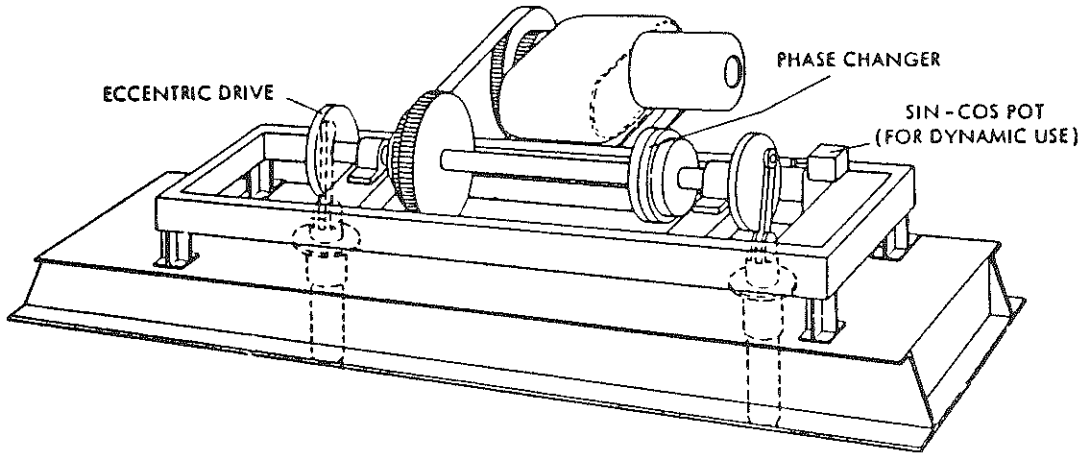

(a) ISOMETRIC OF FORCED MOTION MECHANISM

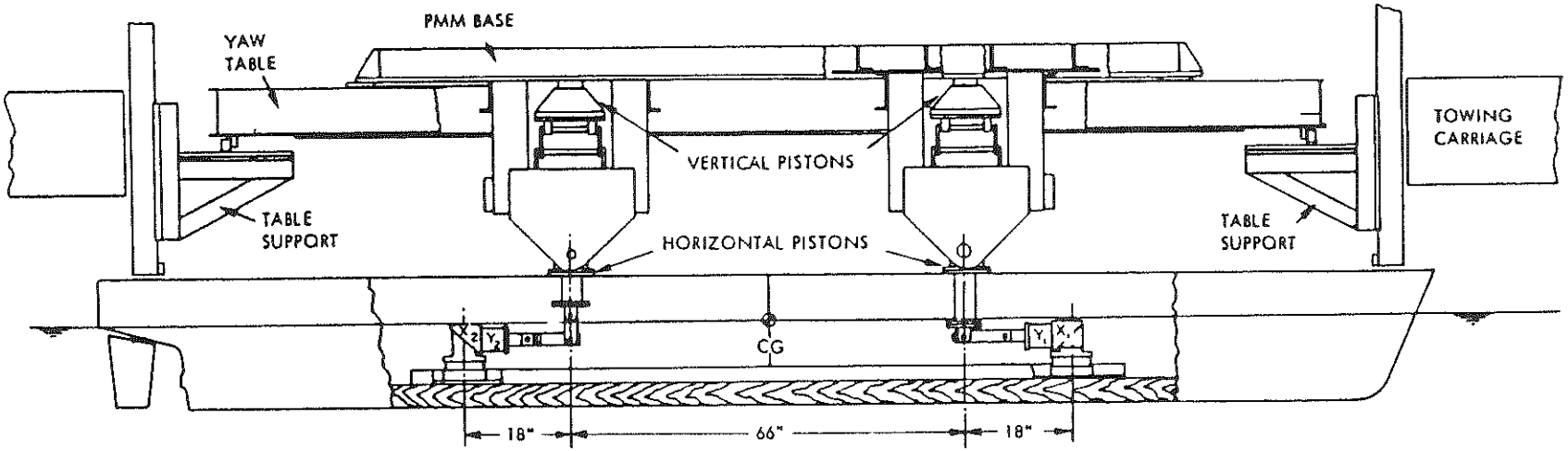

(b) HORIZONTAL ADAPTORS AND MODEL SUPPORT

FIGURE A-2 - SCHEMATIC OF HORIZONTAL PLANAR MOTION MECHANISM USED FOR SURFACE SHIPS

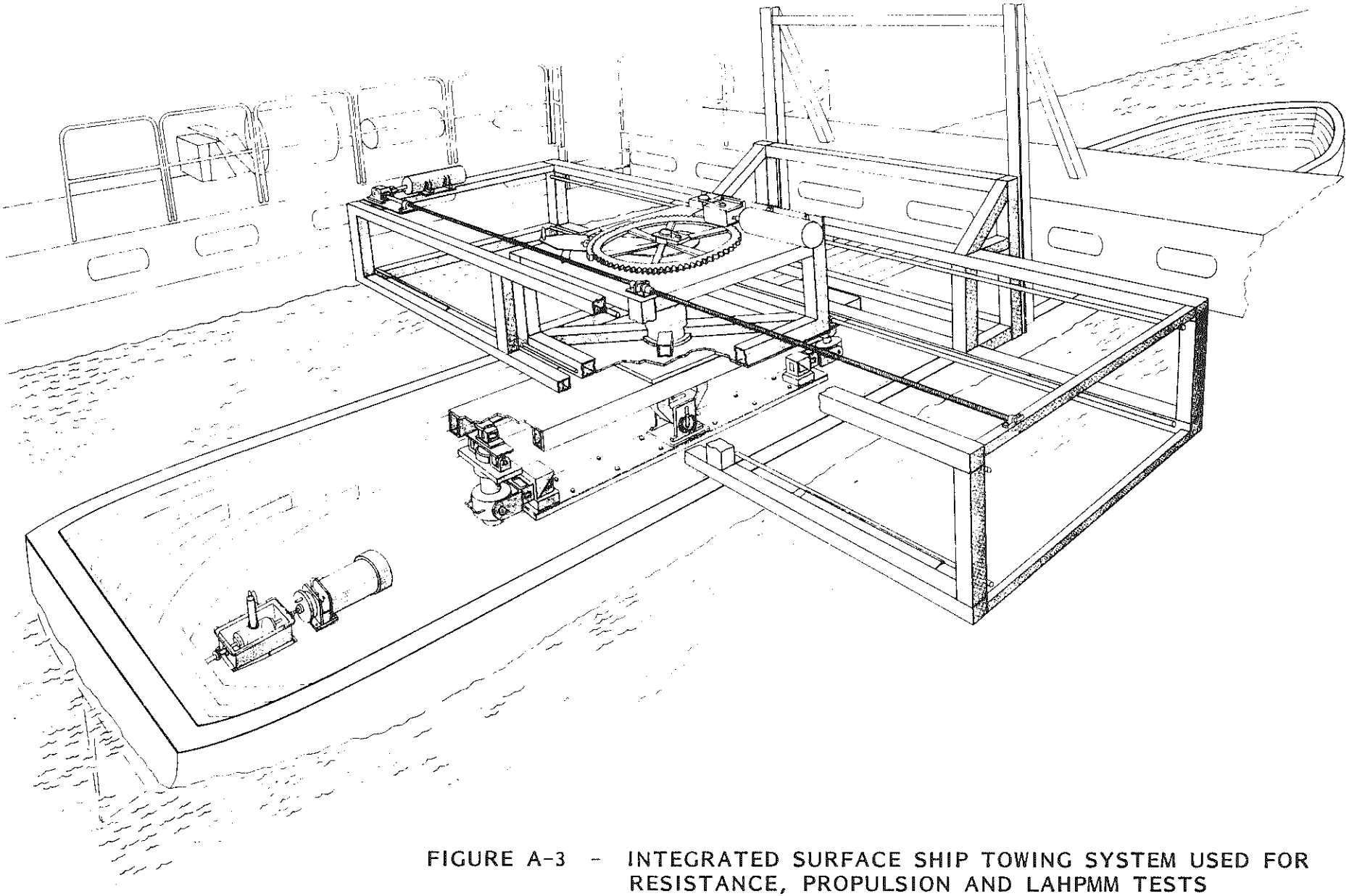

FIGURE A-3 - INTEGRATED SURFACE SHIP TOWING SYSTEM USED FOR RESISTANCE, PROPULSION AND LAHPMM TESTS

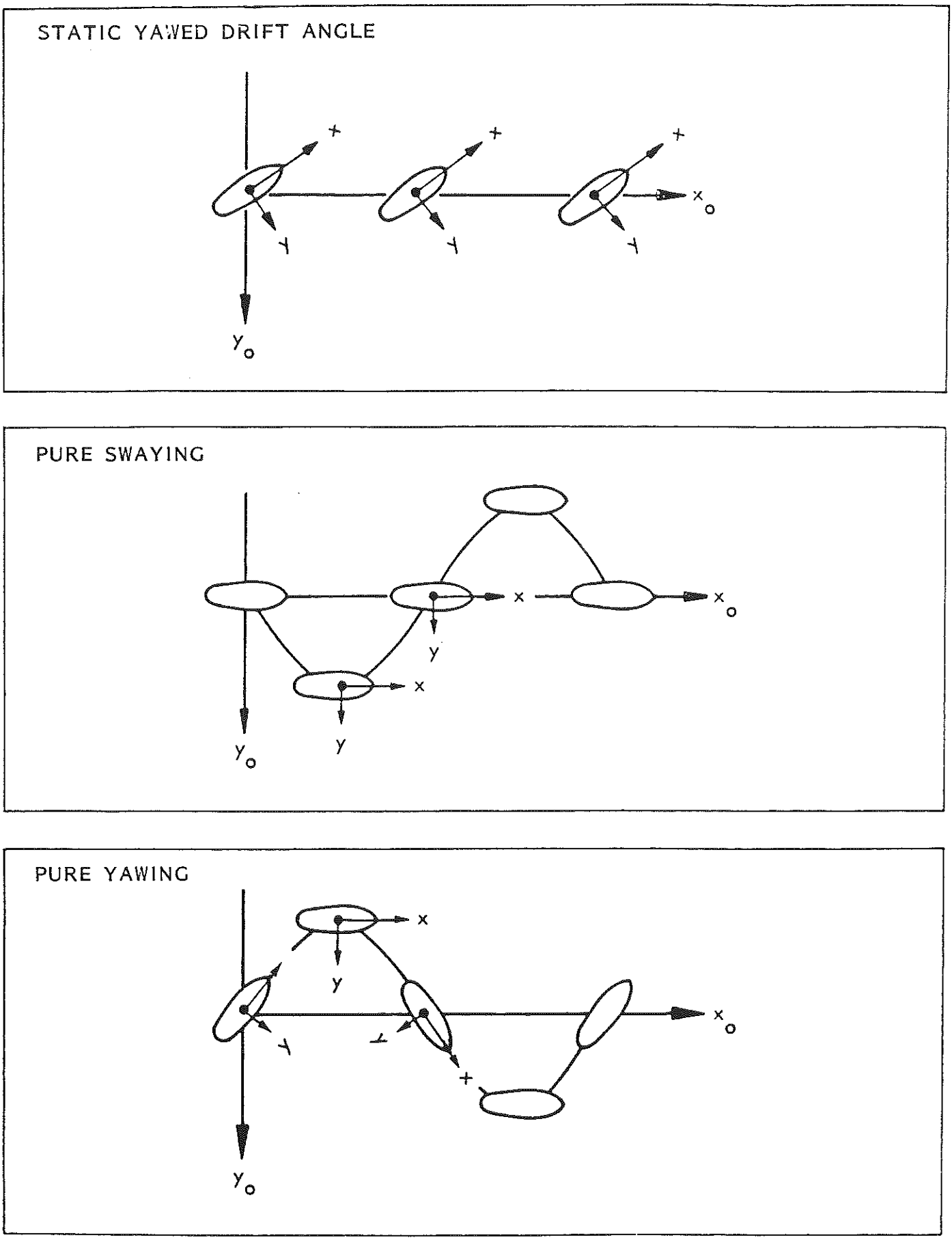

FIGURE A-4 - HORIZONTAL PMM MODES OF MOTION FOR SURFACE SHIP MODEL TESTS

TABLE A-1
Reduction Equations for Horizontal Plane Rotary and Acceleration Derivatives

Derivative	
$Y_{\dot{v}}' - m_m'$	$\frac{\partial[(Y_1')_{in} + (Y_2')_{in}]}{\partial \dot{v}_o'}$
$N_{\dot{v}}' - x_{CG}'m_m'$	$\frac{x}{L}\frac{\partial[(Y_1')_{in} - (Y_2')_{in}]}{\partial \dot{v}_o'}$
$Y_r' - m_m'$	$\frac{\partial[(Y_1')_{out} + (Y_2')_{out}]}{\partial r_o'}$
$N_r' - x_{CG}'m_m'$	$\frac{x}{L}\frac{\partial[(Y_1')_{out} - (Y_2')_{out}]}{\partial \dot{r}_o'}$
$Y_{\dot{r}}' - x_{CG}'m_m'$	$\frac{\partial[(Y_1')_{in} + (Y_2')_{in}]}{\partial \dot{r}_o'}$
$N_{\dot{r}}' - I_{zm}'$	$\frac{x}{L}\frac{\partial[(Y_1')_{in} - (Y_2')_{in}]}{\partial \dot{r}_o'} + \frac{(N_\psi)_m}{\frac{1}{2}\rho L^5 \omega^2}$

APPENDIX B
RESIDUARY RESISTANCE COEFFICIENT CURVES
FOR INDIVIDUAL SERIES SHIPS

APPENDIX B
RESIDUARY RESISTANCE COEFFICIENT CURVES
FOR INDIVIDUAL SERIES SHIPS

350,000 Ton Displacement

NOTES:

(1) The values of C_R in this appendix are based on the use of the 1957 ITTC Friction Line. A Hughes tank blockage correction has been applied to the model resistance versus speed measurements.

(2) Data points for Model A in the full load condition are not available.

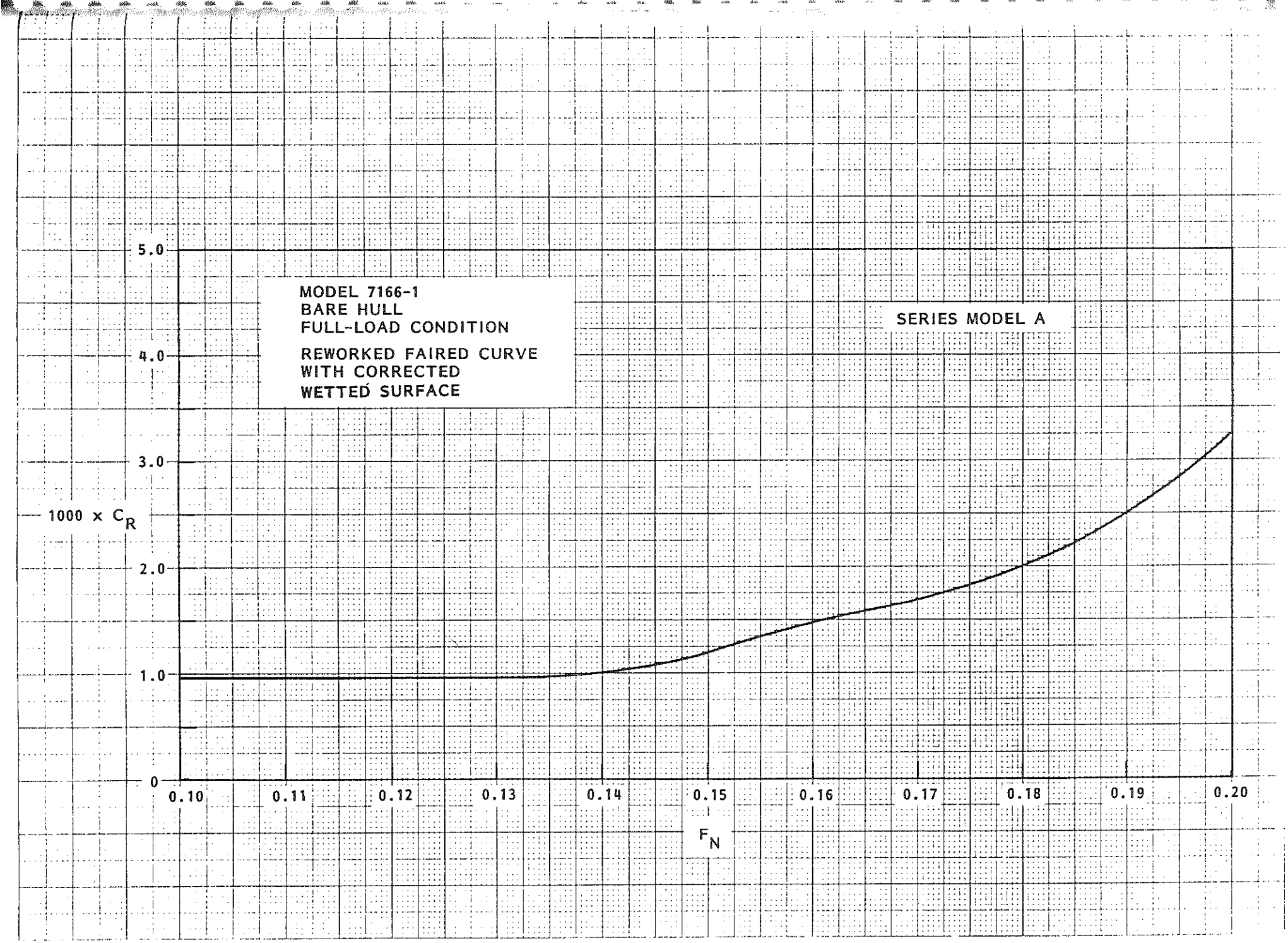
MODEL 7166-1
BARE HULL
FULL-LOAD CONDITION
REWORKED FAIRED CURVE
WITH CORRECTED
WETTED SURFACE
SERIES MODEL A
1000 x C_R
5.0
4.0
3.0
2.0
1.0
0
0.10
0.11
0.12
0.13
0.14
0.15
0.16
0.17
0.18
0.19
0.20
F_N

HYDRONAUTICS, INCORPORATED DATE 5 12 24
MODEL NO. 2166 - 2 TESTED 2 FEB 1973 FULL LOAD
APPENDAGES BARE HULL

SPEED IN KNOTS

11.0 12.0 13.0 14.0 15.0 16.0 17.0 18.0 19.0 20.0 21.0 22.0 23.0

MODEL DATA CORRECTED FOR BLOCKAGE

SERIES MODEL B

1000 C_R

6.00
5.00
4.00
3.00
2.00
1.00
0.00

0.10 0.11 0.12 0.13 0.14 0.15 0.16 0.17 0.18 0.19 0.20

F_N

HYDRONAUTICS, INCORPORATED DATE 5 12 24
MODEL NO. 2166 - 8 TESTED 5 FEB 1923 FULL LOAD
APPENDAGES BARE HULL

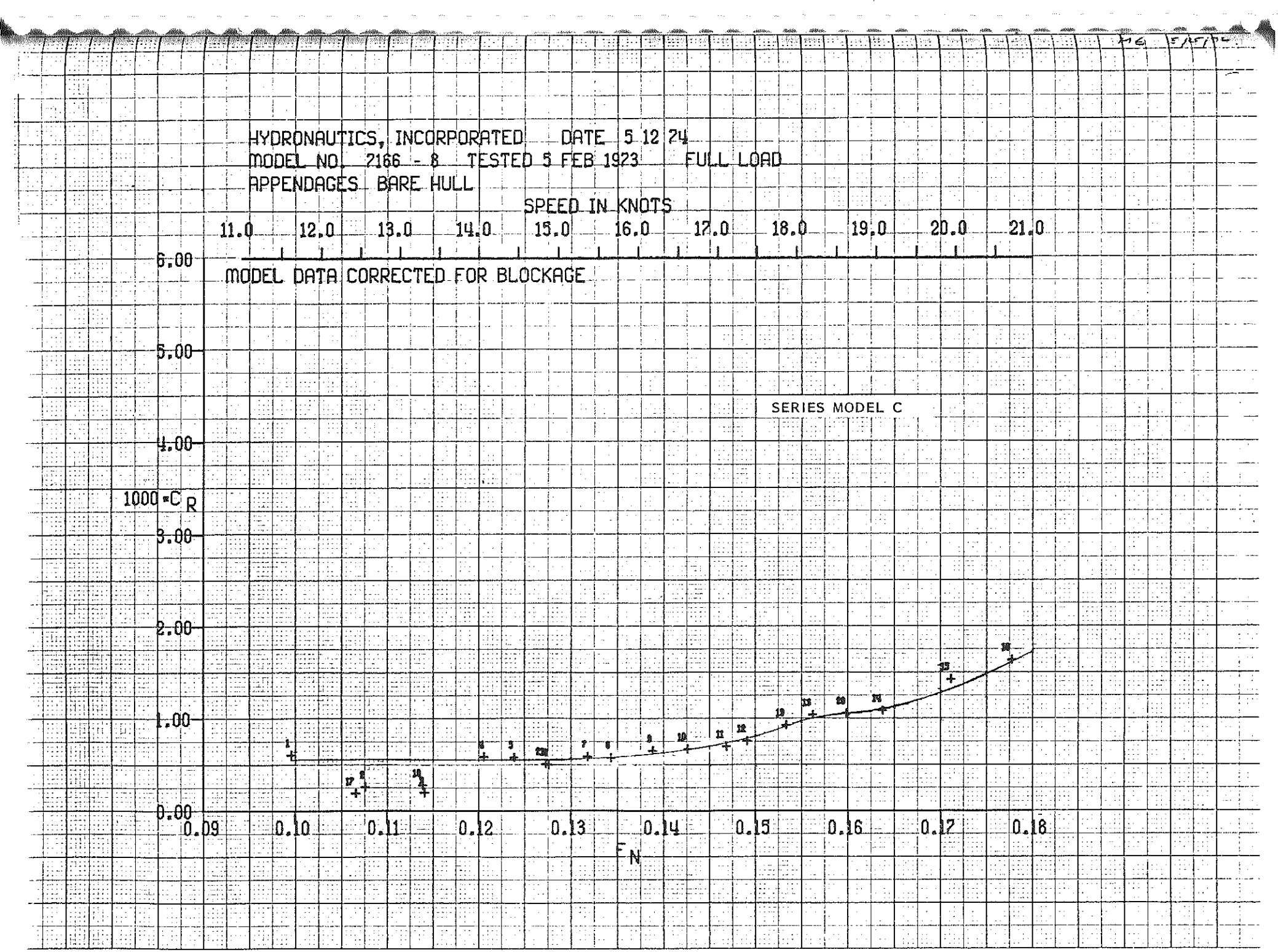

HYDRONAUTICS, INCORPORATED DATE 3 26 24
MODEL NO. 2166-4 TESTED 6 OCT 72 FULL LOAD
APPENDAGES NONE CORRECTED WETTED SURFACE

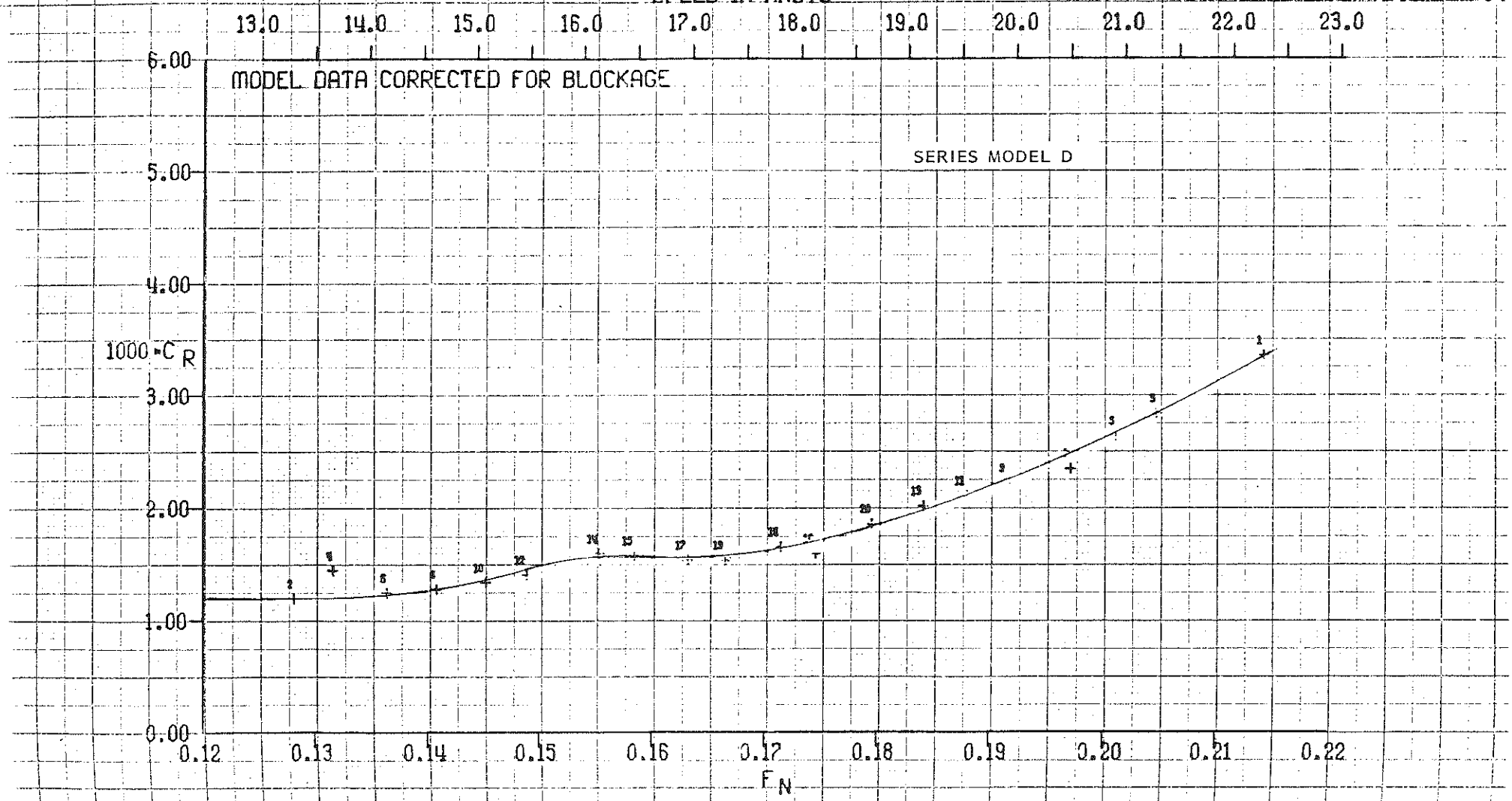

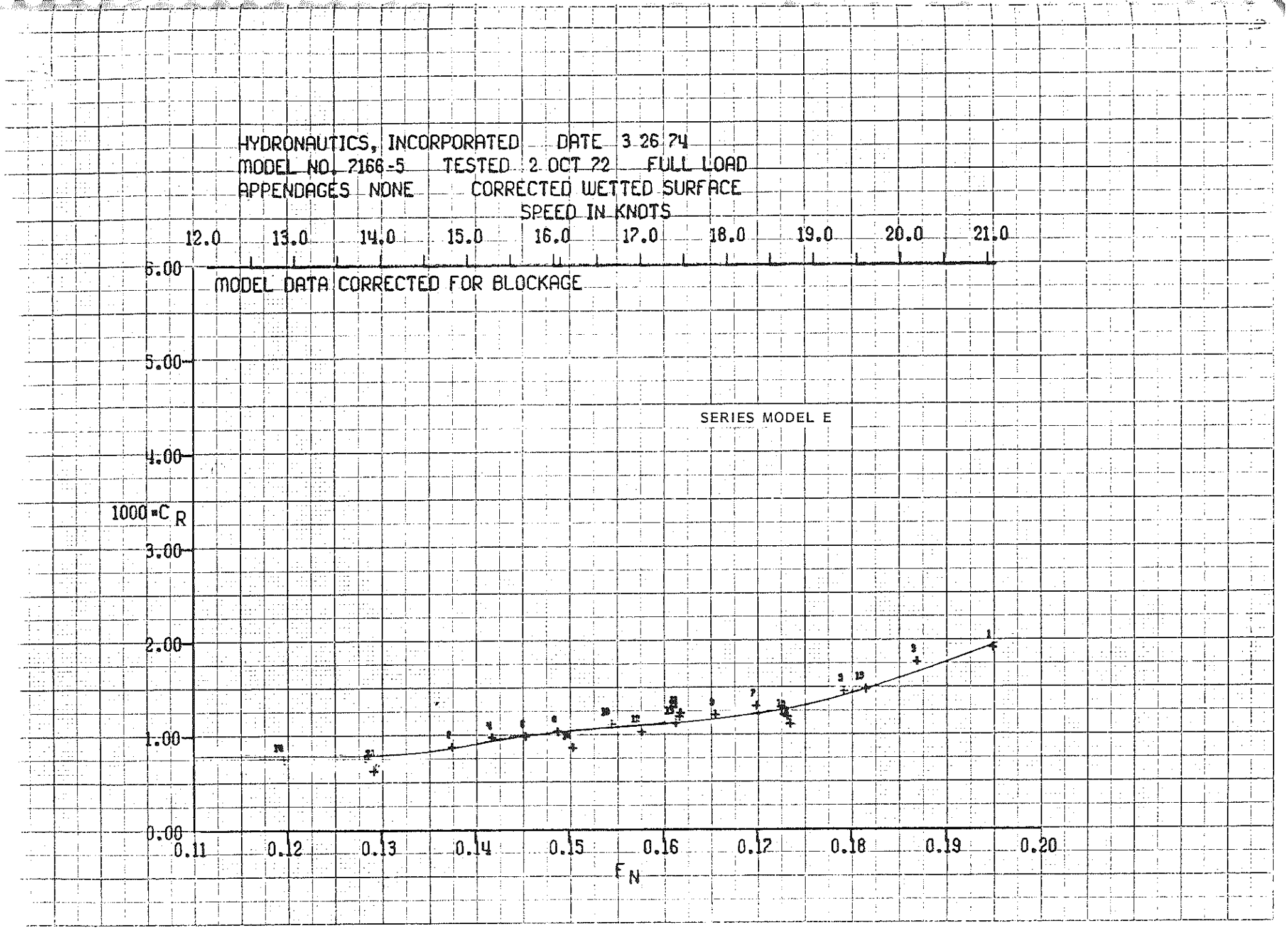
HYDRONAUTICS, INCORPORATED DATE 3 26 74
MODEL NO. 7166-5 TESTED 2 OCT 72 FULL LOAD
APPENDAGES NONE CORRECTED WETTED SURFACE
SPEED IN KNOTS
12.0
13.0
14.0
15.0
16.0
17.0
18.0
19.0
20.0
21.0
6.00
MODEL DATA CORRECTED FOR BLOCKAGE
5.00
SERIES MODEL E
4.00
1000 •C R
3.00
2.00
1.00
0.00
0.11
0.12
0.13
0.14
0.15
0.16
0.17
0.18
0.19
0.20
F N

HYDRONAUTICS, INCORPORATED DATE 3 26 24
MODEL NO. 2168-6 TESTED 15 SEP 24 FULL LOAD
APPENDAGES NONE CORRECTED WETTED SURFACE

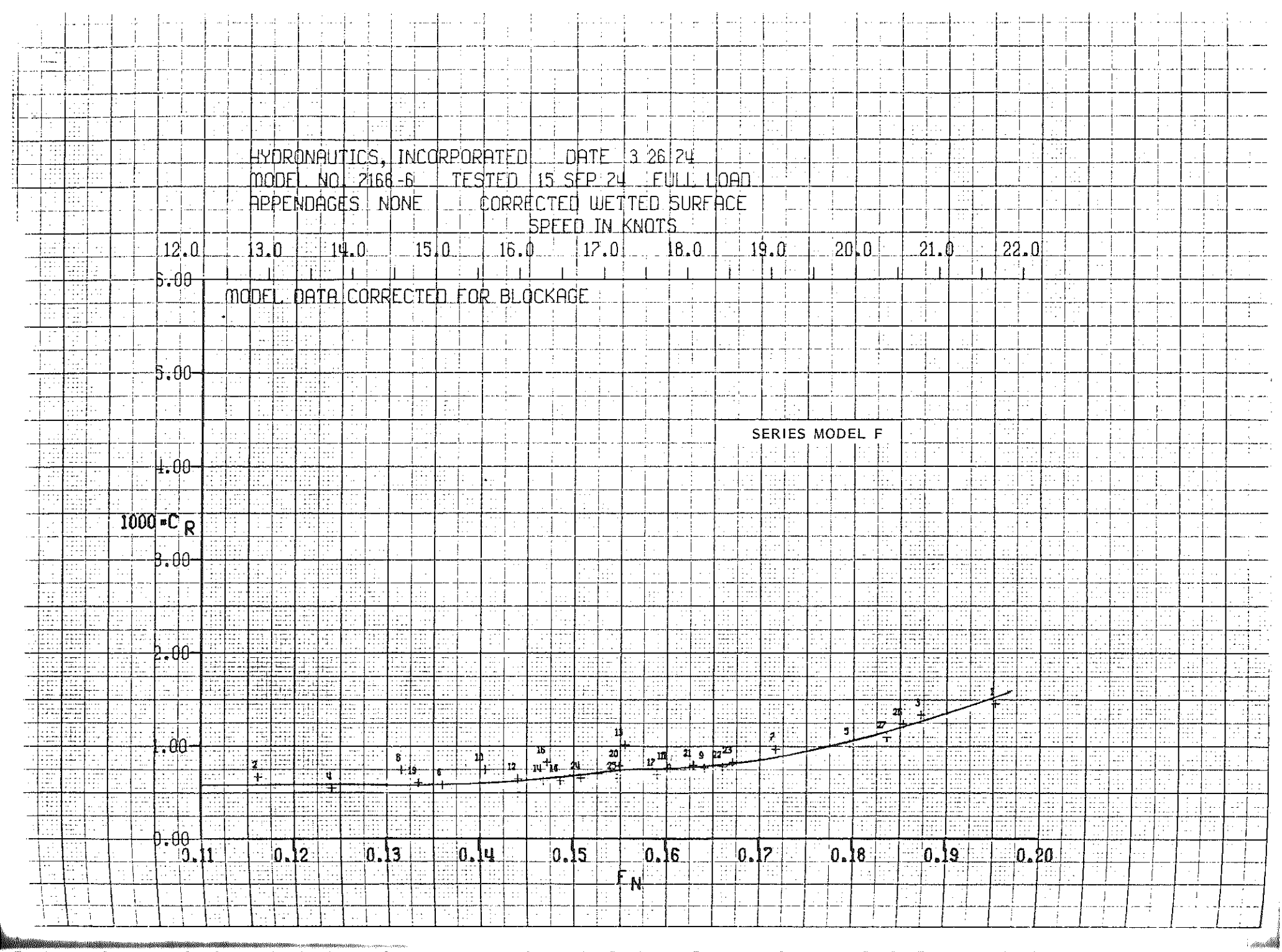

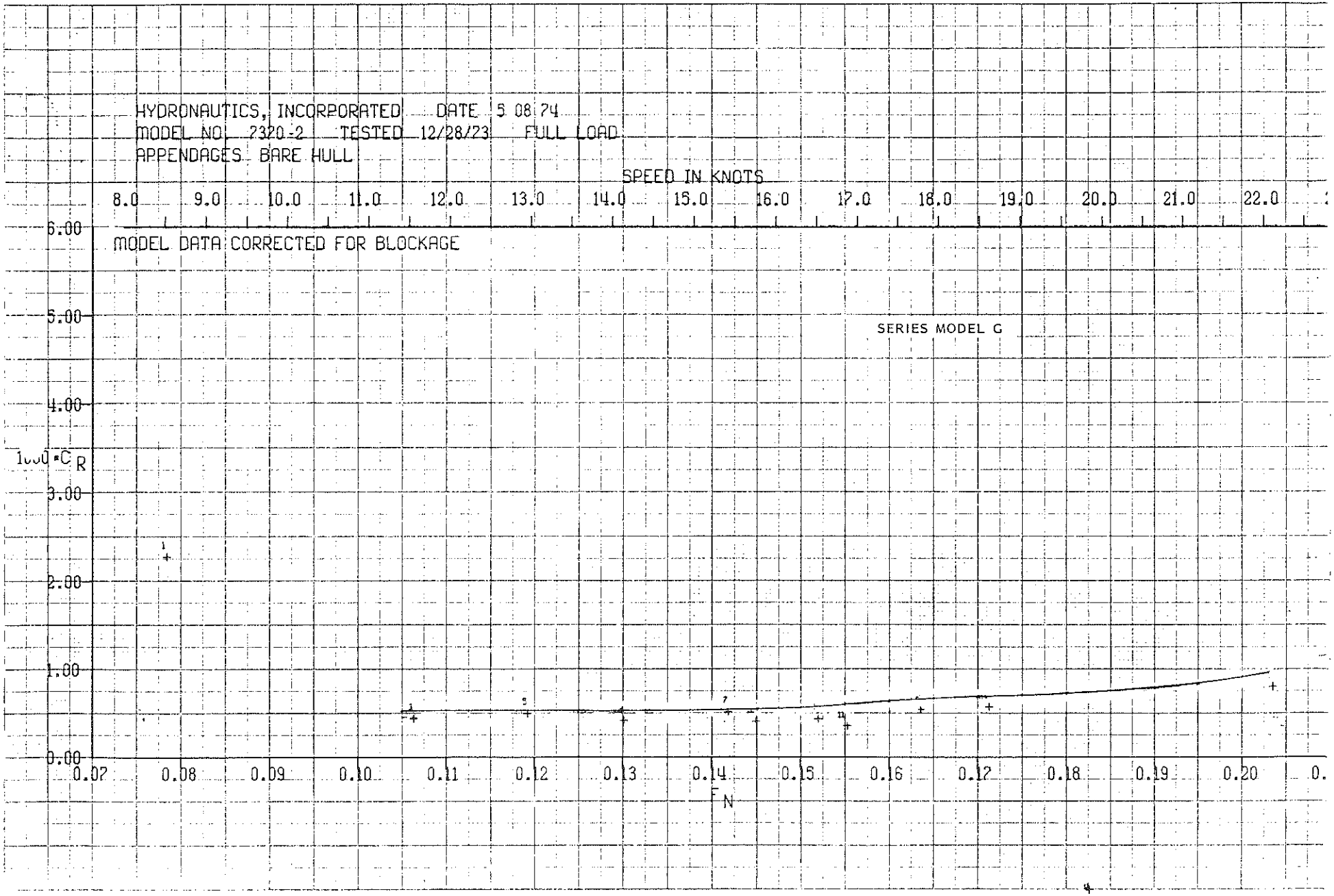
HYDRONAUTICS, INCORPORATED DATE 5 08 74
MODEL NO. 2320-2 TESTED 12/28/23 FULL LOAD
APPENDAGES BARE HULL
SPEED IN KNOTS
8.0
9.0
10.0
11.0
12.0
13.0
14.0
15.0
16.0
17.0
18.0
19.0
20.0
21.0
22.0
MODEL DATA CORRECTED FOR BLOCKAGE
SERIES MODEL G
6.00
5.00
4.00
1000 C R
3.00
2.00
1.00
0.00
0.07
0.08
0.09
0.10
0.11
0.12
0.13
0.14
0.15
0.16
0.17
0.18
0.19
0.20
F N

HYDRONAUTICS, INCORPORATED DATE 3 25 74
MODEL NO. 2320-1 TESTED 10/18/73 FULL LOAD
APPENDAGES BARE

SPEED IN KNOTS

8.0 9.0 10.0 11.0 12.0 13.0 14.0 15.0 16.0 17.0 18.0 19.0 20.0 21.0 22.0 23.0

MODEL DATA CORRECTED FOR BLOCKAGE

SERIES MODEL H

1000 • C_R

6.00
5.00
4.00
3.00
2.00
1.00
0.00

0.07 0.08 0.09 0.10 0.11 0.12 0.13 0.14 0.15 0.16 0.17 0.18 0.19 0.20

F_N

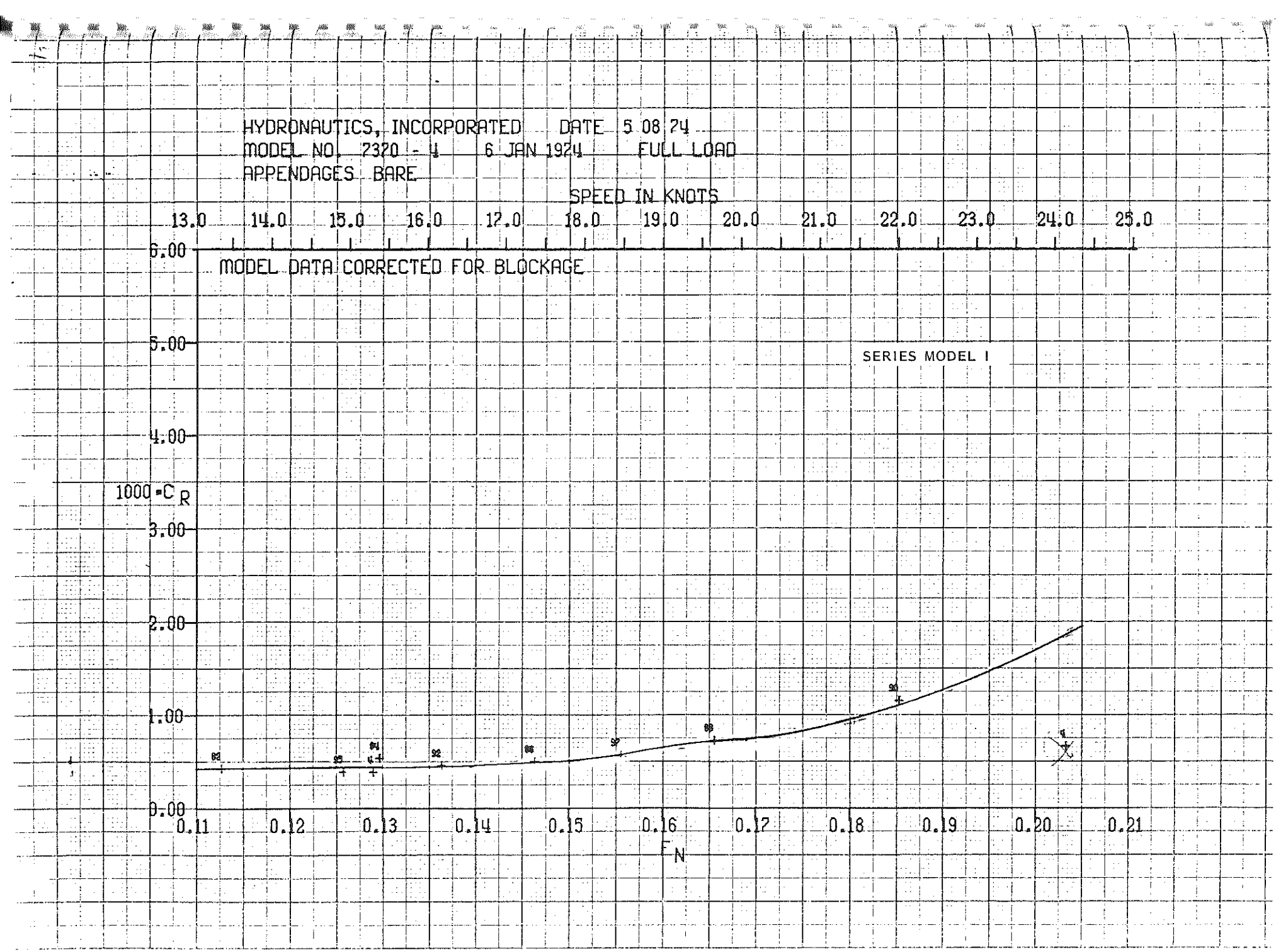
HYDRONAUTICS, INCORPORATED DATE 5 08 24
MODEL NO. 7320 - 4 6 JAN 1924 FULL LOAD
APPENDAGES BARE
SPEED IN KNOTS
13.0 14.0 15.0 16.0 17.0 18.0 19.0 20.0 21.0 22.0 23.0 24.0 25.0
MODEL DATA CORRECTED FOR BLOCKAGE
SERIES MODEL I
1000 • C_R
6.00
5.00
4.00
3.00
2.00
1.00
0.00
0.11 0.12 0.13 0.14 0.15 0.16 0.17 0.18 0.19 0.20 0.21
F_N

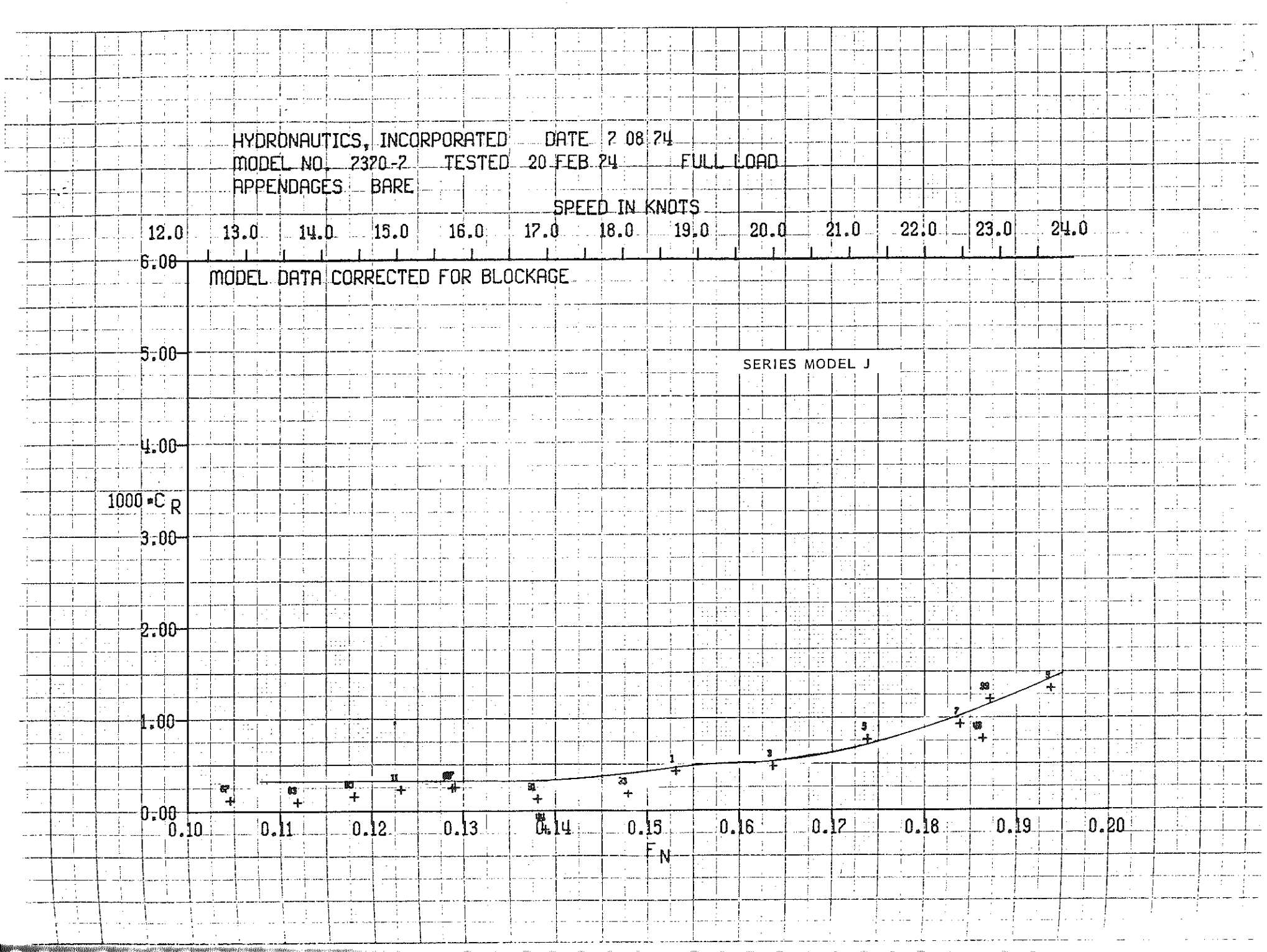
HYDRONAUTICS, INCORPORATED DATE 7 08 74
MODEL NO. 2370-2 TESTED 20 FEB 74 FULL LOAD
APPENDAGES BARE
SPEED IN KNOTS
12.0 13.0 14.0 15.0 16.0 17.0 18.0 19.0 20.0 21.0 22.0 23.0 24.0
MODEL DATA CORRECTED FOR BLOCKAGE
SERIES MODEL J
1000 * C R
6.00
5.00
4.00
3.00
2.00
1.00
0.00
0.10 0.11 0.12 0.13 0.14 0.15 0.16 0.17 0.18 0.19 0.20
F N

HYDRONAUTICS, INCORPORATED DATE 3 25 74
MODEL NO. 2320-3 TESTED 12 OCT 23 FULL LOAD
APPENDAGES BARE

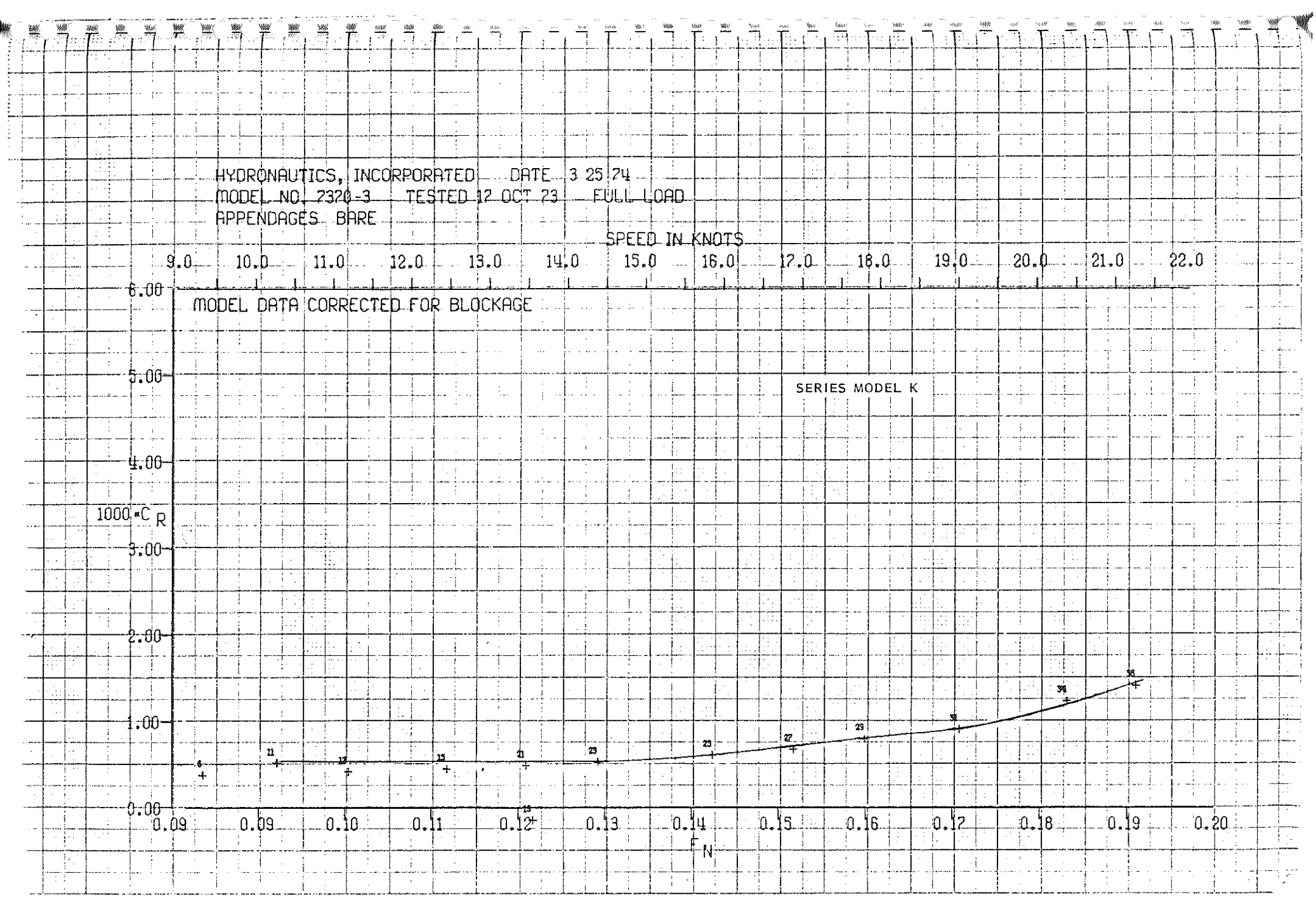

HYDRONAUTICS, INCORPORATED DATE 3 26 74
MODEL NO. 2320-8 TESTED 21 FEB 74 FULL LOAD
APPENDAGES BARE

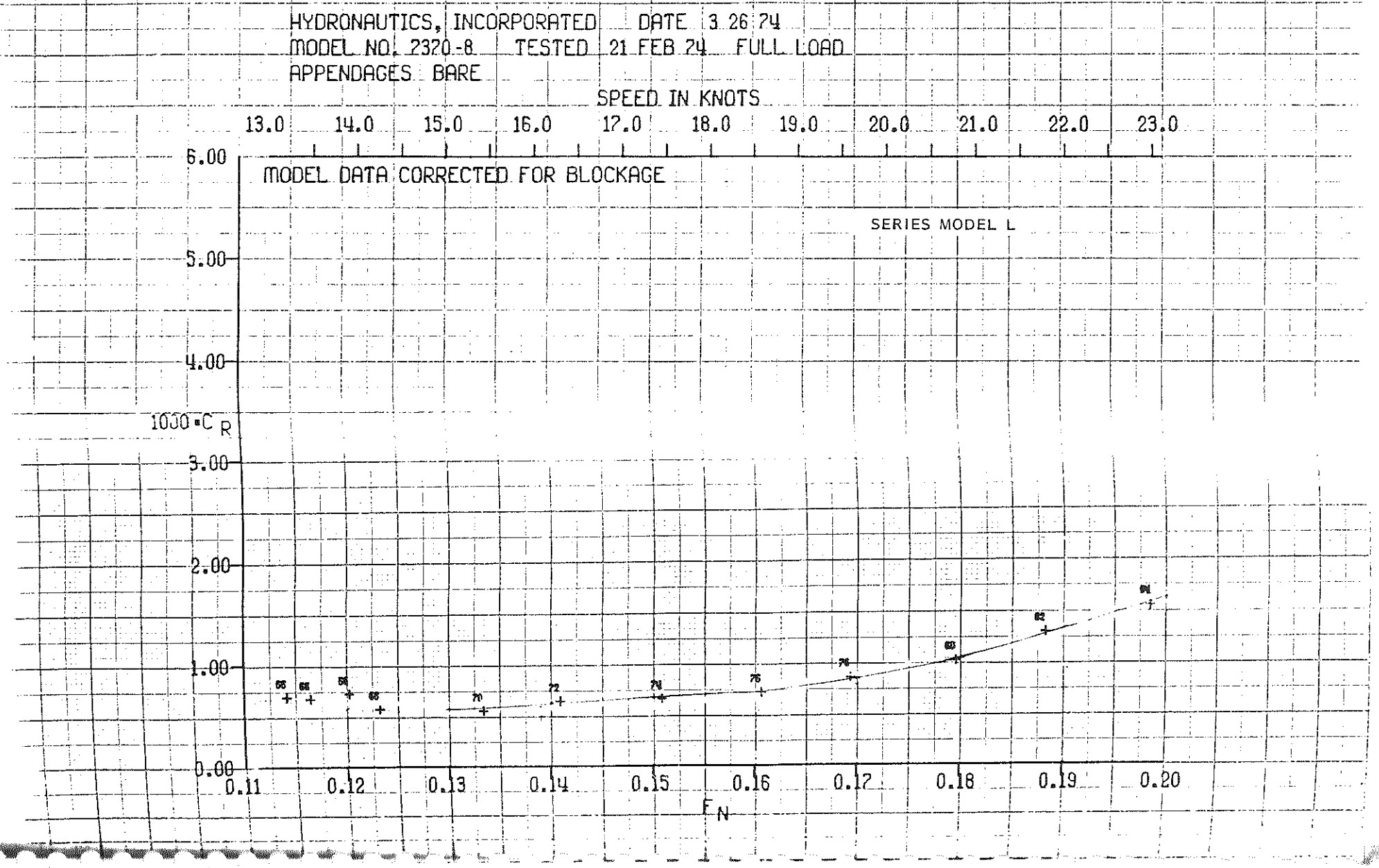

HYDRONAUTICS, INCORPORATED DATE 5 08 74
MODEL NO. 2370 - 6 TESTED 14 FEB 74 FULL LOAD
APPENDAGES BARE

SPEED IN KNOTS

12.0 13.0 14.0 15.0 16.0 17.0 18.0 19.0 20.0 21.0 22.0 23.0 24.0

MODEL DATA CORRECTED FOR BLOCKAGE

SERIES MODEL M

$1000 \cdot C_R$

6.00
5.00
4.00
3.00
2.00
1.00
0.00

0.10 0.11 0.12 0.13 0.14 0.15 0.16 0.17 0.18 0.19 0.20

F_N

HYDRONAUTICS, INCORPORATED DATE 5 09 74
MODEL NO. 2370 - 9 TESTED 25 APR 74 FULL LOAD
APPENDAGES BARE HULL

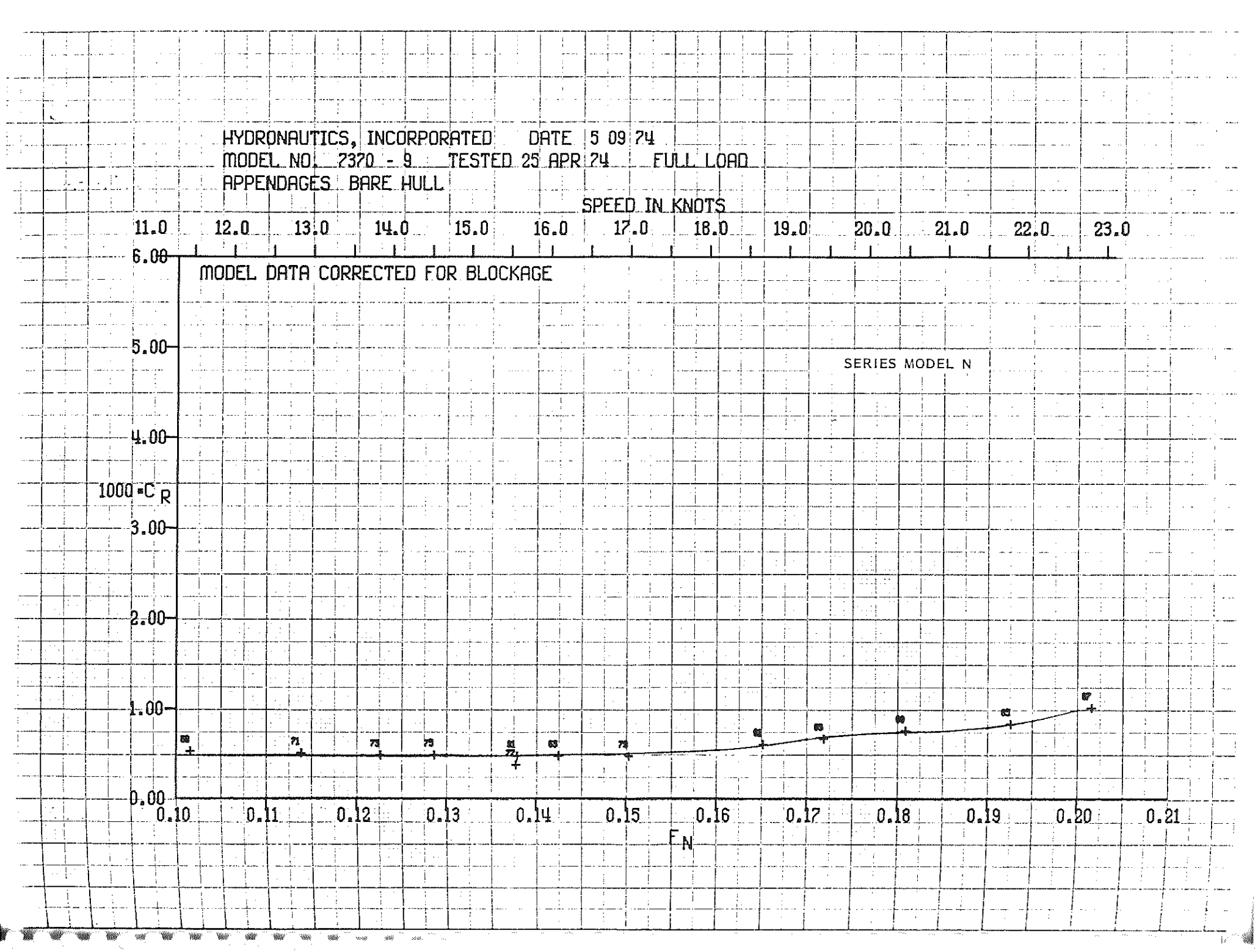

HYDRONAUTICS, INCORPORATED DATE 5 08 24
MODEL NO. 2320-5 TESTED 11 FEB 24 FULL LOAD
APPENDAGES BARE

SPEED IN KNOTS

10.0 11.0 12.0 13.0 14.0 15.0 16.0 17.0 18.0 19.0 20.0 21.0 22.0 23.0

MODEL DATA CORRECTED FOR BLOCKAGE

SERIES MODEL O

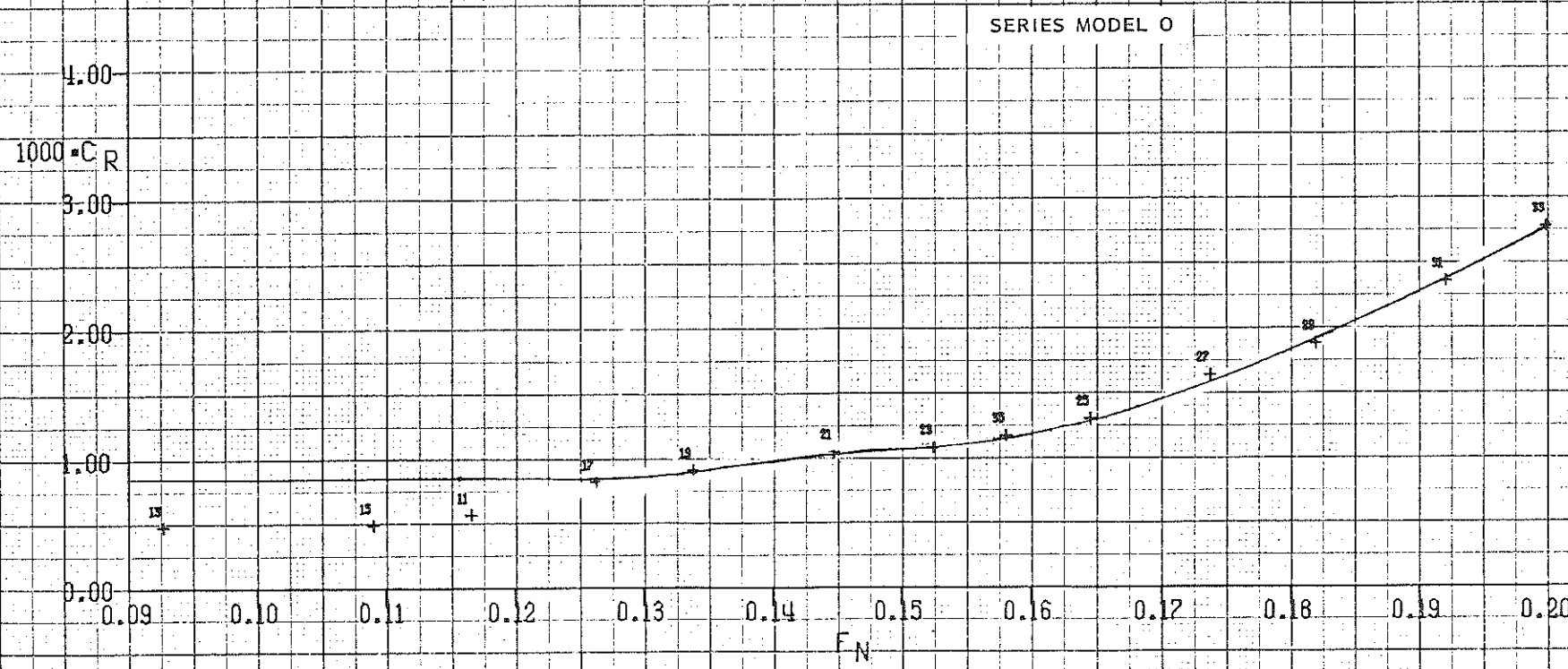

HYDRONAUTICS, INCORPORATED DATE 5 09 74
MODEL NO. 2370 - 10 TESTED 23 APR 74 FULL LOAD
APPENDAGES BARE HULL

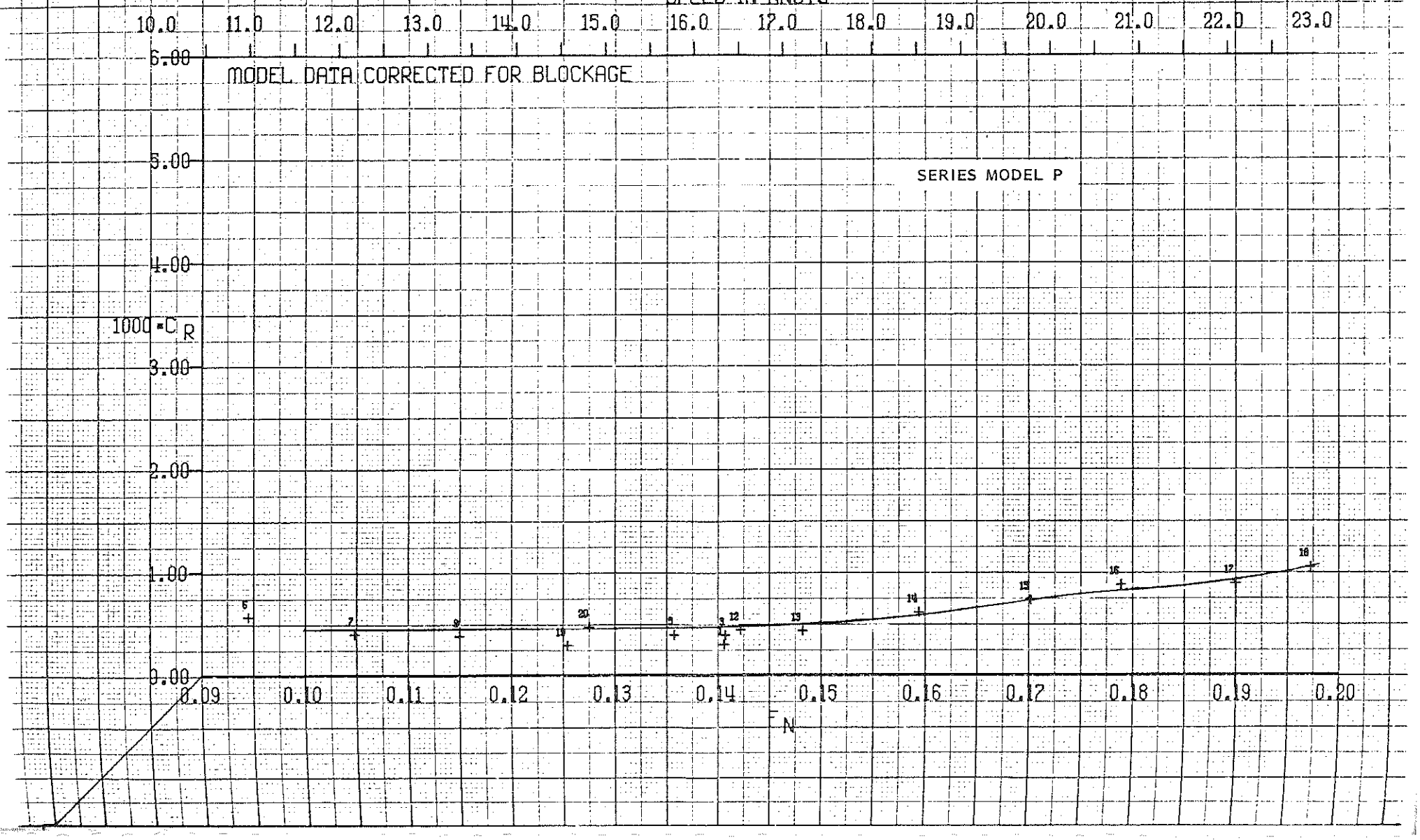

APPENDIX C

PRINCIPAL NUMERICAL MEASURES AND SELECTED COMPUTER PLOTS FOR TURNING AND ZIGZAG MANEUVERS IN DEEP WATER

APPENDIX C
PRINCIPAL NUMERICAL MEASURES AND SELECTED COMPUTER PLOTS FOR TURNING AND ZIGZAG MANEUVERS IN DEEP WATER

Principal numerical results derived for all sixteen ships with 350,000 tons displacement, for 20-20 zigzag and turning maneuvers, are summarized in Tables C-1 and C-2, respectively. Both maneuvers were simulated for 8 knots approach speed. Selected graphical computer plots are presented in Figures C-1 through C-12 for six models having the following principal characteristics:

Model Designation	D	E	F	G	N	P
C_B	0.85	0.85	0.85	0.80	0.80	0.80
L/B	4.50	5.00	5.50	5.00	5.00	5.00
B/T	3.00	3.00	3.00	3.00	3.75	4.50

These selected plots illustrate variation in maneuvering characteristics for variations in L/B and B/T, for block coefficients of 0.85 and 0.80, respectively.

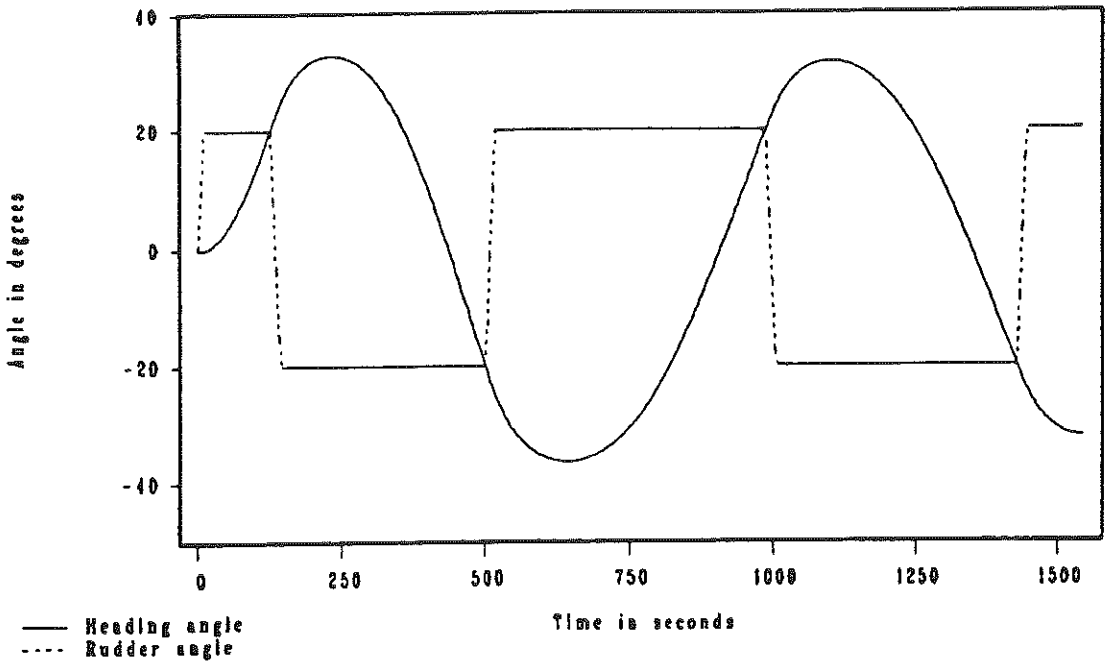

ZIGZAG MANEUVERING CHARACTERISTICS

SHIP IDENTIFICATION: SHIP D MARAD SERIES 350 KT FULL LOAD
RUN IDENTIFICATION: 20/20 ZIG-ZAG, MODIFIED MATH MODEL

SHIP LENGTH (FEET)	=	956.74
RUDDER ANGLE (DEGREES)	=	20.00 R
APPROACH SPEED (KNOTS)	=	8.00
RPM	=	32.41

FIRST OVERSHOOT

TIME TO REACH EXECUTE HEADING CHANGE (SECONDS)	=	123.63
OVERSHOOT ANGLE (DEGREES)	=	12.94
TOTAL HEADING CHANGE (DEGREES)	=	32.94
WIDTH OF PATH AT EXECUTE (FEET)	=	85.19
OVERSHOOT WIDTH OF PATH (FEET)	=	1563.06
TOTAL WIDTH OF PATH (FEET)	=	1648.25
REACH (SECONDS)	=	437.91
SECOND OVERSHOOT HEADING ANGLE (DEGREES)	=	16.54
THIRD OVERSHOOT HEADING ANGLE (DEGREES)	=	11.77
PERIOD (SECONDS)	=	863.59
FOURTH OVERSHOOT HEADING ANGLE (DEGREES)	=	12.17

FIGURE C-1 - TIME HISTORY OF HEADING ANGLE AND NUMERICAL CHARACTERISTICS OF ZIGZAG MANEUVER SHIP D

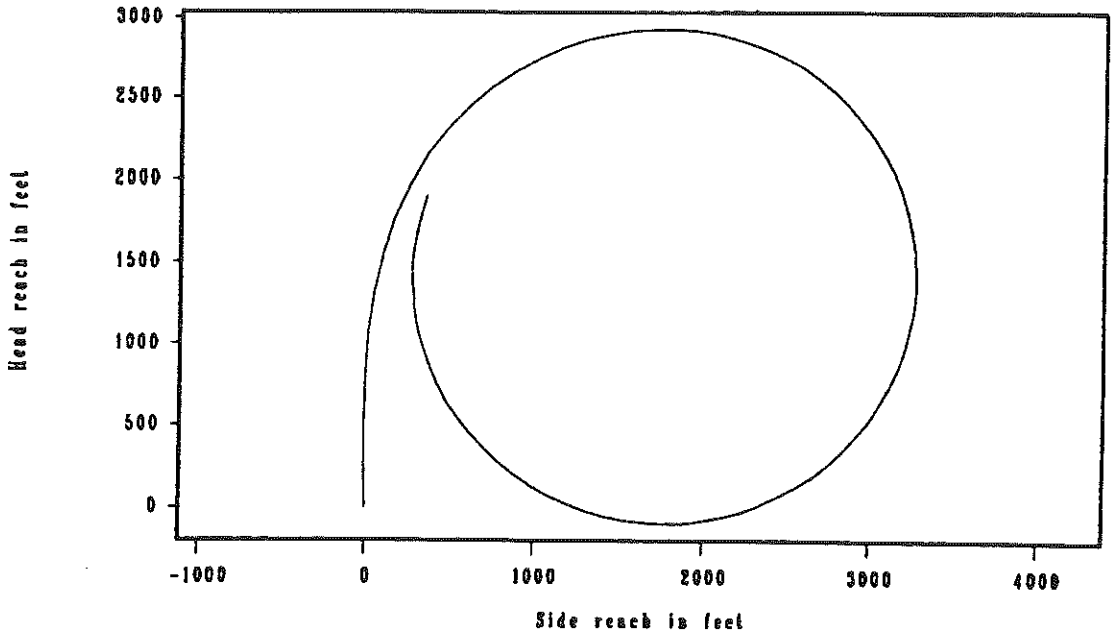

TURNING MANEUVERING CHARACTERISTICS

SHIP IDENTIFICATION: SHIP G MARAD SERIES 350 KT FULL LOAD
RUN IDENTIFICATION: TURN, MODIFIED MATH MODEL

RUDDER ANGLE (DEGREES)	=	35.00 R
APPROACH SPEED (KNOTS)	=	8.00
RPM	=	35.94
SHIP LENGTH, L, (FEET)	=	1047.20
TIME TO CHANGE HEADING 90 DEGREES (SECONDS)	=	303.72
TIME TO CHANGE HEADING 180 DEGREES (SECONDS)	=	678.62
SPEED REMAINING IN STEADY TURN (KNOTS)	=	3.52
SPEED LOSS IN PERCENT	=	56.01
ADVANCE (FEET)	=	2826.60
TRANSFER (FEET)	=	1183.63
TACTICAL DIAMETER, TD, (FEET)	=	3187.22
NONDIMENSIONAL TACTICAL DIAMETER, TD/L	=	3.04
STEADY TURNING DIAMETER, D, (FEET)	=	2995.28
NONDIMENSIONAL STEADY TURNING DIAM, D/L	=	2.86
FINAL DRIFT ANGLE (DEGREES)	=	19.40

FIGURE C-8 - TRAJECTORY PLOT AND NUMERICAL CHARACTERISTICS OF TURNING MANEUVER SHIP G

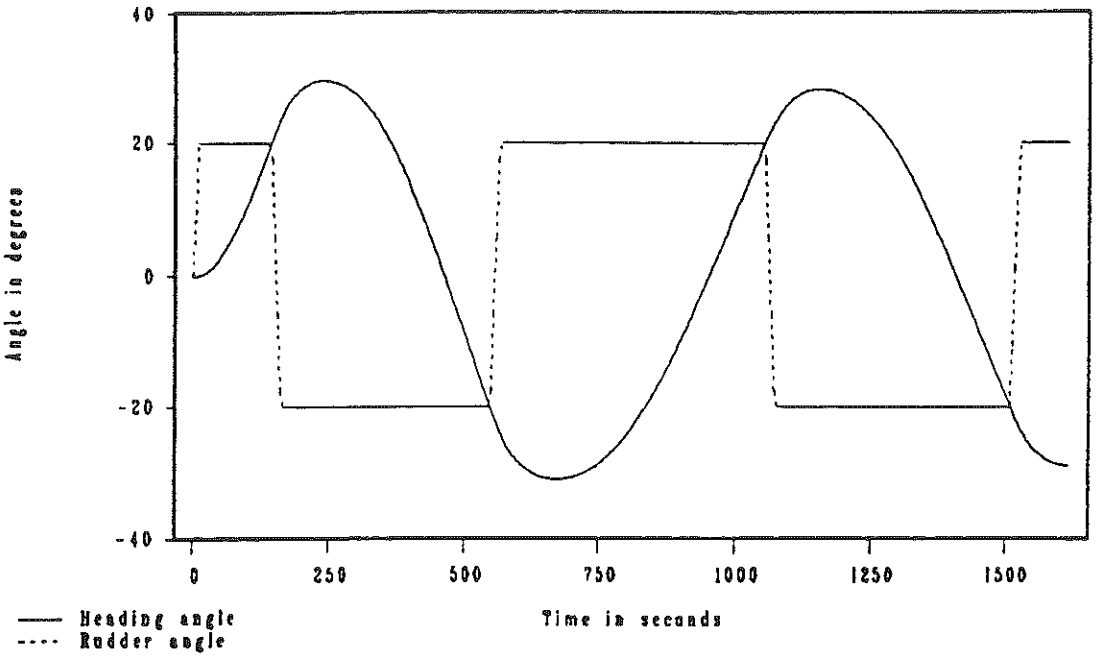


```
                    ZIGZAG MANEUVERING CHARACTERISTICS
                    **********************************

   SHIP IDENTIFICATION:  SHIP N MARAD SERIES 350 KT FULL LOAD
   RUN IDENTIFICATION:   20/20 ZIG-ZAG, MODIFIED MATH MODEL

   SHIP LENGTH (FEET)      = 1128.08
   RUDDER ANGLE (DEGREES) =   20.00 R
   APPROACH SPEED (KNOTS) =    8.00
   RPM                    =   34.43

      ***FIRST OVERSHOOT***

      TIME TO REACH EXECUTE HEADING CHANGE (SECONDS) =    142.32
      OVERSHOOT ANGLE (DEGREES)                      =      9.58
      TOTAL HEADING CHANGE (DEGREES)                 =     29.58
      WIDTH OF PATH AT EXECUTE (FEET)                =     92.01
      OVERSHOOT WIDTH OF PATH (FEET)                 =   1440.92
      TOTAL WIDTH OF PATH (FEET)                     =   1532.93

      REACH (SECONDS)                                =    464.01
      SECOND OVERSHOOT HEADING ANGLE (DEGREES)       =     11.13
      THIRD OVERSHOOT HEADING ANGLE (DEGREES)        =      8.26
      PERIOD (SECONDS)                               =    909.74
      FOURTH OVERSHOOT HEADING ANGLE (DEGREES)       =      8.98
```

FIGURE C-9 - TIME HISTORY OF HEADING ANGLE AND NUMERICAL CHARACTERISTICS OF ZIGZAG MANEUVER SHIP N

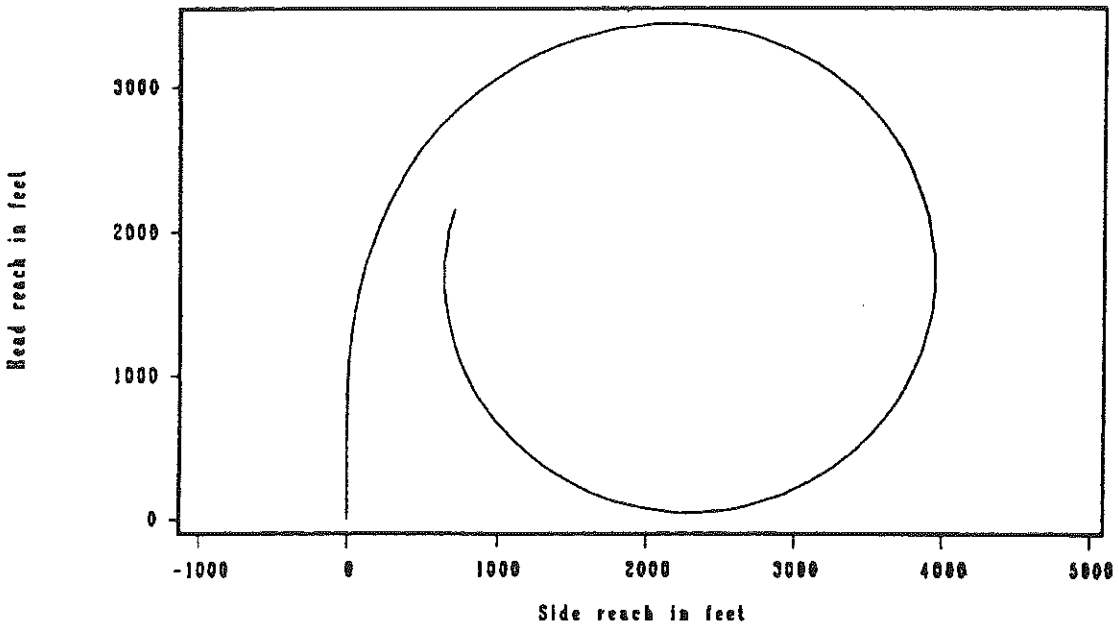

TURNING MANEUVERING CHARACTERISTICS

SHIP IDENTIFICATION: SHIP N MARAD SERIES 350 KT FULL LOAD
RUN IDENTIFICATION: TURN, MODIFIED MATH MODEL

RUDDER ANGLE (DEGREES)	=	35.00 R
APPROACH SPEED (KNOTS)	=	8.00
RPM	=	34.43
SHIP LENGTH, L, (FEET)	=	1128.08
TIME TO CHANGE HEADING 90 DEGREES (SECONDS)	=	364.03
TIME TO CHANGE HEADING 180 DEGREES (SECONDS)	=	867.92
SPEED REMAINING IN STEADY TURN (KNOTS)	=	2.70
SPEED LOSS IN PERCENT	=	66.29
ADVANCE (FEET)	=	3308.82
TRANSFER (FEET)	=	1424.22
TACTICAL DIAMETER, TD, (FEET)	=	3824.53
NONDIMENSIONAL TACTICAL DIAMETER, TD/L	=	3.39
STEADY TURNING DIAMETER, D, (FEET)	=	3294.59
NONDIMENSIONAL STEADY TURNING DIAM, D/L	=	2.92
FINAL DRIFT ANGLE (DEGREES)	=	21.42

FIGURE C-10 - TRAJECTORY PLOT AND NUMERICAL CHARACTERISTICS OF TURNING MANEUVER SHIP N

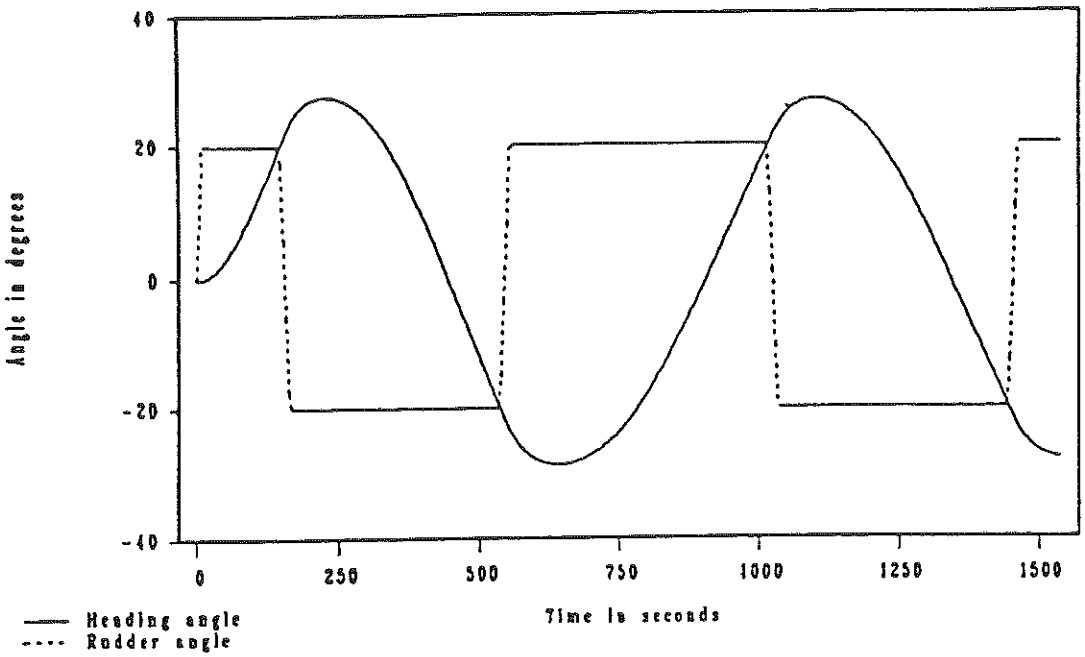

ZIGZAG MANEUVERING CHARACTERISTICS

SHIP IDENTIFICATION: SHIP P MARAD SERIES 350 KT FULL LOAD
RUN IDENTIFICATION: 20/20 ZIG-ZAG, MODIFIED MATH MODEL

SHIP LENGTH (FEET)	= 1198.76
RUDDER ANGLE (DEGREES)	= 20.00 R
APPROACH SPEED (KNOTS)	= 8.00
RPM	= 40.05

FIRST OVERSHOOT

TIME TO REACH EXECUTE HEADING CHANGE (SECONDS)	=	147.92
OVERSHOOT ANGLE (DEGREES)	=	7.45
TOTAL HEADING CHANGE (DEGREES)	=	27.45
WIDTH OF PATH AT EXECUTE (FEET)	=	90.48
OVERSHOOT WIDTH OF PATH (FEET)	=	1230.45
TOTAL WIDTH OF PATH (FEET)	=	1320.93
REACH (SECONDS)	=	485.73
SECOND OVERSHOOT HEADING ANGLE (DEGREES)	=	8.71
THIRD OVERSHOOT HEADING ANGLE (DEGREES)	=	6.71
PERIOD (SECONDS)	=	867.25
FOURTH OVERSHOOT HEADING ANGLE (DEGREES)	=	7.75

FIGURE C-11 - TIME HISTORY OF HEADING ANGLE AND NUMERICAL CHARACTERISTICS OF ZIGZAG MANEUVER SHIP P

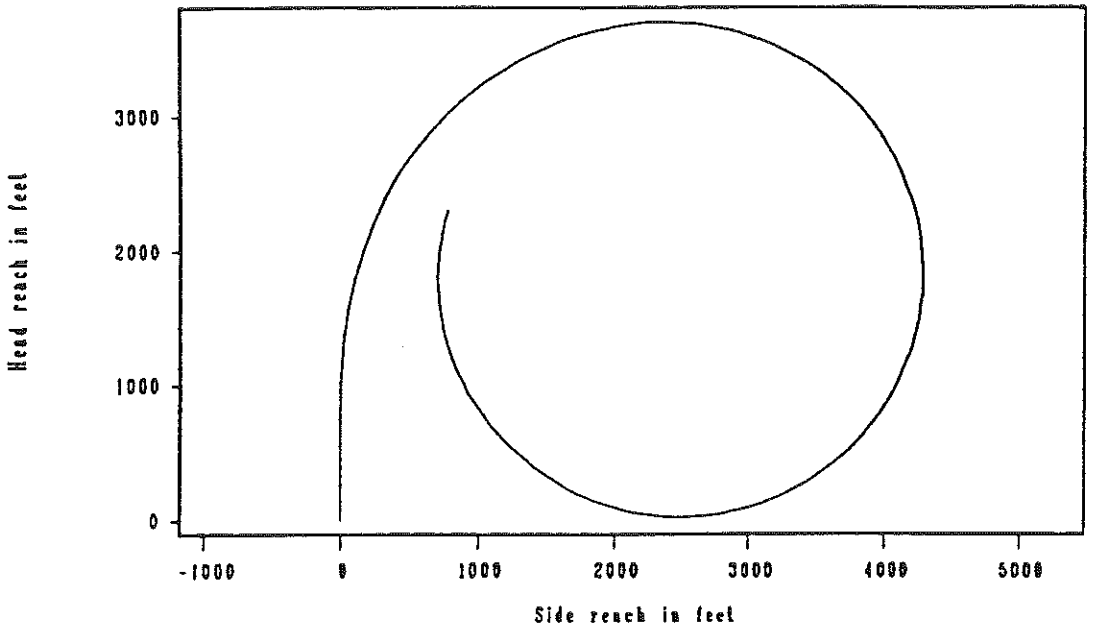

TURNING MANEUVERING CHARACTERISTICS

SHIP IDENTIFICATION: SHIP P MARAD SERIES 350 KT FULL LOAD
RUN IDENTIFICATION: TURN, MODIFIED MATH MODEL

RUDDER ANGLE (DEGREES)	=	35.00 R
APPROACH SPEED (KNOTS)	=	8.00
RPM	=	40.05
SHIP LENGTH, L, (FEET)	=	1198.76
TIME TO CHANGE HEADING 90 DEGREES (SECONDS)	=	396.15
TIME TO CHANGE HEADING 180 DEGREES (SECONDS)	=	913.18
SPEED REMAINING IN STEADY TURN (KNOTS)	=	2.99
SPEED LOSS IN PERCENT	=	62.61
ADVANCE (FEET)	=	3542.59
TRANSFER (FEET)	=	1545.08
TACTICAL DIAMETER, TD, (FEET)	=	4148.78
NONDIMENSIONAL TACTICAL DIAMETER, TD/L	=	3.46
STEADY TURNING DIAMETER, D, (FEET)	=	3570.49
NONDIMENSIONAL STEADY TURNING DIAM, D/L	=	2.98
FINAL DRIFT ANGLE (DEGREES)	=	22.12

FIGURE C-12 - TRAJECTORY PLOT AND NUMERICAL CHARACTERISTICS OF TURNING MANEUVER SHIP P

TABLE C-1

SIMULATED ZIGZAG MANEUVERING CHARACTERISTICS

SHIP IDENTIFICATION	Length, feet	RPM	First Overshoot						Reach (seconds)	Second Overshoot Heading Angle (seconds)	Third Overshoot Heading Angle (degrees)	Period (seconds)	Fourth Overshoot Heading Angle (degrees)
			Time to Reach Execute Heading Change (seconds)	Overshoot Angle (degrees)	Total Heading Change (degrees)	Path Width @ Execute (feet)	Overshoot Path Width (feet)	Total Path Width (feet)					
A	1083.18	36.20	140.21	13.53	33.53	97.60	1799.43	1897.03	500.06	18.65	13.42	994.84	13.81
B	1147.86	36.93	142.27	13.47	33.47	100.27	1824.89	1925.16	507.49	16.14	11.78	991.75	12.31
C	1210.75	37.50	135.29	19.08	39.08	91.88	2368.34	2460.22	557.62	18.54	12.99	1088.90	13.59
D	956.74	32.41	123.63	12.94	32.94	85.19	1563.06	1648.25	437.91	16.54	11.77	863.59	12.17
E	1026.30	36.56	132.17	14.38	34.38	91.58	1803.48	1895.06	483.35	17.45	12.57	946.07	13.46
F	1093.68	34.35	147.57	12.95	32.95	109.57	1874.17	1983.74	524.27	16.14	11.87	1031.44	12.43
G	1047.20	35.94	126.53	12.53	32.53	85.50	1583.40	1668.89	447.79	14.10	11.16	861.49	11.71
H	1222.40	41.66	157.48	9.70	29.70	116.09	1530.11	1646.20	499.20	12.74	9.75	968.54	10.60
I	1248.40	38.56	152.16	9.45	29.45	99.74	1504.45	1604.19	495.39	10.05	7.51	964.99	8.26
J	1326.61	45.19	164.18	7.81	27.81	107.83	1406.37	1514.20	504.30	8.69	6.53	990.86	7.42
K	1105.50	36.24	132.88	10.89	30.89	78.61	1489.73	1568.34	452.76	12.21	9.32	881.22	10.21
L	1174.80	42.16	148.64	8.76	28.76	85.80	1396.17	1481.97	473.17	10.53	7.70	932.49	8.90
M	1304.16	42.39	149.23	9.13	29.13	99.03	1385.37	1484.41	473.46	9.65	7.53	914.77	8.09
N	1128.08	34.43	142.32	9.58	29.58	92.01	1440.92	1532.93	464.01	11.13	8.26	909.74	8.98
O	1166.71	40.23	150.95	10.16	30.16	95.95	1628.96	1724.91	507.15	11.98	9.16	986.11	10.02
P	1198.76	40.05	147.92	7.45	27.45	90.48	1230.45	1320.93	445.73	8.71	6.71	867.25	7.75

NOTES:

1. Rudder angle = 20.00 degrees, right
2. Approach speed = 8.00 knots

TABLE C-2

SIMULATED TURNING MANEUVER CHARACTERISTICS

Ship Identification	Length, L, (feet)	RPM	Time to Change Heading 90 (seconds)	Time to Change Heading 180 (seconds)	Speed Remaining in Steady Turn (knots)	Speed Loss (percent)	Advance (feet)	Transfer (feet)	Tactical Diameter, TD	TD/L	Steady Turning Diameter, D (feet)	D/L	Final Drift Angle (degrees)
A	1083.18	36.20	308.28	708.97	2.38	70.21	2940.87	1098.97	2838.97	2.62	2479.97	2.29	22.87
B	1147.86	36.93	331.04	773.90	2.49	68.84	3057.13	1261.46	3248.51	2.83	2836.23	2.47	19.78
C	1210.75	37.50	328.41	816.77	2.41	69.84	2964.59	1249.99	3355.67	2.77	2986.48	2.47	19.20
D	956.74	32.41	277.57	667.11	2.21	72.33	2670.81	1011.47	2700.48	2.82	2180.11	2.28	24.79
E	1026.30	36.56	300.58	703.46	2.52	68.45	2831.42	1112.86	2930.13	2.86	2512.52	2.45	21.79
F	1093.68	34.35	344.65	803.71	2.72	65.95	3181.34	139.01	3436.25	3.14	3093.11	2.83	18.98
G	1047.20	35.94	303.72	678.62	3.52	56.01	2826.60	1183.63	3187.22	3.04	2995.28	2.86	19.40
H	1222.40	41.66	370.44	815.12	2.62	67.27	3350.62	1441.31	3507.49	2.87	2915.50	2.39	18.96
I	1248.80	38.56	410.23	981.79	2.66	66.69	3549.39	1597.54	4187.00	3.35	3589.70	2.88	20.03
J	1326.61	45.19	459.59	1071.68	2.79	65.13	3910.22	1798.23	4645.51	3.50	3936.29	2.97	20.33
K	1105.50	36.24	340.04	815.24	2.74	65.80	3125.73	1281.72	3579.13	3.24	3105.70	2.81	23.14
L	1174.80	42.16	388.01	906.12	2.74	65.70	3503.96	1435.57	3930.21	3.35	3309.83	2.82	23.96
M	1304.16	42.39	398.58	946.11	2.54	68.19	3401.94	1521.37	3922.52	3.01	3312.30	2.54	19.69
N	1128.08	34.43	364.03	867.92	2.70	66.29	3308.82	1424.22	3824.53	3.39	3294.59	2.92	21.42
O	1166.71	40.23	380.32	870.84	3.08	61.55	3483.22	1488.95	3974.74	3.41	3566.16	3.06	20.55
P	1198.76	40.05	396.15	913.18	2.99	62.61	3542.59	1545.08	4148.78	3.46	3570.49	2.98	22.12

NOTES:

1. Rudder angle = 35.00 degrees, right
2. Approach speed = 8 knots

APPENDIX D

HULL FORM GEOMETRY AND POWERING ESTIMATE COMPUTER PROGRAMS

Note: The following pages, D-1 through D-10, are an abridged version of Appendix D. The full text with program listings is included in microfiche form in an insert at the back of this volume.

APPENDIX D

HULL FORM GEOMETRY AND POWERING ESTIMATE COMPUTER PROGRAMS

Introduction

The two computer programs described in this appendix provide the means for development of hull form geometry and the determination of the resistance and propulsion data for a hull form derived from the MARAD Series. This appendix was derived from Reference (4).

Symbols not defined in this appendix are included in the Notation section preceding Chapter 1.

Hull Form Geometry Program

The hull form geometry computer program was developed for the definition of hull forms derived from the MARAD Series. The characteristics of the derived hull form design must lie within the matrix of model characteristics defined in Chapter 1.

The data base for the hull form geometry is described in Chapter 1. Subsequent to the completion of the Series model tests, lengthened versions of the Series hull form were designed, for possible high L/B applications such as Great Lakes bulk carrier hull forms, as reported in Reference (4). Accordingly, the hull form geometry program can be used to develop lines for the following extended range of form coefficients:

$$0.80 \leq C_B \leq 0.90$$
$$4.5 \leq L/B \leq 10.0$$
$$2.5 \leq B/T \leq 4.5$$

Hull Form Description

A preliminary body plan, waterlines and buttocks, can be developed from the Series parent form data and algorithms for given values of L, B, T, LCB location, and C_B. The program will not define the stern profile for the reasons discussed in

Chapter 2. This limitation is of little practical importance, however, since the run and aperture geometry must be developed independently to suit specific propeller and aperture configurations.

Program Input Description

The following input data is required:

- L, B, T, LCB (defined as percentage of L, forward of amidships), and C_B;
- Station, waterline, and buttock spacing and location.

Note that the stations are defined as follows: Station x is located (x • L)/20 ft from FP. Thus x = 0,1,2,...,20 are the standard stations. Fractional stations such as station 1.25 can also be defined.

The maximum number of stations and waterlines are 30 each. Maximum number of buttocks is 10.

If the user does not supply the abovementioned information, the program provides the following default conditions:

Stations at 0,1,2...,20

Waterlines at $(i-1)\times T/10$, i = 1,2,...,16

Buttocks at $(B/2)\times i/5$, i = 1,2,3,4

Program Output

Depending upon the chosen option, the output includes:

- Title page
- Summary of output options selected
- Input hull data
- Output station, waterline, and buttock locations
- Computed values of lengths of entrance, parallel middle body and run
- Offset tables
- Scaled body plan offsets as plotted
- Bow profile data
- Bow waterline data

- Plotted and listed offsets for bow waterlines and buttocks
- Plotted and listed offsets for run waterlines and buttocks.

Resistance and Powering Estimates

The resistance and powering characteristics of any given Series offspring hull form is based on the data included in Chapters 4 and 5.

Algorithm Description

The powering estimates are obtained by interpolating over tabulated entries for B/T, L/B, C_B, and FN, following the interpolation sequence described in Chapter 8.

Correlation Allowance

C_A = Model-ship correlation allowance coefficient

$= R_A/(1/2\rho v^2 S)$

Unless otherwise input, a zero correlation allowance is used.

Wetted Surface

The wetted surface is calculated from the expression:

$$S = C_S \sqrt{\nabla L}$$

The wetted surface coefficients of the series are given in Chapter 2 as functions of L/B, B/T, and C_B.

The following algorithms were developed for computation of the C_S values:

$$C_S = D - [(0.008414 - 0.0023\ B/T + 0.0004888\ (B/T)^2)\ L/B - 0.002666\ C_B\ L/B]$$

where

$$D = 3.15757 - 0.54846\ B/T + 0.092\ (B/T)^2 - (0.4189 - 0.588\ B/T + 0.0816\ (B/T)^2)\ C_B$$

These algorithms approximate the C_S values within 1/2 percent of the values given in Chapter 2. The variations of C_S with respect to L/B and C_B are linear; the variation of C_S with respect to B/T is parabolic.

Nondimensional Wetted Surface

The wetted surface algorithm producing a nondimensional value is:

$$S' = \frac{S}{\nabla^{2/3}}$$

Effective Horsepower

The total effective horsepower is calculated as follows:

$$EHP_{Total} = EHP_{BH} + EHP_{APP}$$

where

EHP_{BH} = effective horsepower, bare hull = R_T v/550

and

EHP_{APP} = effective horsepower, appended

= (appendage allowance) • (EHP_{BH})

Propulsive Factors

Values for 1-t, 1-w, and e_{rr} are given in Chapter 5 as functions of B/T, L/B, and C_B, and are constant with F_N.

For a given B/T, L/B, and C_B, the values of 1-t, 1-w, and e_{rr} are determined as follows:

- Interpolate on B/T, using a three-point parabolic fit.
- Interpolate on L/B, using a three-point parabolic fit.

- Interpolate on C_B as follows:
  for $0.80 \leq C_B \leq 0.850$, a weighted average of a linear and a second order polynomial interpolation;
  for $0.85 < C_B \leq 0.875$, a second order polynomial interpolation;
  for $0.875 < C_B \leq 0.90$, a linear extrapolation using slope between $C_B = 0.865$ and $C_B = 0.875$ as determined by a second order polynomial.
- Calculate $e_h = (1-t)/(1-w)$
- Calculate PC = = $(e_h)(e_p)(e_{rr})$

The propeller open water efficiency is obtained from the open water tests of the Wageningen B-screw series four and five-bladed propellers, as stated in Chapter 5. The propeller is optimized for the design speed with respect to operating RPM, blade-area ratio (BAR), pitch-diameter ratio (P/D), and diameter (D).

Shaft Horsepower

The shaft horsepower is calculated from the expression:

$$SHP = \frac{EHP_{Total}}{PC}$$

Ballast Draft

The ballast drafts are defined in Chapter 3. The curves of ballast draft/full load draft, as a function of B/T, have been approximated by the following algorithms:

Draft at AP:

$$\frac{\text{ballast draft}}{\text{full load draft}} = 0.8886 - 0.2305\ B/T + 0.0893\ (B/T)^2 - 0.0112\ (B/T)^3 - 0.00064\ (B/T)^4 + 0.00017\ (B/T)^5$$

Draft at FP:

$$\frac{\text{ballast draft}}{\text{full load draft}} = 0.7083 - 0.2201\ B/T + 0.0758\ (B/T)^2 - 0.00621\ (B/T)^3 - 0.0014\ (B/T)^4 + 0.00021\ (B/T)^5$$

Mean ballast draft:

$$\frac{\text{ballast draft}}{\text{full load draft}} = 0.7290 - 0.1392\ B/T + 0.0426\ (B/T)^2 - 0.000178\ (B/T)^3 - 0.00182\ (B/T)^4 + 0.00021\ (B/T)^5$$

Ballast Displacement

Ballast displacement is calculated from the expression:

$$\Delta_B = (LBP)\ (B)\ (T_{B,mean})\ C_{B_{Ballast}}/(1/\rho)$$

where,

$1/\rho$ = 35 for salt water and 36 for fresh water

$T_{B,mean}$ = ballast condition mean draft, ft

$C_{B_{Ballast}}$ = the ballast condition block coefficient.

$C_{B_{Ballast}}$ is a function of the full load block coefficient and is approximated by the following algorithm:

$$C_{B_{Ballast}} = 2.3879 - 6.6224\ C_{B_{FL}} + 7.6145\ (C_{B_{FL}})^2 - 6.8270\ (C_{B_{FL}})^3 + 10.4332\ (C_{B_{FL}})^4 - 6.1172\ (C_{B_{FL}})^5$$

where

$C_{B_{FL}}$ = the full load condition block coefficient

Ballast Wetted Surface

The ballast condition wetted surfaced is determined by the expression:

$$S_B = fS \sqrt{\frac{\Delta_B}{\Delta_{FL}}}$$

where,

Δ_B = ballast displacement

Δ_{FL} = full load displacement

S = full load wetted surface

f = factor which is a function of B/T and C_B, and is approximated by the following equations for the respective values of C_B:

$$f(C_{B_{FL}} = 0.800) = 1.0667 - 0.2713\ B/T + 0.1552\ (B/T)^2 - 0.0203\ (B/T)^3 - 0.00238\ (B/T)^4 + 0.00049\ (B/T)^5$$

$$f(C_{B_{FL}} = 0.850) = 1.4759 - 0.7606\ B/T + 0.3368\ (B/T)^2 - 0.0338\ (B/T)^3 - 0.00688\ (B/T)^4 + 0.0011\ (B/T)^5$$

$$f(C_{B_{FL}} = 0.875) = 0.4609 + 0.2668\ B/T + 0.0184\ (B/T)^2 - 0.0221\ (B/T)^3 + 0.00263\ (B/T)^4 - 0.000005\ (B/T)^5$$

After the value of f is determined for each of the three values of C_B, an interpolation is made on C_B to find the final value of f. This interpolation is made using a three-point parabolic approximation.

Ballast EHP

Ballast C_T, C_F, C_R, and EHP values are calculated in the same manner as for the full load condition using the C_R values for the ballast condition obtained from Chapter 4.

Powering Estimate Program Output

The program output consists of a summary of input ship characteristics, and resistance and propulsion data. The following table lists items and corresponding abbreviations output by the program.

Full Load and Ballast Conditions

Abbreviation	Item
	Project number
	Project title
	Project engineer
	Date
V, KNOTS	Speed in knots
FN	Froude number
SLR	speed-length ratio
CIRC-K	(K)
EHP BARE HULL	Effective horsepower, bare hull
EHP APP	Effective horsepower, appended
EHP TOTAL	Effective horsepower, total
REY NO.	Reynolds number
CF × 1000	Frictional resistance coefficient, × 1000
CA × 1000	Correlation allowance, × 1000
CR × 1000	Residuary resistance coefficient, × 1000
CT × 1000	Total resistance coefficient, × 1000
CIRC-C	(C)
	Appendage allowance
	Correlation allowance

Full Load Condition Only

Abbreviation	Item
LBP	Length between perpendiculars
BEAM	Breadth
DRAFT	Full load draft
W.S.	Wetted surface
DISPL.	Displacement
LCB	Longitudinal center of buoyancy, percent of LBP from amidships. + is fwd, - is aft
CB	Block coefficient
L/B	Length-beam ratio
B/T	Beam-draft ratio
CS	Wetted surface coefficient
CIRC-S	(S)
PROP. DIAM.	Propeller diameter
PITCH/DIAM	Propeller pitch-diameter ratio
BAR	Blade area ratio
NO. OF BLADES	Number of propeller blades
SHP	Shaft horsepower
PC	Propulsive coefficient
1-T	Thrust deduction factor
1-W	Wake fraction
EH	Hull efficiency
ERR	Relative rotative efficiency
EP	Open water propeller efficiency
RPM	Propeller RPM

Ballast Condition Only

Abbreviation	Item
F.L. DRAFT	Full load draft
F.L. DISPL	Full load displacement
F.L. CB	Full load block coefficient
BALLAST DRAFTS:	
F.P.	Ballast draft at FP
A.P.	Ballast draft at AP
MEAN	Mean ballast draft
BALLAST DISPL	Ballast displacement
BALLAST CB	Ballast block coefficient
BALLAST W.S.	Ballast wetted surface

REFERENCES

1. Gertler, M., Kohl, R. E., and Kirkman, K. L., "Experimental Investigations of a Systematic Series of Low Length-Beam Ratio, High Block Coefficient Merchant Ship Forms," Hydronautics, Incorporated Technical Report No. 7166-1, June 1973.
2. Gertler, M. and Kohl, R. E., "Resistance Propulsion and Maneuverability Characteristics of MarAd Systematic Series for Large Full-Form Merchant Ships," Hydronautics, Incorporated Technical Report 7370-1, November 1974.
3. Gertler, M., Miller, E. R., and Ankudinov, V., "Shallow-Water Maneuverability Characteristics of MarAd Systematic Series for Large Full-Form Merchant Ships," Hydronautics, Incorporated Technical Report No. 7568-1, August 1977.
4. Tomassoni, C., Rawat, P., Sauer, T., and Setterstrom, C., "Development of Means of Rapid Retrieval of Hull Form Geometry and Performance Data for the MarAd Standard Series," Hydronautics, Incorporated Technical Report No. 7644-1, June 1977.
5. Gertler, M., "A Reanalysis of the Original Test Data for the Taylor Standard Series," TMB Report 806, U. S. Government Printing Office, 1954.
6. Todd, F. H., "Series 60 Methodical Experiments with Models of Single-Screw Ships," TMB Report 1712, U. S. Government Printing Office, July, 1963.
7. Moor, D. I., Parker, and Pattulo, R.N.M., "The BSRA Methodical Series - An Overall Presentation," Transactions RINA, Volume 103, 1961.
8. Edstrand, H., et al, "Experiments with Tanker Models," SSPA Publication Nos. 23, 26, 29, 36 and 37, 1953-56; also NECI, Volume 72, 1955-56 for Summary.
9. Yokoo, Koichi, "Systematic Series Model Tests in Japan Concerning the Propulsive Performance of Full Ship Forms," Japan Shipbuilding and Marine Engineering Volume 1, Number 2, May 1966.

10. Muntjewerf, J. J., "Methodical Series Experiments on Cylindrical Bows," Transactions of RINA, Volume 112, Number 2, April 1970.
11. Modellversuchsergebnisse von Einschrauben - Frachtschiffen mit einer Volligkeit C_B = 0.85 - Forschungszentrum des Deutschen Schiffbaus Bericht Nr. 2/1968.
12. Hughes, G., "Tank Boundary Effects on Model Resistance," Transactions RINA, Volume 103, 1961.
13. Hadler, J. B.," Coefficients for International Towing Tank Conference 1957 Model-Ship Correlation Line," DTMB Report 1185, April 1958.
14. Mandel, P., Ship Manuevering and Control, Principles of Naval Architecture, Chapter VIII, SNAME, 1967.
15. van Berlekom, William B. and Goddard, Thomas A., "Maneuvering of Large Tankers," Transactions SNAME, Vol. 80, 1972.
16. Goodman, A., "Description and Operation of Planar Motion Mechanism Instrumentation System," HYDRONAUTICS, Incorporated Technical Report 818-1, February 1968.
17. Gertler, M. and Hagen, G. R., "Standard Equations of Motion for Submarine Simulation," NSRDC Report 2510, June 1967.
18. Gertler, M., "The ITTC Standard Captive-Model Test Program - A Review and Preliminary Analysis of Data Received Prior to May 1966," Appendix II of Maneuverability Committee Report, Proceedings of 11th ITTC, 1966.
19. Gertler, M., "Final Analysis of First Phase of ITTC Standard Captive-Model Test Program," Appendix 3, Part 2 of Maneuverability Committee Report, Proceedings of the 12th ITTC, 1969.
20. Gertler, M., "Some Recent Advances in Dynamic Stability and Control of Submerged Vehicles," Proceedings of IUTAM Symposium on Directional Stability and Control of Bodies Moving in Water," London, England 17-21 April 1972.

21. Norrbin, N., H., "Theory and Observations on the Use of a Mathematical Model for Ship Maneuvering in Deep and Confined Waters," SSPA Publication No. 68, 1971.
22. Gertler, M., "Cooperative Test Program-Review and Status of Second Phase of Standard Captive-Model Test Program," Appendix VI of Maneuverability Committee Report Proceedings of 13th ITTC, 1972.
23. Abkowitz, M. A., "Lecture on Ship Hydrodynamics - Steering and Maneuverability," Hydro - and Aerodynamics Laboratory Report Hy-5, May 1964.
24. Chislett, M. S. and Strom-Tejsen, J., "Planar Motion Mechanism Tests and Full-Scale Steering and Maneuvering Predictions for a MARINER Class Vessel," Hydro - and Aerodynamic Laboratory Report Hy-6, April 1965.
25. Strom-Tejsen, J., "A Digital Computer Technique for Predication of Standard Maneuvers of Surface Ships," TMB Report 2130, December 1965.
26. Smitt, L. W. and Chislett, M. S., "X_{vr}' for Models of a Fast Container Vessel and Two Large Tankers," Written Contribution to 13th ITTC, September 1972.
27. Smitt, L. W. and Landsburg, A. C., "Note on Added Mass in Surge Measurements with Model of Large Tanker," Written Contribution to 13th ITTC, September 1972.
28. Gertler, M. and Gover, S. C., "Handling Quality Criteria for Surface Ships," Presented before the Chesapeake Section of SNAME, May 1959; TMB Report 1514, April 1961.
29. Crane, C. L., "Maneuvering Trials of the 278,000 DWT ESSO OSAKA in Shallow and Deep Waters", EXXON International Company Report No. E11. 4TM.79, January 1979.
30. Norrbin, N. H., "Theory and Observations on the Use of a Mathematical Model for Ship Manoeuvring in Deep and Confinded Waters" SSPA Publication Nr 68, 1971.
31. Comstock, J. P. and Hancock, C. H., "The Effect of Size of Towing Tank on Model Resistance," Transactions SNAME, 1942.

32. Schlichting, O., "Ship Resistance in Water of Limited Depth-Resistance of Sea-Going Vessels in Shallow Water," Jahrbuck der STG, Vol. 35, 1934, EMB Translation 56, January 1940.

33. Landweber, L., "Tests of a Model in Restricted Channels," EMB Report 460, May 1939.

34. Todd, F. H., "Resistance and Propulsion - Shallow-Water Effects," Principles of Naval Architecture, Chapter VII, Section 5.5, SNAME, 1967.

35. Saunders, H. E. Hydrodynamics in Ship Design, Vol. II, Chapter 61 entitled "The Prediction of Ship Behavior in Confined Waters," SNAME, 1957.

36. Fujino, M., "Experimental Studies on Ship Manoeuvrability in Restricted Waters," Part I - International Shipbuilding Progress, Vol. 15, No. 168, August 1968.

37. Van Berlekom, W. B. and Goddard, T. A., "Maneuvering of Large Tankers," Transactions SNAME, 1971.

38. Goodman, A., Gertler, M., and Kohl, R., "Experimental Techniques and Methods of Analysis Used at HYDRONAUTICS for Surface-Ship Maneuvering Predictions," Proceedings of the Eleventh ONR Symposium on Naval Hydrodynamics, April 1976, HYDRONAUTICS, Incorporated Technical Report 7600-1, June 1976.

39. van Oortmerssen, G., "Influences of the Water Depth on the Maneuvering Characteristics of Ships," Proceedings of Symposium on "Ship Handling," NSMB Publication No. 451, November 1973.

40. Kohl, R., Young, B., Altmann, R., and Schaefer, K., "Model Tests to Determine the Resistance, Propulsion, Wake, Maneuvering, Hydrodynamic Rudder Torque and Propeller Cavitation Characteristics of a 390,000 DWT Bulk Oil Carrier," Hydronautics Technical Report No. 7530-1, July 1975.

41. Teledyne Hastings-Raydist, "Raydist Trial Report, U.S.T. ATLANTIC," Report R281, February 1979.

42. Tomassoni, C., Rawat, P., Sauer, T., and Setterstrom, C., "Development of Means for Rapid Retrieval of Hull Form Geometry and Performance Data for the MARAD Standard Series," Hydronautics, Inc. Technical Report No. 7644-1, June 1977.

43. van Lammeren, W. P. A., van Manen, J. D., and Oosterveld, M. W. C., "The Wageningen B-Screw Series," Transactions SNAME, Volume 77, p. 269, 1969.

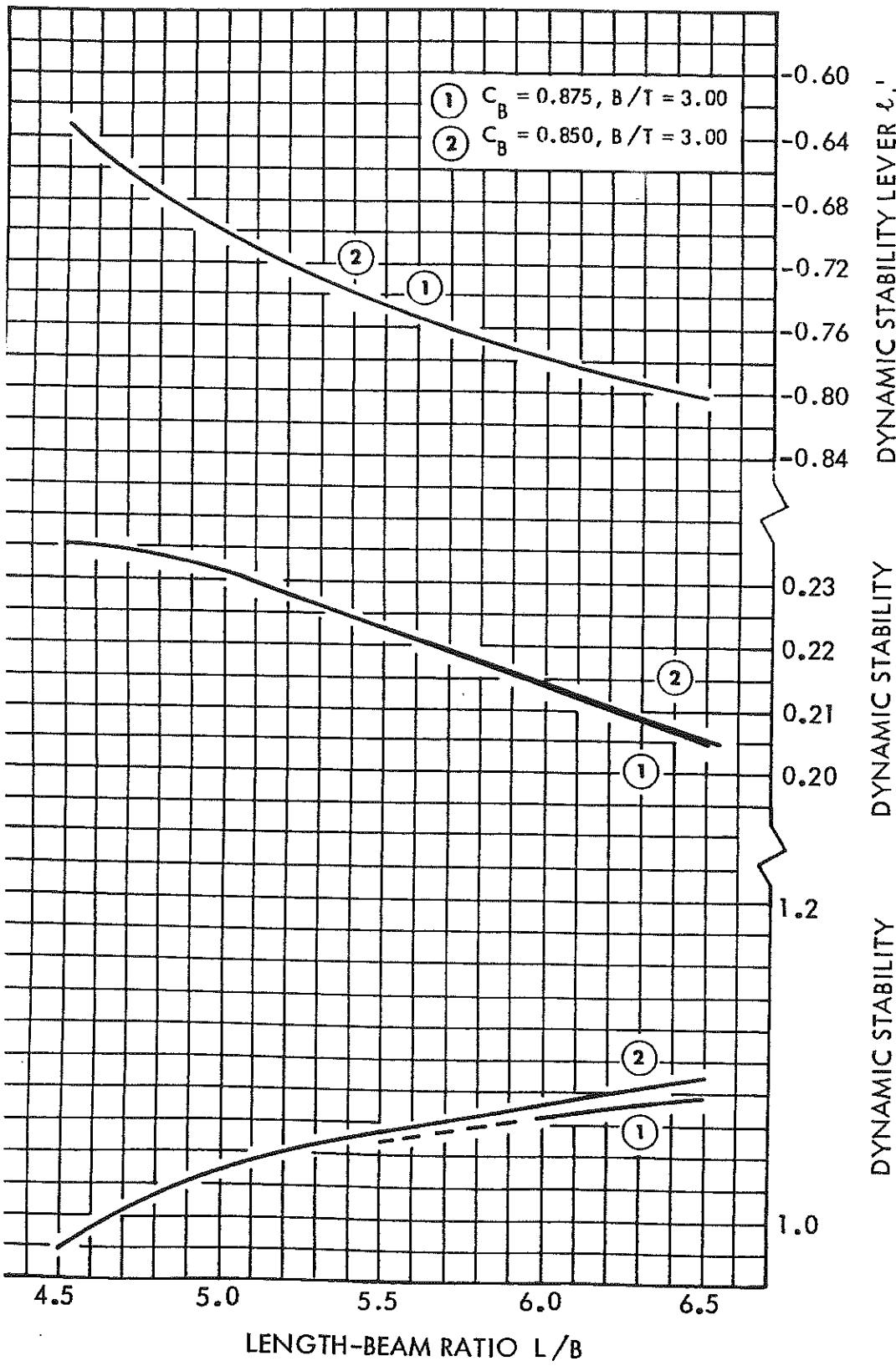

$\ell_d' = \frac{\ell_d}{L} = \frac{\ell_r - \ell_s}{L}$

$\ell_r' = \frac{\ell_r}{L} = \frac{N_r'}{Y_r' - m'}$

$\ell_s' = \frac{\ell_s}{L} = \frac{N_s'}{Y_s'}$

(vari versus)

RE 6-3 – EFFECT OF L/B VARIATION ON DYNAMIC STABILITY INDICES – BARE HULL

$$\sigma_{1,2} = -\frac{B}{2A} \pm \sqrt{\left(\frac{B}{2A}\right)^2 - \frac{C}{A}}$$

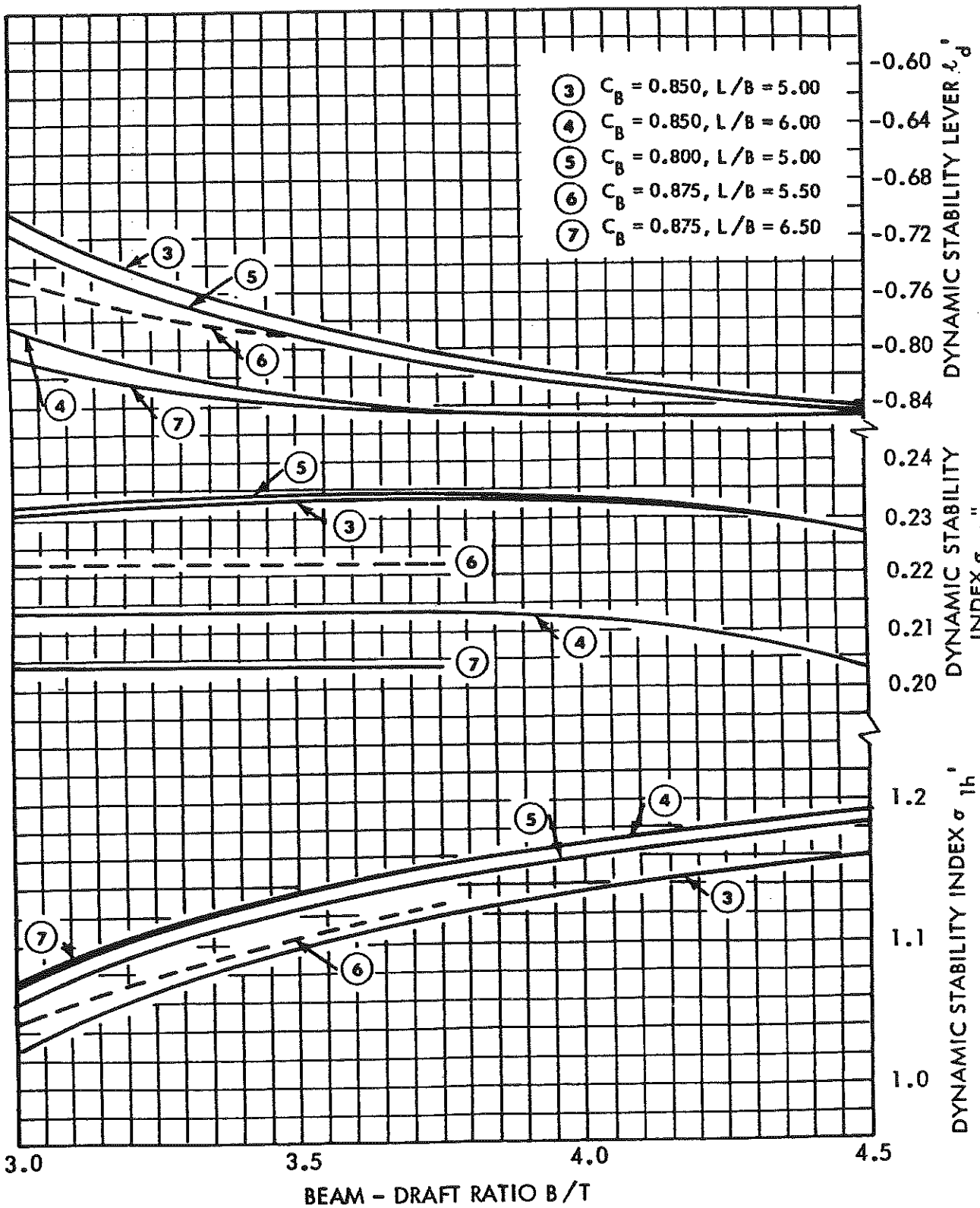

FIGURE 6-4 - EFFECT OF B/T VARIATION ON DYNAMIC STABILITY INDICES - BARE HULL

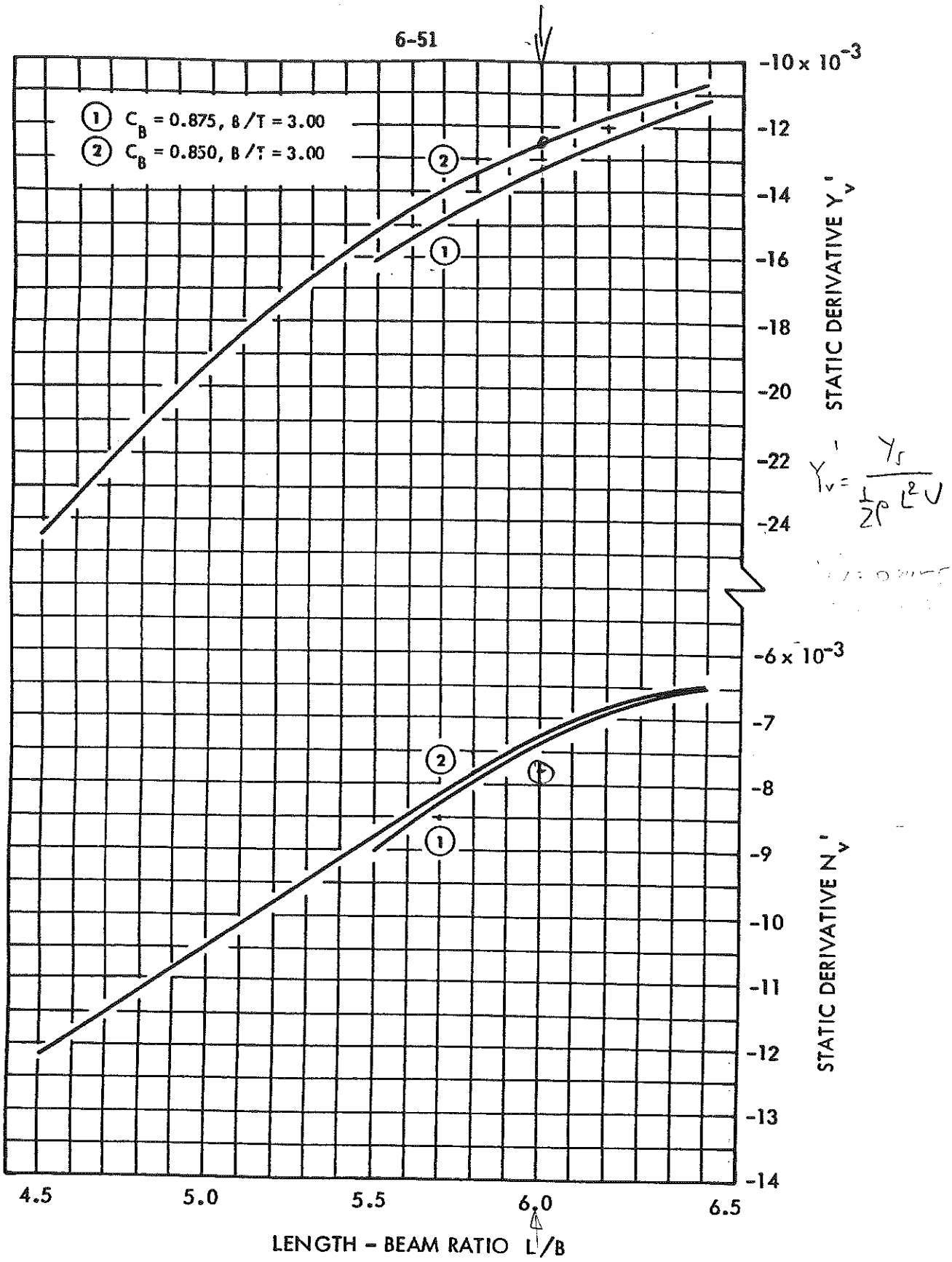

(a) Static Derivatives

FIGURE 6-5 - EFFECT OF L/B VARIATION ON STATIC, ROTARY, AND ACCELERATION DERIVATIVES - WITH STAND